Aromatization of *n*-Hexane over Metal Modified H-ZSM-5 Zeolite Catalysts

Themba Emmanuel Tshabalala

A dissertation submitted to the Faculty of Science, University of the Witwatersrand, Johannesburg, in fulfillment of the requirements for the degree of Master of Science.

Johannesburg, 2009

Declaration

I declare that this dissertation is my own, unaided work. It is being submitted for the Degree of Master of Science in the University of the Witwatersrand, Johannesburg. It has not been submitted before for any degree or examination in any other University.

_____

(Signature of candidate)

_____ Day of _____ 2009

TO MY GRANDPARENTS

NONTOMBI GRACE SUKA

And the late

DUBULA JOHN SUKA

To my late aunts,

Sisi Kholiwe and Sisi Nondaba

May their souls rest in peace.

Abstract

The aromatization of *n*-hexane was studied over H-ZSM-5 (SiO_2/Al_2O_3 = 70 and %XRD crystallinity = 66%), Ga/H-ZSM-5, Zn/H-ZSM-5 and Mo/H-ZSM-5 catalysts prepared by the incipient impregnation method and calcined at 500^oC. The aromatization reactions were carried out at 500^oC. BET, NH_3-TPD, H_2-TPR and XRD techniques were used in characterization of the catalysts in a preliminary attempt to correlate structure and catalytic behaviour. The catalytic activity of H-ZSM-5 was improved when impregnated with gallium and zinc. High conversions were obtained and the aromatic selectivity was above 50% when the gallium loading was 0.5 wt%. For Zn/H-ZSM-5 catalysts the activity increased with increase in zinc loading. The 3%Zn/H-ZSM-5 was the most active catalyst attaining a conversion of 88% and aromatic selectivity above 40%. The impregnation of H-ZSM-5 with molybdenum led to a decrease in activity and aromatic selectivity. As the molybdenum content was increased the deactivation rate increased with time-on-stream. This may be attributed to less dispersion of molybdenum species in the H-ZSM-5 channels leading to the blockage of the pore and active sites. The NH_3-TPD profiles suggested that an increase in the molybdenum content decreased the concentration of Brønsted acid sites hence decreased the activity of the H-SM-5 catalysts. The results obtained showed that Ga/H-ZSM-5 and Zn/H-ZSM-5 catalysts are good catalysts for the aromatization of *n*-hexane due to their dehydrogenation activity.

The results on the effect of percentage XRD crystallinity (from 5 to 86%) of H-ZSM-5 on the activity of H-ZSM-5 modified by loading 2 wt% of metal showed that conversion of *n*-hexane increased with %XRD crystallinity. The Ga/H-ZSM-5 and Zn/H-ZSM-5 catalysts with %XRD crystallinity above 30% showed more aromatic selectivity than Mo/H-ZSM-5 catalysts. The Mo/H-ZSM-5 catalysts were more selective to the cracked products due to the absence of the dehydrogenation activity that is possessed by gallium and zinc metals.

The effect of reaction temperature (between 500 and 600^{o}) on the aromatization of n-hexane over H-ZSM-5 containing 2 wt% metal content was investigated. The activity of catalysts increased with temperature for the 1 hour on-stream studies and as the time-on-stream increased a decrease in activity was observed. But at 550^{o}C Ga/H-ZSM-5 and Mo/H-ZSM-5 showed good stability with increase in time-on-stream. A rapid deactivation on Zn/H-SM-5 is associated with zinc leaving the catalyst bed.

Acknowledgements

I would like to thank the following people who offered their support during my MSc:

My supervisor, Prof. Mike Scurrell for his knowledge and support which he offered during the course of this project. I will not forget the meeting we held and the ideas that you suggested for progress in research.

To the man who technically ensured that my GC and TPD were working fine, Mr. Basil Chassoulas. You are the technical master mind in CATOMAT Group.

CATOMAT Group you make working easier with the kind of relationship we have.

I would like to thank the University of the Witwatersrand for offering me the opportunity and facility to do research. SASOL for financing the experimental part of this research project.

NRF for the Financial Support

Dr. Maropeng Ngobeni (Fe-Man), you have done a great job by introducing me to this catalysis world. And the advice you gave during my Honours degree. You will not be forgotten in my academic sphere.

To my family, Mama, Sipho, Phumla and Zubi you rock. Mampinga ndiyabulela.

Nongaka you have been supporting me all the way and I thank you for that. Know that you are LOVED always. '*SEMPER FIDELIS*'

And to the Almighty God. For strength He gave during my MSc duration. *Col 3: 23-24*

Presentations

Poster Presentation

Themba Tshabalala and Mike Scurrell, **Aromatization of *n*-Hexane over Metal Modified H-ZSM-5 Zeolite Catalysts** in: CATSA catalysis Conference at Ikhaya Bhubezi Parys, 9-12 November 2008.

List of Tables

CHAPTER 3

CHAPTER 4

List of Figures

CHAPTER 2

CHAPTER 3

CHAPTER 4

Table of Contents

CHAPTER 1

CHAPTER 2

CHAPTER 3

CHAPTER 4

CHAPTER 5

Chapter 1

Introduction

1.1.BRIEF BACKGROUND

The abundance and lower cost of light alkanes have generated extraordinary interest in converting them into useful compounds that may be of benefit to other industries. The conversion of light alkanes (C_2-C_4) into aromatic compounds mainly benzene, toluene and xylenes (BTX) is one of the important industrial processes that has attracted much attention due to the industrial application of BTX compounds [1]. These small alkanes are produced by processes such as Fischer-Tropsch synthesis, from oil refineries and are also found in natural gas. Aromatic compounds are regarded as highly useful compounds in the petroleum and chemical industries. In the petroleum industry aromatic compounds are used as additives in gasoline for the enhancement of the octane levels in gasoline. These aromatics can also be used as raw materials in other chemical industries for synthesizing other chemicals; in the polymer industry they are used as monomers in polyester engineering plastics, and they are also intermediates for detergents, pharmaceuticals, agricultural products and explosives manufacture [2].

Different catalytic processes have been utilized in producing aromatic compounds, mainly benzene, toluene and xylenes (BTX) from different feed stocks. The catalytic reforming of naphtha was regarded as an effective process for producing petroleum-derived aromatics, however; it was considered not economical due to its inability to convert light hydrocarbons [2]. Csicsery [3] discovered a process of converting light alkanes to BTX called dehydrocylodimerization. The process required high temperature i.e. above 500^{o}C and bi-functional catalysts. The dehydrocyclodimerization catalytic process had an advantage over catalytic reforming of naphtha in producing aromatics containing more carbon atoms than the

reactant paraffin. The catalysts that were used in this process are platinum metal on alumina (Pt/Al_2O_3) and chromia on alumina (Cr/Al_2O_3). These catalysts were susceptible to coke formed on the catalysts resulting in the deactivation of the catalyst. These studies triggered new developments in finding catalysts that would be coke resistant. The H-ZSM-5 zeolites were considered because of their unique properties. This aluminosilicate material is relatively coke resistant. The shape selective property prevents the polynuclear aromatic compounds from forming within the pores of the catalysts. Formation and dehydrogenation of these compounds leads to the formation of coke. Thus the use of H-ZSM-5 reduces the formation of coke and the catalyst remains active for a longer time.

Mobil developed a process called M2-Forming in which light alkanes are converted into BTX an over unmodified H-ZSM-5 zeolite catalyst. Unfortunately, the unmodified H-ZSM-5 suffers fast deactivation and possesses substantial cracking activity that leads to a large selectivity for C_1 and C_2 products. However, the problem is overcome by adding activating agents which are transition metals such as such as Cr, Cu, Fe, Mn, Mo, Ni, Os, Pt, V, W and Zn, including Ga. These metals were added in the form of extra-framework species to facilitate the dehydrogenation function [4-6]. Gallium, platinum and zinc appeared to be more active and selective towards aromatic compounds. However, gallium and zinc were more advantageous than platinum [7]. Platinum has a high activity for the dehydrogenation of paraffins. Loading platinum increases considerably the conversion of alkanes into aromatics. However, the aromatization reaction is accompanied by the production of unreactive alkanes, methane and ethane through hydrogenolysis, hydrogenation, and dealkylation reactions [8]. The improved activity and selectivity due to the addition of extra-framework species has made possible commercial application of the other processes, i.e. the Cyclar process which was developed by BP and UOP, and Aroforming [9].

1.2.AIMS AND OBJECTIVES

A fluctuation in the price of crude oil and coal depletion, the two resources which are needed in the petroleum industry has led to some comprehensive developments in finding economical processes and alternative resources that can be used in producing gasoline, diesel and other important chemicals that will be of good use in the chemical industry. The catalytic conversion of alkanes into desired chemical compounds is one promising process that can be of good utilization in enhancing the economic state of the petroleum industry, especially in South Africa.

The C_6 reactants can be converted to a large variety of hydrocarbons comprising C_1-C_4 compounds, iso-paraffins, alkycyclopentanes, and aromatics (mainly BTX). The selectivity towards each of the products depends strongly on various factors such as, metal dispersion, metal alloy formation, carbon deposition on the catalyst, acidity of the support and reaction conditions. Therefore, in this project we aim to study some factors that have been mentioned above that influence the catalytic activities in the aromatization of *n*-hexane over gallium, zinc and molybdenum loaded H-ZSM-5 based catalysts. The latter catalysts have been studied for the conversion of short (C_1-C_4) alkanes but relatively little work has been carried out on longer (C_6-C_8) alkanes. This study involves the investigation of the effect of metal loading on the catalytic conversion of *n*-hexane to aromatic compounds and the selectivity towards aromatics. Parameters such as reaction temperature and the effect of percentage XRD crystallinity of H-ZSM-5 will also be studied. Characterization techniques such as BET surface area and pore volume analysis, temperature programmed reduction/desorption methods, Fourier Transform infrared (FT-IR) spectroscopy and X-ray powder diffraction (XRD) were also used in this study.

1.3.OUTLINE OF THE THESIS

Chapter 2 presents a literature review of the chemistry and background of zeolites as supports in catalysis. Several factors that are important in the preparation of zeolites are briefly discussed. Techniques that can be employed to characterize zeolites samples are also given. The conversion of alkanes over metal modified H-ZSM-5 zeolites catalysts are reported in this chapter. Metals that were previously studied include gallium, zinc, and more recently molybdenum. A survey of the aromatization of *n*-hexane over metal modified zeolites catalysts is also presented.

Chapter 3 is the experimental section of this paper and deals with the description of the preparation of H-ZSM-5 zeolites catalysts using hydrothermal treatment methods. The incorporation of metals such as gallium, zinc and molybdenum using the incipient wetness impregnation method is also presented. The characterization methods that were used to study the characteristics of the prepared samples are also presented.

The results obtained on the study of the aromatization of n-hexane are documented and discussed in Chapter 4. Several variables were investigated. The results show the effects of variables such as metal loading, percentage XRD crystallinity of H-ZSM-5 with 2 wt% metal loading and reaction temperature on the aromatization of n-hexane.

The general conclusions are presented in Chapter 5.

1.4.REFERENCE LIST

[1] L. Cheng, H. Guo, X. Guo, H. Liu and G. Li, *Catal. Commun.*, **8** (2007) 416.

[2] W.J.H. Dehertog and G.F. Fromen, *Appl. Catal. A: General*, **189** (1999) 63.

[3] S.M. Ciscsery, *J. Catal*., **17** (1970) 207.

[4] Y. Xu and L. Lin, *Appl. Catal*., **188** (1999) 53.

[5] Y. Shu and M. Ichikawa, *Catal. Today*., **71** (2001) 55.

[6] Y. Xu, X. Bao and L. Lin*, J. Catal.,* **216** (2003) 386.

[7] M.G. Sanchez, Characterization of Gallium-containing Zeolites for Catalytic Application, PhD Thesis, Eindhoven University of Technology, Netherlands, 2003.

[8] P. Meriaudead and C. Naccache, *Catal. Rev-Sci. Eng*., **39** (1997) 5.

Chapter 2

Literature Review

2.1. BACKGROUND ON ZEOLITES

The history of zeolites began with discovery of stilbite in 1756 by a Swedish mineralogist Cronsted [1]. The name zeolite is derived from Greek word *zeo*-to boil and *lithos*-stones. The name was derived from the behavior of the mineral when subjected to heating; stilbite loses water on heating and thus seems to boil (boiling stone) [2]. Natural zeolite is a framework aluminosilicates whose structure contains channels filled with water and exchangeable cations, with a general chemical formula:

$$m/yM^{y+}[(SiO_2)_n(AlO_2)_m] .xH_2O \qquad (1)$$

where M can be cation, e.g.: Na^+, Ca^{2+}, K^+, or H^+. The presence of water in the channels allows the mobility of cations for ion-exchange to occur at lower temperatures (100^{o}C). Water is lost at 250^{o}C and reversibly re-adsorbed at room temperature [3].

Zeolites are known to be porous material on a molecular scale with structures revealing their regular arrays of channels and cavities of 3-15 Å. This pores and channels are the most important properties that are associated with molecular sieving ability [4]. The primary building units are the TO_4 tetrahedra, where T represents Si and Al atoms. The adjacent tetrahedra atoms are held together by apical oxygens forming a T-O-T chain which gives a framework ratio of O/(Si+Al) of two. The linkage of Al and Si is facilitated by the apical oxygen leading to a formation of channels and cavities of a certain molecular dimension which allows molecules of appropriate size to access intracrystalline pores. Thus the number of tetrahedra forming a ring/window is important since it governs the accessibility of the intracrystalline channels. The

sizes of intracrystalline pores lie in the range 0.3-1 nm, depending on the structure of the zeolite. For ZSM-5 the pores are built from 10 tetrahedra, but different arrangements of secondary building units normally result in formation of smaller/larger sized pores in other zeolites.

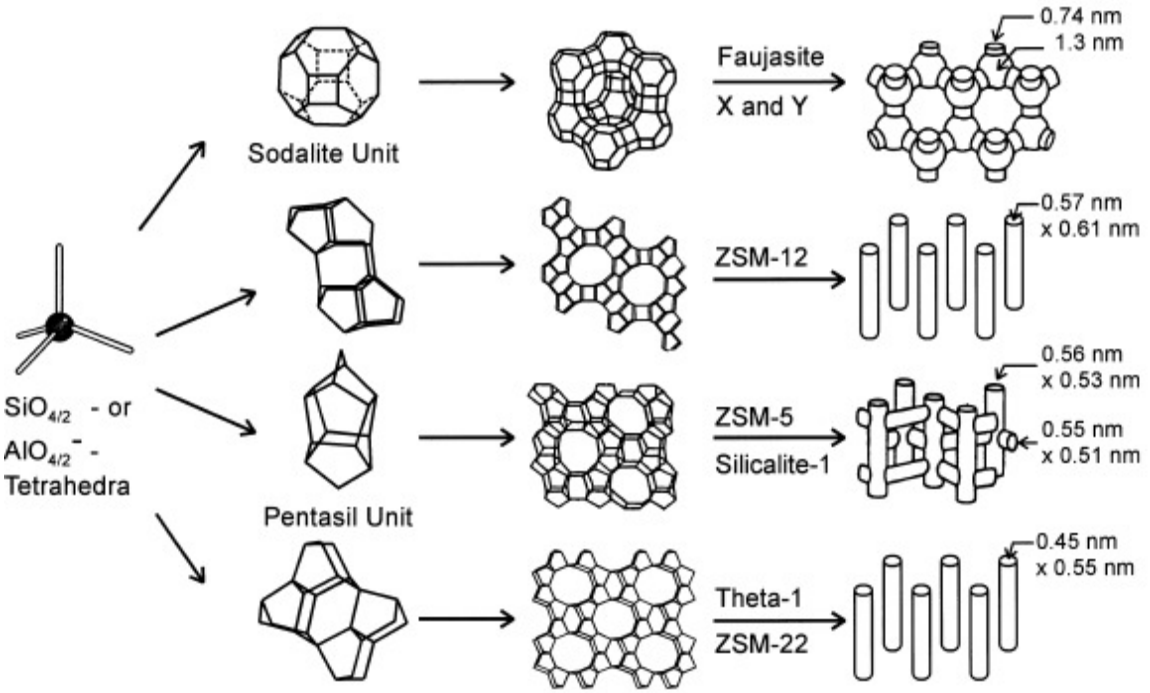

Figure 2.1: Structure of the four selected zeolites and their micropore systems and dimensions [5].

The type and size of cavities is based on the secondary building units (sodalite unit or pentasil unit) that consists of 24 silica or alumina tetrahedral linked together to form a sodalite cage. The secondary building units are linked either through the 5 or 6 member rings to form a cage of a certain dimensions resulting in the formation of faujasite i.e. zeolite X, Y types. The zeolite Y is considered as one of the important zeolite types in heterogeneous catalysis. Its pore system is relatively spacious and consists of spherical cages referred to as supercages with diameter of 1.3 nm connected tetrahedrally with four neighbouring cages through windows with a diameter of 0.74 nm formed by 12 tetrahedra. Zeolite ZSM-5 and its all silica analogue silicates are built

from the pentasil units. They contain intersecting systems of ten-membered–ring pores with one being straight and the other sinusoidal [5].

The unique features of zeolites compared to other conventional solid catalysts or supports are: (i) their strictly uniform diameters and (ii) pore width in the order of molecule dimensions. According to the IUPAC classification [6] of porous materials, zeolites are classified as microporous materials.

2.2. APPLICATION OF ZEOLITES

Zeolites possess good properties that enable them to be interesting materials for use in different industrial applications. The size of the channels and cavities mean that such materials can be used as molecular sieves because of their size and shape exclusion character. There are three different molecular shape selective catalysis mechanisms that take place within/outside the pores of zeolites; which are summarized below:

Reactant Selectivity demonstrates the phenomenon when the microporous character of zeolite acts as a molecular sieve. This occurs when only one part of the reactant molecules is small enough to diffuse through the pores while bulky molecules are excluded from entering the intracrystalline pores. This exclusion limit can be varied over a wide range of different zeolites and related microporous solids.

Product Selectivity describes the diffusion of reaction products formed in the microporous pore and crystal size of the catalyst particles out of the zeolite. The less sterically favoured molecules diffuse through the pores leaving the framework of zeolites, whereas the bulky ones stay longer

in the framework and some are further transformed to less sterically hindered product molecules while others are converted into coke which leads to catalyst deactivation.

Restricted Transition-State Selectivity is the prevention of reactions that involve formation of large intermediate molecules or transition states in the pores of molecular sieves. This means the formation of intermediates or transition states is sterically limited due to the shape and size of the microporous lattice allowing the access species formed to interact with the active sites. Neither the reactants nor products are hindered in diffusing through the pores and only the transition state is hindered.

These shape selectivity properties allow zeolites to be used in separation processes such as catalytic dewaxing. This is the selective removal of the long chain n-paraffin in the gas phase from oil using ZSM-5 as catalysts. Several medium pore and microporous types of zeolites including ZSM-11, ZSM-23 and SAPO-11 have been used in catalytic dewaxing [7].

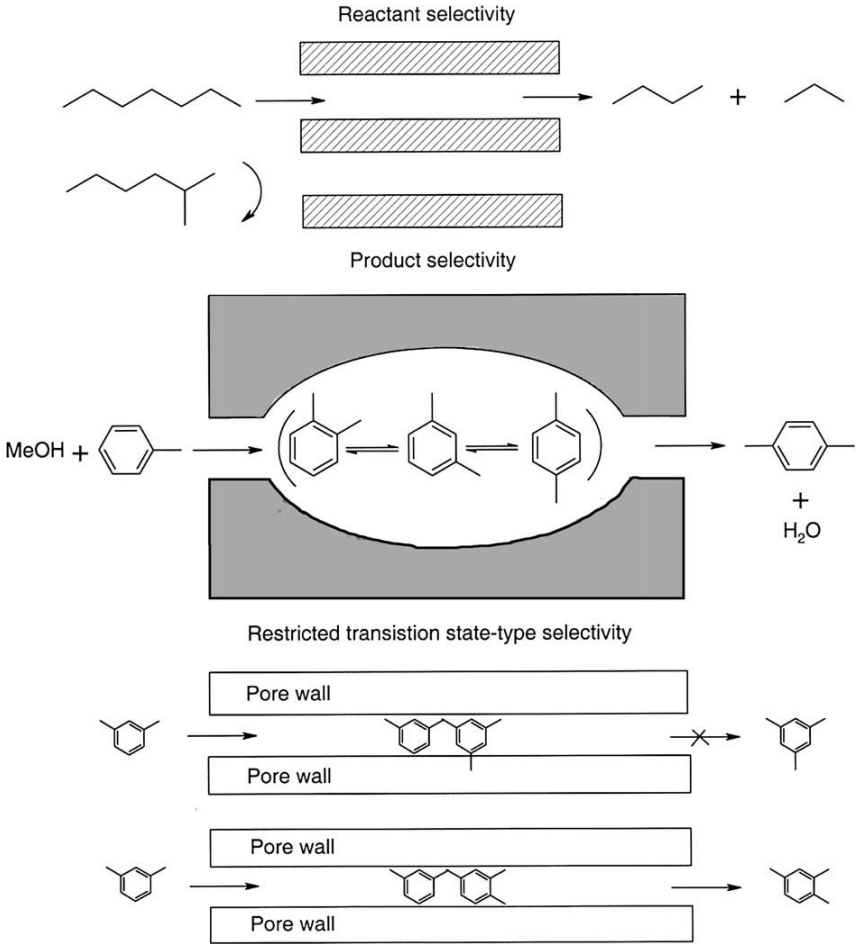

Figure 2.2: Representation of size and shape selectivity of a zeolite relative to the size of the molecule [8].

2.2.1. Ion-Exchange

It has been mentioned that the framework of zeolites contain cations Na^+ and K^+ (depending on the alkaline based used during synthesis) in the channels and cavities which are free to move. The mobility of metal ions permits ion-exchange to take place easily in the cages of zeolites. This makes zeolites suitable for ion exchange in aqueous solution. The exchange of Na^+ by Ca^{2+} and Mg^{2+} in reducing the hardness of water is a classical example of zeolites application in the washing powder industry. Zeolites are used as additives in washing powder to allow ion-exchange to take place during washing resulting in the reduction of hardness of water.

Considering environmental aspects, zeolites have been used in reducing water waste contamination containing heavy metal effluents and in nuclear radioactive isotope clean up applications [9]. In the 1960s one natural occurring zeolite called clinoptilolite was found to be highly selective to ammonium ions by ion-exchange. This led to zeolites finding a place in a water industry. Clinoptilolite is used to treat sewage and agricultural effluents. Most municipal water supplies are processed through zeolites before public consumption. This is done to reduce the concentration of ammonium ions and other metallic cations and to enhance the user friendly character of water.

2.2.2. Catalytic Applications

The acidic nature that zeolites possess has led to these materials finding a special place in many industrial applications. The petroleum industry is interested in the increase in compounds that are associated with an enhancement of octane levels of gasoline, and the production of other fuels. The conversion of hydrocarbons is mainly dependent on the formation of carbocations on zeolites and other related catalysts [8]. The major role of acid sites is to function as a proton source in this manner, leading to the formation of carbocations. These carbocations result in processes such as polymerization, alkylation, isomerization, and cracking, leading to the formation of products with high octane levels which can be useful in other ways.

In the oil refinery business, zeolitic catalysis impact is noticed in Fluid Catalytic Cracking (FCC) where crude oil fractions are converted into gasoline. In the conversion of methanol to gasoline (MTG), acid sites dehydrate the methanol which results in the formation of DME, and then the mixture of DME and methanol is converted into hydrocarbons which are within the gasoline range [10]. Many developments in the oil refinery and petroleum industry have made use of zeolites in the conversion of hydrocarbon into valuable products. Currently there is ongoing

research on the conversion of methane to liquid hydrocarbons using ZSM-5 zeolite type. However, the results are still confined to low conversion and selectivity [11].

2.3. SYNTHESIS OF ZEOLITE

Aluminosilicate zeolites are usually synthesized by hydrothermal treatment methods from reactive gels containing an aluminum and silicon source, an organic template and an alkaline metal base. The gel mixture is heated at temperatures between 60 and 200^{o}C under a closed system (autoclave vessel) for several days. It is well known that the natural zeolite synthesis is sensitive to several parameters such as temperature, pH, the type of alkaline cation, reaction time, template agent and raw material used i.e. origin of silica and alumina.

The formation of zeolites is governed by two reactions: nucleation and crystal growth, which are also influenced by the parameters mentioned above. The nucleation process occurs in the liquid-solid solution and it can be homogeneous or heterogeneous. The heterogeneous nucleation process is induced by the impurities that other particles present in the solution of the starting material and the homogeneous nucleation process occurs spontaneously. The formation of zeolites starts by aggregation and densification of primary units formed during nucleation in the gel phase. The first crystals formed are largely due to the defects in the un-finished aggregation or densification processes. Crystal growth process occurs at the crystal-solution interface by condensation of dissolved species onto the crystal surface formed during nucleation process. This happens through the incorporation and aggregation of primary units present in the amorphous gel followed a by densification process. A crystal growth reaction reduces the size of crystals formed during nucleation [12].

2.3.1. Alkaline Metal Base

The base metal is considered as the mineralizer in this process and it has control over the pH of synthesis mixture. The mineralizer in this case is an alkaline metal base (OH^- and F^- anions) used for hydrothermal synthesis of zeolite. The F^- anion in the mineralizer reduces nucleation and crystallization rates making the process of zeolite synthesis faster; larger crystals are formed. Murayama et al. [13] investigated different alkaline species (NaOH, Na_2CO_3 and KOH) that can be used in the hydrothermal synthesis of zeolites. He found that the best alkaline cation to be used in the synthesis of zeolites is Na^+ because its contribution to the crystallization of zeolites and the hydroxide ion promotes the dissolution of silica and alumina.

The concentration of the hydroxide ion is important since it controls the pH of the solution gel. The alkalinity of the solution has an influence on the crystallinity and zeolite growth. Wong et al. [14] studied the effect of concentration of OH^-. They established that the highest growth rate and crystallinity was obtained at 0.03 M concentration of hydroxide ion. At concentrations above 0.03 M a slow growth rate of the zeolite and low crystallinity were reported.

2.3.2. Template Reagent

A chemical species is regarded as a template or structure directing agent, if crystallization of the specific zeolite structure is induced that could be not formed in the absence of the reagent. The roles of the template are:

- Behaves as a structure directing agent
- Acts as a gel modifier, particularly influencing the Si/Al ratio
- Acts as a void filler

- Influences chemically and physically the formation and aging of the gels and the crystallization process.

Most of the templates used in the zeolite synthesis are positively charged molecules. The structure making agents also influences the rate of crystallization. In zeolite synthesis the most used templates are quaternary tetraalkylammonium cations e.g. tetramethylammonium (TMA^+), tetraethylammonium (TEA^+), tetrapropylammonium (TPA^+) and dihydroxyethyldimethylammonium. For synthesis of ZSM-5 zeolites a TPA^+ cation is used [15]. These templates possess the hydrophobic character generally from the alkyl group which is responsible for the arrangement of water molecules. The organic cation is surrounded by many water molecules forming an organized cloud of water molecules. The organized cloud of water molecules can be replaced by silicate and aluminate tetrahedra and this contributes to the formation of cage-like structures as shown in Figure 2.3 [16].

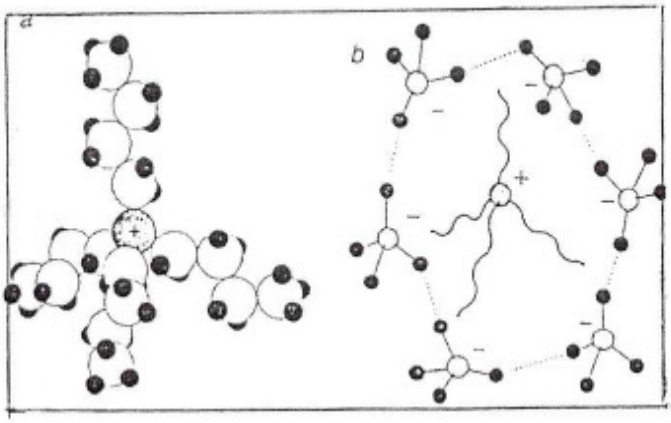

Figure 2.3: Tetraalkylammonium ions (a), in which a positively charged nitrogen atom contains a four carbon chain, (b) template ion surrounded by silicate and aluminate ions linking together to form zeolite cavities [16].

2.3.3. Synthesis Temperature

The reaction temperature influences the zeolitization process both kinetically and thermodynamically. Different structural zeolite phases are obtained at various reaction temperatures at equal reaction times. The zeolite phases formed at high temperature have a low degree of hydration and are thermodynamically stability. The reaction temperature has a beneficial effect on the induction time for crystallization and an increase in conversion of raw material to crystalline material leads to zeolitization taking place at a faster rate, thereby shortening the reaction time [17].

2.3.4. Formation of Acid Sites

Acidity and basicity of zeolites are the important properties in heterogeneous catalysis which are classified in to two types; Brønsted type (proton donating/hydroxyl anion-donating site) and Lewis type (electron donating or electron withdrawing site). The concentration of aluminum is one factor that has an effect on the acid site distribution or concentration. This can be monitored by noting at the silica/alumina ratio. The other factors that influence the acidity of zeolites are thermal stability and the chemical nature of substrates used to modify the zeolite surface, primarily referring to the metal.

The Brønsted acid sites arise from the hydroxyl bridging groups within the pore structure of the zeolite. These hydroxyl groups which most of the time are referred to as protons are associated with a negatively charged framework oxygens linked with alumina tetrahedra and give Brønsted acid sites. They are formed during the calcination process of NH_4-ZSM-5 or Cation-ZSM-5 zeolite forms which are ion-exchangeable. High temperatures enhance the mobility of protons in zeolite pores and are quite mobile due to the presence of water molecules. At temperatures above 500^{o}C they are lost, as with water molecules resulting to the formation of Lewis acid sites [8]. However, it has not been clearly discussed which specific atom within or outside the

framework of zeolites act as the Lewis acid site. The dealumination process which takes place concurrently with dehydroxylation liberates aluminium atoms from the zeolite framework. It is believed that non-framework aluminium atoms in tri-coordination act as Lewis acid sites. Chen et al. [18] study the effect of calcination temperature on the formation of Lewis acid sites. They found that the increase in calcination temperature favours the formation of non-framework aluminium which leads to an increase in the concentration of Lewis acid sites within zeolites. They concluded that the non-framework aluminium acts as a Lewis acid site.

The acid sites i.e. Brønsted and Lewis, are the most important sites in zeolites as catalytic reactions take place on them. The catalytic reaction of methanol to gasoline aromatic compounds is reported to be driven by the presence of acid sites in the zeolites [19]. Sulikowskil and Klinowski [20] found that the addition ZSM-5 in the FCC catalyst increased the concentration of aromatics while the concentration of olefins decreased. This was attributed to the presence of Brønsted acid sites from zeolites catalysts.

2.4. CHARACTERIZATION TECHNIQUES

Characterization is important in linking the catalytic behavior with the physical and chemical properties of the catalysts. Many techniques and instruments have been developed and used to characterize solid phase catalysts. Zeolites are characterized using Powder-X-Ray Diffraction (XRD), Temperature Programmed Reduction/Desorption (TPR/TPD), nitrogen-adsorption surface area determination technique (BET), Fourier Transform Infra Red spectroscopy (FT-IR). These techniques will give detailed description of zeolites samples in terms of crystallinity, strength of acid sites, structure; oxidation state of metal and temperature reduction.

2.4.3. Powder X-Ray Diffraction

The powder X-Ray Diffraction method is a non-destructive technique applied to crystalline materials. The technique has been traditionally used for phase identification, quantitative analysis and the determination of structure imperfections. With growing interest in crystallography more applications have been extended to new areas, such as the determination of crystal structures and the extraction of three-dimensional micro-structural properties. Various kinds of micro- and nano-crystalline materials can be characterized from X-ray powder diffraction, including inorganics, organics, drugs, minerals, zeolites, catalysts, metals and ceramics. The physical state of the materials can be loose powders, thin films, polycrystalline and bulk materials. For most applications, the amount of information which is possible to extract depends on the nature of the sample microstructure (crystallinity, structure imperfections and crystallite size), and the complexity of the crystal structure (number of atoms in the asymmetric unit cell, unit cell volume) [21].

The diffraction line profiles in a powder diffraction pattern are distributions of intensities I (2θ) defined by several parameters:

- The reflection angle position 2θ at the maximum intensity which is related to the lattice spacing d of the diffracting *hkl* plane and the wavelength λ by Bragg's law,

$$\lambda = 2d_{hkl} \sin\theta \qquad (2)$$

- The dispersion of the distribution, full-width at half-maximum and integral breadth
- Line shape factor
- Integrated intensity which is said to be proportional to the square of the structure factor amplitude

In zeolites, the powder XRD technique is used for sample identification and to calculate the degree of crystallinity of the zeolite sample relative to a reference sample. The diffraction pattern is regarded as the fingerprint of the respective sample. Hence, a zeolite structure can be identified by using d-spacing or 2 theta values of the of the typical Bragg reflections of the respective sample in comparison with the standard sample [22]. The crystalline and amorphous nature and also the presence of contaminates is verified by comparing the prepared sample with suitable standards. If there are no traces of impurities in the diffraction pattern the sample can be declared to be pure.

The intensities or areas under the peaks can be used to determine the degree of crystallinity or percentage XRD crystallinity of zeolite samples relative to the reference sample with high crystallinity. Applying the method, the summation of seven, five or three major peaks in the diffraction pattern has been used. The intensities of these particular peaks are compared with those of the reference sample. From the three methods, the three peaks method was proven to be the most efficient and reliable method to calculate %XRD crystallinity [23, 24].

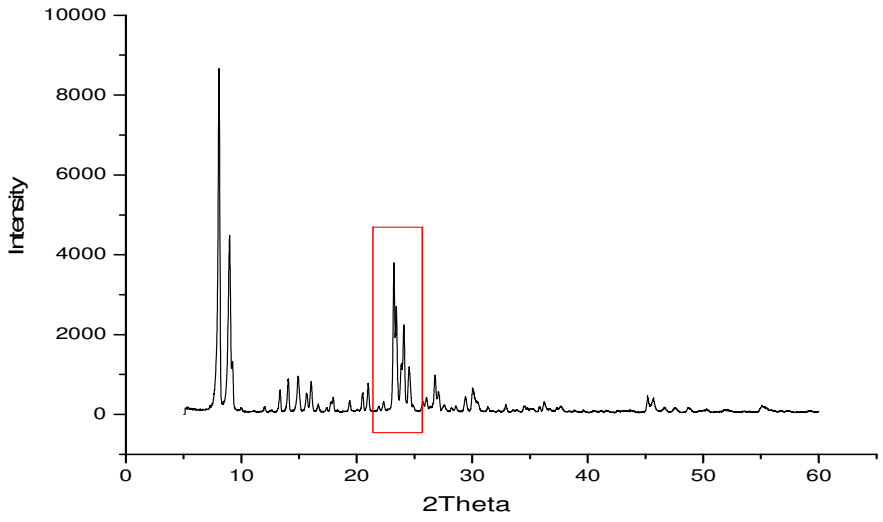

Figure 2.4: X-ray powder diffraction pattern of H-ZSM-5 (SiO_2/Al_2O_3=70).

This is done by calculating the sum intensities or areas of the peaks between 2 (theta angles) 22 and 25°.

$$\%\ XRD\ Crystallinity = \frac{\Sigma I_{sample}}{\Sigma I_{reference}} \times 100\% \qquad (3)$$

Different factors affect the %XRD crystallinity of zeolites such as size, shape of crystals, dispersion and homogeneity, etc. zeolite samples with crystalline particle size may yield low percentage XRD crystallinity, and this was attributed to the crystalline small particles being below the detection limit. The other factor is related to the amorphous phase of the sample giving a broad and weak diffraction line or no diffraction at all and in consequence the percentage crystallinity of the sample would be difficult to determine.

2.4.2. Thermal Techniques

There are several surface techniques that may be used in to analyze catalysts and thermal techniques such as temperature-programmed reduction (TPR) and temperature-programmed desorption (TPD) are some of those that are used. These techniques are applied in heterogeneous catalysis to monitor surface bulk reactions between a solid which is the catalyst and a gas which is the reactant while increasing temperature.

2.4.2.1. Temperature Programmed Desorption (TPD)

Temperature-programmed desorption (TPD) or thermal desorption spectroscopy (TDS) studies employ probe molecule to examine interactions of the surface of the catalyst with the gas or liquid-phase molecules. The probe molecules are chosen with respect to the nature of the adsorbed species believed to be important in the catalytic reaction under study or chosen to

provide information on the specific character of the of surface of the catalyst e.g. acid sites. The temperature of the desorption peak maximum is indicative of the strength with which the adsorbate is bound to the surface [25]. The higher the temperature of the desorption peak the stronger the bond between the adsorbate and the surface. Ammonia and pyridine are the probe molecules that are frequently used to study the acid character of solid catalysts because of their ability to distinguish between the Lewis and Brønsted acid sites. However, the size of the probe molecule is of pivotal importance because it affects the accessibility to specific sites as well as influences the rate of diffusion in the TPD instrument. It has been reported that pyridine desorption from zeolites, i.e. ZSM-5 is limited by molecular diffusion in the zeolite crystals, and hence ammonia is widely used rather than pyridine.

In a typical TPD experiment, the sample is placed in a tube fluxed by an inert gas. The substance to be adsorbed is fed; pulsed or continuously, till the equilibrium is reached. After out gassing the physisorbed fraction, the temperature is raised at a constant rate, so the adsorbate undergoes a progressive release. At temperatures which are high imply that the interaction with the surface of the catalysts is strong. A detector system is placed beyond the sample reactor to monitor the changes of the interaction between the adsorbate and solid surface of the catalyst [26]. Figure 2.5 below shows an ammonia-TPD profile.

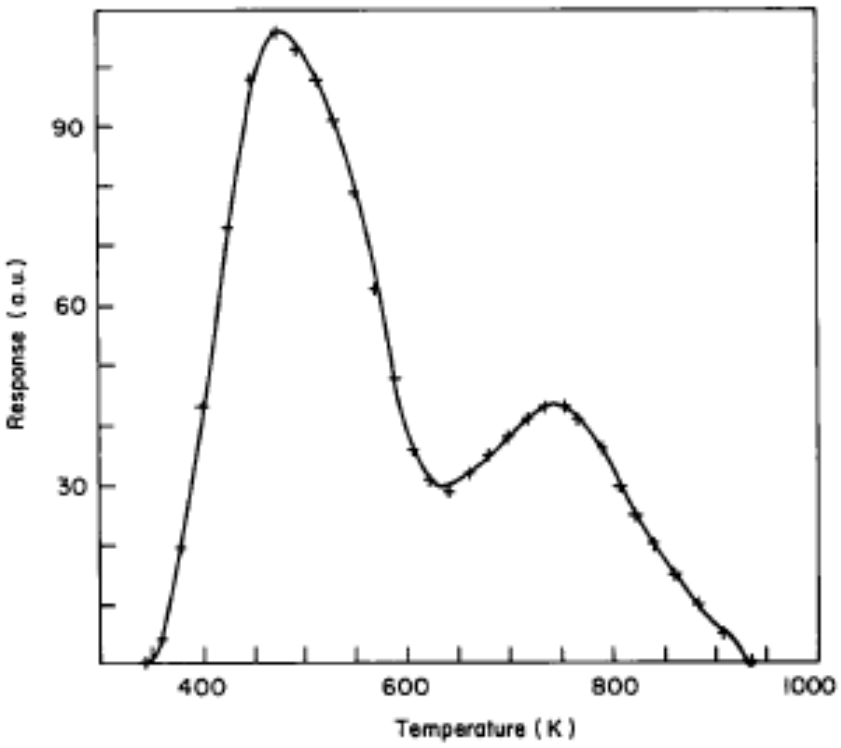

Figure 2.5: Typical ammonia-TPD profile for catalyst [27].

Two peaks observed, one at low temperature (LT) and the other at high temperature (HT). The LT peak represent the desorption of weakly attached ammonia gas molecules from acid sites in the zeolite and the HT peak is the desorption of ammonia that is strongly attached to the acid sites. The desorption peak at high temperature is due to the migration of ammonia from the strong Brønsted acid sites and the interaction has been attributed to the IR band observed at 3610 cm^{-1}. The interaction of Lewis acid sites with the ammonia molecule is represented by the desorption peak at low temperature and the IR band at 3680 cm^{-1}. The IR band shows the interaction of the ammonia with the aluminium in the zeolite framework. The nitrogen from the ammonia has a lone pair which will attack the vacant orbital possessed by the aluminium forming a covalent bond [28].

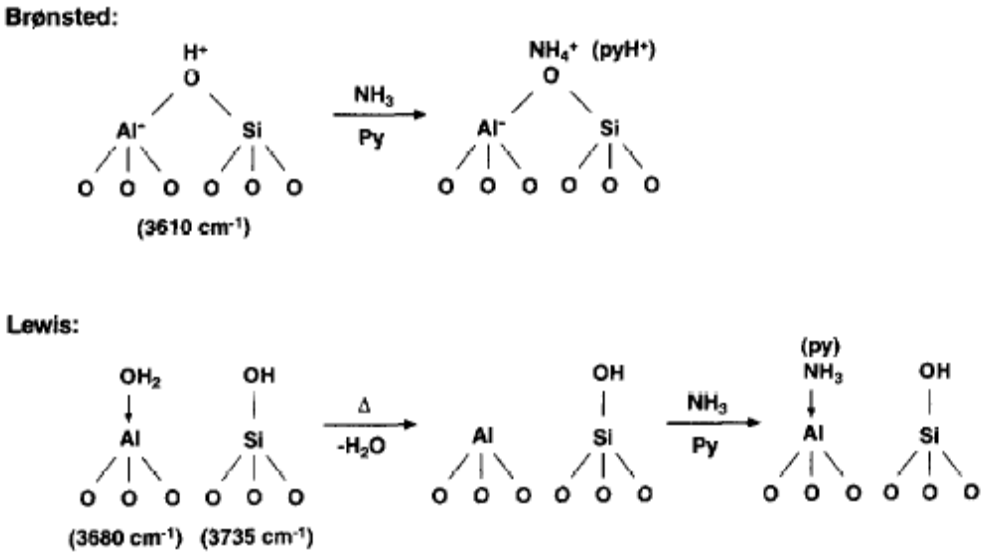

Figure 2.6: Representation of ammonia interaction with Brønsted and Lewis acid sites of zeolites [28].

2.4.2.2. Temperature Programmed Reduction (TPR)

The TPR technique has proved to be an effectivel tool to analyze the reduction kinetics of oxidic catalyst precursors. In the thermal reduction technique, a reducible oxidic catalyst or catalyst precursor is exposed to a flow of a reducing gas mixture (nitrogen/hydrogen or argon/hydrogen containing a few volume per cent of hydrogen) while of temperature is increasing linearly. The reduction of metal oxide by H_2 is described by the equation:

$$MO_n + nH_2 \longrightarrow M + nH_2O$$

The degree of reduction is continuously monitored by measuring the hydrogen gas consumption. The experiment allows the determination of the total amount of hydrogen consumed during reduction. From the degree of reduction the average oxidation state of the catalyst or precursor after reduction can be calculated [29].

The reduction reactions of metal oxides by hydrogen start with dissociative adsorption of H_2, which is a much more difficult process on an oxide than on metals. The atomic hydrogen is a pro-molecule for the actual reduction reaction. The rate of reduction is dependent on the activation of H_2. In TPR the degree of reduction of the catalyst is proportional to the function of time, while the temperature increases at a linear rate. Hurst et al. [30] derived a rate expression for the reduction reaction. They assumed that the reversible reaction of reduction from metal to oxide is unfeasible.

$$\frac{-d[MO_n]}{dt} = k_{red}[H_2]^p f([MO_n]) \quad (4)$$

Where

$[MO_n]$ concentration of metal oxide

$[H_2]$ concentration of hydrogen

k_{red} rate constant of reduction

p order of the reaction in hydrogen gas

f function which describes the dependence of the rate of reduction on the concentration of metal oxide

t time

2.4.3. Surface Area Determination

Heterogeneous catalysts are porous solids and the porosity arises due to the preparation method involved. In zeolites synthesis, crystallization using hydrothermal conditions produces zeolites. The peculiar disposition of the building units generates intracrystalline cavities of molecular size.

During thermal treatment the volatile material (template) is burnt off and cavities that represent both the solid arrangement and exit of the removed material are produced. Post-treatment of the catalysts further alter the morphological characteristics and physical properties of the catalyst. The catalytic activity may be only indirectly related to the total surface, and so determination of surface area is generally considered to be an important requirement in catalyst characterization [25]. It is necessary to know the nature of the pore structure since this may control the transport of reactants and products of catalytic reactions. Other physical properties which may influence the path of catalytic reactions are pore size and shape [31].

There are various techniques used for surface area and pore determinations, and the right choice depends on the type of pores and pore structure of the catalysts to be studied. The gas adsorption methods are widely used to determine the surface area and pore size distribution of catalysts. The technique accurately determines the amount of gas adsorbed on a solid material, which is a direct measure of the porous properties and structure. The technique involves the determination of the adsorption isotherm of the probe gas volume adsorbed against its relative pressure [32].

The adsorption isotherm obtained from adsorption measurements provides information on the surface area, pore volume, and pore size distribution [33–35]. Different probe gases including N_2, Ar, and CO_2 are frequently used as adsorptives, depending on the nature of the material (adsorbent) and the information required. The adsorption of N_2 at 77 K and at sub-atmospheric pressures has remained universally pre-eminent and can be used for routine quality control, as well as for investigation of new materials [36]. The N_2 adsorption at 77 K allows the determination of:

- Total surface area of the solid by the BET method
- Total surface, external to micropores by t-plot or α_s plot methods
- Mesopore surface distribution vs. their size by the Barrett-Joiner-Halenda (BJH) method
- Micropore volume by t-plot or α_s plot methods

- Mesopore volume and volume distribution vs. their size by Gurvitsch and BJH methods

The BET method is widely used, despite its limitations, for the evaluation of surface area from a physisorption isotherm. There are two stages in the application of BET procedure that are pivotal in the determination of BET surface area. The first stage is the derivation of the monolayer capacity n_m^a, defined as the amount of the adsorbate required to form a complete monolayer on the surface of a unit mass of the adsorbent. The specific surface a_s(BET), is then obtained from n_m^a by taking an average area a_m, occupied by an adsorbate molecule in the monolayer. Hence

$$a_s(BET) = n_m^a \; L \; a_m \qquad (5)$$

where *L* is the Avogadro number.

Langmuir's kinetic model [37] can be incorporated to the BET theory for multilayer adsorption analysis. In the multilayer adsorption it is assumed in the first layer of molecules are located on a set of equivalent surface sites and act as sites for the second layer. Additional assumptions were made to derive an isotherm equation, (i) adsorption–desorption conditions are identical for all layers excluding the first layer, (ii) The energy of adsorption and desorption is equal to the condensation energy and (iii) when $p = p_o$, the multilayer has infinite thickness. These assumptions led to the birth a simplified BET linear equation,

$$\frac{\frac{p}{p_o}}{n^a\left(1-\frac{p}{p_o}\right)} = \frac{1}{n_m^a c} + \frac{c-1}{n_m^a c}\frac{p}{p_o} \qquad (6)$$

P_0 Saturation vapour pressure of the adsorptive

P Equilibrium Pressure

n_m^a Monolayer capacity

n^a Amount of gas adsorbed per unit mass of adsorbent

C Value which gives indication of isotherm shape and the order of magnitude of the adsorbent-adsorbate interactions. This value can be determined mathematically from the isotherm plots.

2.4.4. Fourier Transform Infrared Spectroscopy (FT-IR)

Infrared spectroscopy is one of the techniques that is commonly used to identify the acidity of zeolites. It is considered to be a direct method for characterization of the H^+-form of a zeolite specifically focusing on the OH stretch frequencies. Other spectrocopic changes may also be observed when small probe molecules are absorbed hence yielding useful information regarding the zeolite sample that is investigated. The IR spectroscopic technique is simmilar to temperature programme desorption (TPD) which allows one to look at the interaction of hydroxyl groups present with basic probe molecule, hence allowing the determination of the type of acid sites and the acid strength [38].

2.5. AROMATIZATION OF ALKANES OVER H-ZSM-5 ZEOLITE CATALYSTS

The aromatization of alkanes was discovered by Csicsery in the early 1970s. This reforming process used a dual-function catalyst having dehydrogenating and acid properties that catalyze the dehydrocyclodimerization of light alkanes, into aromatics. The catalysts that were used were platinum-Al_2O_3 and chromia-Al_2O_3. The problem with these catalysts was low selectivity towards aromatics and low conversions that were observed due to deactivation of the catalyst [39]. Great interest has been shown in the development of high selectivity catalysts for the transformation of alkanes into more valuable organic compounds. So, Mobil introduced high a silica zeolites, viz. ZSM-5, to enhance the selectivity of the catalysts. This zeolite type has been used in a number of different commercial reactions, such as conversion of methanol and ethanol

to gasoline and aromatics [40], alkylation of benzene [41], isomerization of xylenes [42], etc. The H-ZSM-5 zeolite was found to be the most suitable catalyst for aromatization of alkanes. H-ZSM-5 is a strong acidic catalyst and possesses a very narrow acid strength which is an important factor in simplifying kinetic analysis and shape selective effects due to the molecular sieving properties associated with well-defined crystal pore sizes [43].

Processes such as M-2 Forming, Cyclar and Aroforming have been used for the transformations of these alkanes into more useful aromatic compounds, mainly BTX. M-2 Forming is the Mobil technology used in conversion of light alkanes into BTX over a H-ZSM-5 zeolite catalyst. Unfortunately, the unmodified H-ZSM-5 suffers fast deactivation and possesses substantial cracking activity that leads to a large selectivity for C_1 and C_2 products. However, the problem is overcome by adding activating agents which are transition metals such as such as Cr, Cu, Fe, Ga, Mn, Mo, Ni, Os, Pt, V, W and Zn. These metals were added in the form of extra-framework species to facilitate the dehydrogenation function [44-46]. Gallium, platinum and zinc appeared to more active and selective. However, gallium and zinc were found to be more advantageous over platinum [47]. Platinum has a high activity for the dehydrogenation of paraffins. Loading platinum increases considerably the conversion of alkanes into aromatics. However, the aromatization reaction is accompanied by the production of unreactive alkanes, methane and ethane through hydrogenolysis, hydrogenation, and dealkylation reactions [48]. The improved activity and selectivity due to the addition of extra-framework species has made possible commercial application of the other processes mentioned above i.e. Cyclar and Aroforming.

2.5.1. Mechanistic Steps in the Aromatization of Alkanes over H-ZSM-5

Conversion of alkanes into aromatic compounds involves a number of mechanical steps that are facilitated by Lewis and Brønsted acid sites. The dehydrogenation and cracking activities of the catalysts has to be taken into consideration during preparation of H-ZSM-5 catalysts [49]. These activities can be altered by loading metal promoters that enhance the Lewis character of the catalysts. The introduction of metal species on H-ZSM-5 increases the rate and selectivity of

aromatization reactions by inhibiting the cracking side reaction from occurring rapidly leading to loss of carbon to undesired products.

Much work has been done on the aromatization of light alkanes, and most researchers report that the aromatization of light alkanes occurs in two stages; formation of alkenes from the starting alkane and transformation of alkenes into aromatic compounds. However, there are a number of reactions that occur in between the reactant and final products, such as protolysis of alkanes, cracking of carbonium ions that form alkanes and alkenes, oligomerization of alkenes, cyclization of oligomerized products and aromatics formation from cyclic rings by hydrogen transfer [50]. Nguyen et al. [51] summarized the mechanism of aromatization of alkanes as occurring in three steps as shown in Figure 2.7:

- transformation of alkanes into alkenes
- interconversion of alkenes
- alkene aromatization

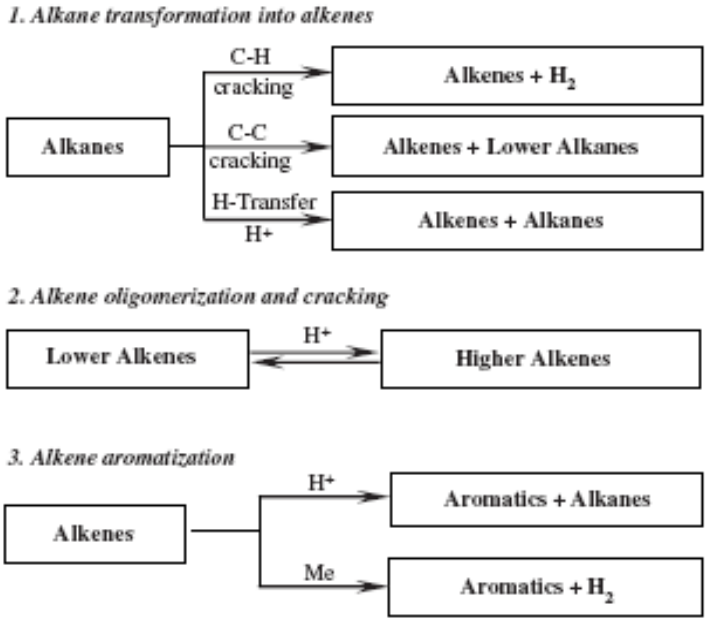

Figure 2.7: Reaction mechanism of alkane aromatization over metal promoted H-ZSM-5 catalysts [51].

The first step is the transformation of an alkane occurring in two routes cracking and hydrogen transfer (dehydrogenation). The hydrogen transfer route involves the reaction between the alkane with the product alkane adsorbed on the acid sites of zeolites. The interconversion step includes isomerization of alkenes, oligomerization and cracking steps. The third step, aromatization of alkenes produced by H-ZSM-5 during interconversion of alkene, the aromatization route, proceeds via cyclization and dehydrogenation reactions.

Gallium and zinc supported on H-ZSM-5 were found to be exceptionally effective catalysts for aromatization reactions. However, only a few papers have reported on the mechanistic reaction of n-hexane over H-ZSM-5 and the role of metal cations. More has been done on the aromatization of propane and butane to investigate the role of gallium and zinc metal species in H-ZSM-5 catalysts. Kanai and Kawata [52] reported that the aromatization of n-hexane over Zn/H-ZSM-5 can be considered to be a bifunctional process where zinc species act as dehydrogenating sites catalyzing the initial reaction of n-hexane to hexane and of oligomerized products to aromatics. Gnep et al. [53] studied the role of gallium for the reaction, and they concluded that gallium catalyzes the dehydrogenation reaction. Inui et al. studied the activity and selectivity of Pt ion-exchanged Ga-silicate and their results showed that Pt promoted the conversion of paraffin to olefins by dehydrogenation and Ga promoted the selective conversion of the produced olefin to aromatics and reduced the rate of coke formation [54].

The dehydrogenation character of zinc and gallium was studied in the aromatization of propane. Biscardi and Iglesia reported that introduction of zinc and gallium enhanced the conversion of propane to proplyene by removing H-atoms from acid sites that activate C-H bonds, allowing acid sites to turnover without the formation of cracking products. Ga and Zn act as portholes [55] and catalyze the re-combinative desorption of H-atoms, formed from acid catalyzed C-H

bond cleavage as H_2. The removal of H_2 was reported to be beneficial in minimizing the formation of the unwanted by-products such as methane and ethane [56].

2.5.2. Aromatization of Alkanes over Gallium based H-ZSM-5 zeolite catalysts

Aromatization of alkanes has been extensively studied over gallium based ZSM-5 type zeolites, viz. physically mixed Ga_2O_3 and H-ZSM-5, Ga-exchanged or impregnated HZSM-5, H-Gallosilicates (H-GaMFI) and H-Galloaluminosilicates (H-GaAlMFI). The high aromatization activity of Ga-modified ZSM-5 type catalysts arises due to the bifunctional nature of these zeolites. This is manifested by the high dehydrogenation function due to the gallium species in combination with zeolitic protons. Among the gallium modified zeolites, the H-Galloaluminosilicates (H-GaAlMFI) showed high activity and selectivity for n-hexane [57] and n-heptane [58]. This superior performance has also been reported for the aromatization of propane [59]. The high performance of these Ga-zeolites can be attributed to the presence of highly dispersed gallium oxide species in close vicinity to zeolitic acid sites. The high dispersion of gallium oxide species is expected due to degalliation during thermal treatment.

Kitagawa et al. [60] studied the aromatization of propane over a gallium modified H-ZSM-5 zeolite catalyst. Their gallium samples were prepared by an ion-exchange method made from a $Ga(NO_3)_3.9H_2O$ solution. The results showed that the conversion of and selectivity to aromatic compounds of Ga-exchanged H-ZSM-5 catalysts increased with gallium content reaching a value corresponding to 100% ion-exchange. Further increase in gallium content only caused a slight increase in conversion and selectivity to aromatic compounds.

Nash et al. [61] investigated the effect of preparation method on the aromatization of long carbon chain compounds i.e. 1-hexene and octane. They used gallium modified H-ZSM-5 catalysts prepared by impregnation (imp), ion-exchange (ix) with gallium nitrate and by physical mixing (mix) with β-gallium oxide crystallites. The conversion of feedstock was reported to be 100% at reaction temperatures above 350^{o}C. The Ga(mix), Ga(imp) and Ga(ix) catalysts showed aromatic

selectivity above 20% despite their differences in preparation and the actual amounts of gallium loaded on of H-ZSM-5. The gallium loading for Ga(ix) was 18 wt% as opposed to 5 wt% for other Ga/H-ZSM-5 samples. The fact that Ga(ix) exhibited similar aromatic selectivity to the other Ga/H-ZSM-5 catalysts is parallel to the results reported by Kitagawa [60], who showed that aromatic selectivity increased with increasing gallium loading until the gallium content reaches the value that correspond to 100% ion exchange capacity. They then concluded that varying the method of preparation does not change the product selectivity as long as there was intimate mixing and good dispersion of gallium species.

Hydrogen pretreatment of gallium catalysts improved the performance of the Ga(mix) by increasing the dispersion of gallium species. This was due to the change in nature of gallium species present, that is, the reduction and the migration of the gallium species in the interior of the zeolite crystals [62]. However, for the catalysts in which the gallium was already dispersed hydrogen pretreatment had a negative effect due to the reduction of Ga^{3+} which is considered as the most active gallium species to less active Ga^{1+}.

The influence of preparation method was also investigated by Bayense and van Hooff [63]. They studied the aromatization of propane over gallium containing H-ZSM-5 catalysts prepared by impregnation and physical mixing methods. Their reactions were carried out at temperatures between 350 and 600^{o}C. From the results they concluded that the cavity of the catalysts was independent on the method of preparation. However, the presence of gallium enhanced the aromatic selectivity from 35 to 60%, and these measures were taken at 80% conversion. The activity of the catalysts showed a decrease with time-on-stream and the catalyst prepared by impregnation showed a comparable deactivation with that prepared by physical mixing. The rate of coke formation increased with the degree of isomorphous substitution of gallium in the framework, while much higher rates of coke formation were observed for the physically mixed sample.

The incorporation of gallium in a zeolite framework by substituting Al with Ga species has led to enhancement of the dehydrogenation activity of alkanes with the catalyst having much increased selectivity for the formation of aromatics from lower alkanes. Other researchers have reported that the high dehydrogenation activity of Ga/H-ZSM-5 is due to the presence of non-framework gallium species formed by its degalliation during calcination or pretreatment steps [64]. Choundry et al. [65] and Nishi et al. [66] studied the influence of Si/Ga ratio on the activity and deactivation during the aromatization of propane. The Si/Ga ratio for the investigated catalysts ranged from 12.5 to 129.6. The increase in gallium content led to an increase in zeolitic acidity and the extra framework Ga_2O_3 increased with increase in calcination temperature. At high gallium loading they observed low conversion of propane and in the case of low gallium content the conversions were high. These were attributed to the decrease in the acid amount due to the extraction of gallium from the MFI-framework.

Kanai and Kawata [67] studied the aromatization of *n*-hexane over gallosilicate, galloaluminosilicate and Ga_2O_3/H-ZSM-5 catalysts to promote the dehydrogenation of *n*-hexane to hexane then into the aromatic compounds. For the conversion of *n*-hexane over Ga_2O_3/H-ZSM-5 catalysts they observed a conversion of 100% in all experiments and the yield of aromatics increased with increase in Ga_2O_3 content up to 1.5 wt%. The hydrogen production was interrelated with aromatic selectivity and Ga_2O_3 content. The *n*-hexane conversion and specific surface area decreased with increase in Ga_2O_3 content in the zeolite catalysts. They suggested that the loading of Ga_2O_3 on the external surface area of H-ZSM-5 and low dispersion caused the pore blockages, and hence a decrease in n-hexane conversion.

The aromatization of n-hexane was studied on gallosilicate catalysts i.e. H-Si-Ga, H-Si-Ga pretreated with HCl solution and Ga^{3+}-exchanged H-Si-Ga pretreated with HCl. H-Si-Ga showed a high activity for the aromatization of n-hexane whereas H-Si-Ga (HCl) containing 3 wt % of gallium content showed much less activity prepared than samples by different methods. The activity was enhanced by addition of a small amount of Ga^{3+} (0.7 wt%). This suggested that the active gallium species are not in the framework but outside the framework. The effect of

HCl pretreatment was studied by Scherser and Bass [68] and they reported that aluminum species outside the framework are more easily removed by HCl acid than those incorporated in the framework structure. This agrees with the low activity of H-Si-Ga pretreated with HCl acid, because the non-framework gallium species of H-Si-Ga were removed by HCl acid during washing.

2.5.3. Aromatization of Alkanes over Zinc based H-ZSM-5 Zeolite Catalysts

Mole and Anderson [69] investigated the conversion of propane to aromatic compounds at temperatures in the range 457 to 547^{o}C over zinc modified H-ZSM-5 catalysts prepared by ion-exchange. They observed the propane conversion to be significant for both H-ZSM-5 and Zn/H-ZSM-5 at a reaction temperature of 457^{o}C. The Zn/H-ZSM5 catalysts showed better BTX selectivity between 60 and 70% and other products were formed C_1 and C_2 hydrocarbons and C_{9+} aromatics. The total conversion of propane was improved by the addition of zinc or gallium species in the zeolite, with a BTX selectivity of 35.6% obtained with a 1.3 wt% Zn/H-ZSM-5 catalyst [70].

Heemsoth et al. [71] studied the aromatization of ethane over zinc modified H-ZSM-5 catalysts, prepared by solid state reduction mixing and impregnation methods. The catalyst prepared by the impregnation method was used as a reference. The conversion of ethane was observed to be 21% at 550^{o}C and the BTX selectivity was 57% for both Zn/H-ZSM-5 catalysts. The results showed that the solid state prepared catalyst exhibits the same properties as the one prepared by the impregnation method.

The preparation methods have an effect on the structure and location of the zinc species inside or outside the channels of the zeolites. The structure of the zinc species formed during catalyst preparation was studied by Biscardi and Iglesia [72]. They observed that the impregnation method led to the formation of both exchanged Zn cations and extracrystalline Zn-O crystals. At

higher loading the Zn impregnated catalyst contains small fraction of Zn-Zn next nearest neighbours, consistent with the presence of external ZnO crystals. These extracrystalline ZnO particles are poorly dispersed and do not significantly contribute to the conversion of alkanes or to recombinative hydrogen desorption. The catalysts prepared by ion-exchange contain only Zn-O species nearest neighbours, suggesting that Zn is present as isolated Zn species at the zeolitic exchange site. Direct exchange is possible because of the smaller coordination sphere of the divalent cations such as Zn^{2+}.

Berndt et al. [73] investigated the influence of the method preparation on the conversion of propane over a zinc modified zeolite catalyst. The Zn/H-ZSM-5 catalysts were prepared by ion-exchange and impregnation methods using a zinc nitrate solution. They observed that the activity of the catalysts was affected by the method of preparation. The catalyst prepared by ion-exchange was observed to exhibit higher activity than the impregnated catalysts. Biscardi and Iglesia [72] attributed the low activity of impregnated catalyst to the presence of ZnO species formed during synthesis. These are responsible for blocking the channels of the zeolite and preventing access to some acid sites.

The properties (size, shape and aluminium distribution) of zeolites have an influence on the activity and selectivity in aromatization of alkanes. The activity and selectivity of Zn/H-ZSM-5 catalysts with loadings between 0.04 to 0.369 mmol Zn/g zeolite prepared by ion-exchange from two samples of H-ZSM-5 having different size particles ($\leq$1 and $\geq$ 4 μm) were investigated. The aromatization of *n*-hexane over H-ZSM-5 is affected by the particle size of the zeolite. The activity/selectivity of the monofunctional acid catalyst is significantly higher on the H-ZSM-5 with particle size $\leq$ 1μm. The selectivity towards BTX increased as Zn species were introduced and increase in concentration. At higher concentration of Zn species the catalytic performance of Zn/H-ZSM-5 is different, probably due to the fact that Zn species are different in H-ZSM-5 at high concentrations [74], as highlighted by Bisarcadi and Iglesia [72]

The Smieskova and Rojasova group [75, 76] focused on the role of Zn in the aromatization of light alkanes using the probe molecules *n*-hexane, hexene and cyclohexane. From the IR results

they observed that zinc in the cationic position represented the Lewis acid sites and the NH_3-TPD measurements revealed that the portion of ammonia adsorbed above 450^oC from Zn/H-ZSM-5 increased compared with H-ZSM-5. The catalytic results showed that for H-ZSM-5 without zinc being loaded, the BTX yield from the conversion of 1-hexene and cyclohexane was very significant but for n-hexane the formation of BTX was low. The conversion of n-hexane over Zn/H-ZSM-5 increased compared to that of the H-ZSM-5 catalyst and the production of BTX products on Zn/H-ZSM-5 is many times higher. The increase in the production of aromatic compounds was attributed to the high concentration of olefins formed during the reaction. From the results with cyclohexane on Zn/H-ZSM-5 catalyst, they concluded that the Zn species possess high dehydrogenation activity for converting cyclic intermediates into aromatic compounds. They compared the production of benzene from *n*-hexane and cyclohexane. The concentration of benzene from the aromatization of cyclohexane was found to higher than *n*-hexane. On the Zn/H-ZSM-5 catalyst the transformation of cyclic intermediates into the corresponding aromatics proceeds also by a direct dehydrogenation reaction.

Furthermore, they studied the effect of activating the Zn/H-ZSM-5 catalyst with hydrogen and air. An increase in the activity and selectivity was observed for the catalysts activated with hydrogen when compared with the activity and selectivity of that activated with air. They attributed the increase in activity to the partial reduction of Zn^{2+} cations and as a result the hydro-dehydrogenation activity of the catalyst increased.

2.5.4. Aromatization of Alkanes over Molybdenum based H-ZSM-5 Zeolite Catalysts

Molybdenum-based ZSM-5 catalysts have been regarded as the best catalysts for the aromatization of methane. In 1993 a Chinese group [77] studied the dehydrogenation and aromatization of methane on modified ZSM-5 zeolite catalysts under non-oxidizing conditions. They observed that a MoO_3/H-ZSM-5 catalyst can transform methane into benzene with 80-100% selectivity at a conversion of 10-12%. These findings led to subsequent studies in aromatization of long chain alkanes. Wang and co-workers [78] studied the aromatization of

propane over Mo/H-ZSM-5 catalysts prepared by impregnation, mechanical mixing and hydrothermal treatment methods. It was reported that the hydrothermal treated catalyst showed high selectivity toward aromatics and activity towards propane conversion. This was attributed to the fact that the hydrothermal treatment method favored the dispersion of Mo species on H-ZSM-5, which promoted the penetration of Mo species into the HZSM-5 channels.

Methane, which is regarded as a very stable compound, is converted into benzene by Mo/H-ZSM-5 catalysts at temperatures above 700^{o}C. The mode of action is said to involve the formation of molybdenum carbide species for the methane activation. Solymosi et al. [78, 79] studied the aromatization of *n*-heptane and *n*-octane over MoC_2 catalysts supported on different supports, viz. H-ZSM-5, SiO_2 and Al_2O_3. The results showed that MoC_2 catalyzed the dehydrogenation and aromatization of *n*-heptane and *n*-octane at 350-500^{o}C. The selectivity to aromatics was measured to be 51% at a conversion of 23% for *n*-heptane, and for *n*-octane aromatic selectivity reached 23% at conversion of 33%. The catalytic performance of MoC_2 was considerable enhanced when it was dispersed on H-ZSM-5, SiO_2 and Al_2O_3. The MoC_2/H-ZSM-5 catalyst showed high performance with a yield of aromatics for *n*-heptane and *n*-octane of 48% and 50-55% respectively.

2.6. BRIEF SUMMARY OF THE LITERATURE REVIEW

In general, the incorporation of gallium and zinc species into catalysts increased the catalytic activity and BTX selectivity by the enhancement of the dehydrogenation activity. However, at a higher metal loading a decrease in catalytic activity has been reported. The method of preparation was found to be influenced by the behavior of catalysts by dictating the nature and location of gallium, zinc or molybdenum species present in the channels of the zeolite.

Other researchers focused on the effect of the added metal in the conversion of alkanes to aromatic compounds. It was found that the metal species facilitate the activation of alkane by

extraction of hydrogen from alkane to form alkene. This was considered to be the rate limiting step for the aromatization of alkanes. It was concluded that the aromatization of alkanes follows a bifunctional mechanism.

2.7. REFERENCE LIST

[1] D.S. Coombs, A.J. Ellis, W.S. Fyfe and A.M. Taylor, *Qeochimlca et Cosmochimica Acta*, **17** (1957) 53.

[2] R.M Barrer, *Hydrothermal Chemistry of Zeolites*, Academic Press, London (1982) p 35.

[3] G. Gottardi and E. Galli*, Natural Zeolites*, Springer-Verlag Berlin Heidelberg (1985) p. 1.

[4] A. Chatterjee, D. Bhattacharya, M. Chatterjee and T.Iwasaki, *Microporous and Mesoporous Mater.*, 32 (1999) 189.

[5] J. Wietkamp, *Solid State Ionics*, **131** (2000) 175.

[6] D.H. Everett, *Pure Appl. Chem*., **31** (1972) 585.

[7] S.M. Csicsery, *Zeolites*, **4** (1984) 202.

[8] M. Stocker, *Microporous and Mesoporous Mater.*, **82** (2005) 257.

[9] S. B. Semosa, MSc Thesis, University of the Witwatersrand, Johannesburg (2005).

[10] B. Sulikowski and J. Klinowski, *Appl. Catal. A: General*, **89** (1992) 69.

[11] T. R Keshav, S. Basu, *Fuel Processing Technology,* **88** (2007) 493.

[12] D.P. Serrano, R. Van Grieken, P. Sánchez, R. Sanz and L. Rodríguez, *Microporous and Mesoporous Mater.*, **46** (2001) 35.

[13] N. Murayama, H. Yamamoto and J. Shibata, *Int. J. Miner. Process*, **64 (**2002) 1.

[14] W.C. Wong, L.T.Y. Au, C.T. Ariso and K. L. Yeung, *J. Membrane Science* **191** (2001) 143.

[15] A.V. Goretsky, L.W. Beck, S.I. Zones and M.E. Davis, *Microporous and Mesoporous Mater.*, **28** (1999) 387.

[16] C.N. Mbileni, PhD. Thesis, University of the Witwatersrand, (2006).

[17] N. Burriesci, L.M. Saija, R. Ottana, N. Giordano, J.C.J. Bart, *Materials Chemistry and Physics*, **8** (1983) 305.

[19] T. Chen, A. Men, P. Sun, J. Zhou, Z. Yuan, Z. Guo, J. Wang, D. Ding, H. Li, *Catal. Today*, **30** (1996) 189.

[20] C. D. Chang and A.J. Silvestri, *J. Catal*., **47** (1977) 249.

[21] B. Sulikowskil and J. Klinowski, *Appl. Catal. A: General,* **89** (1992) 69.

[22] http://www.mf.mpg.de/de/abteilungen/mittemeijer/english/commentary/Powder%20Diffraction%20in%20Mat.Sci.pdf. 30/09/2008

[23] W. Robert and F.R.S Cahn, Concise Encyclopedia of Material Characterization, **2nd** Edition, Elsevier (2005), p. 983.

[24] T.A.J. Hardenberg, L. Mertens, P. Mesman, H.C. Muller, and C.P. Nicolaides, *Zeolites*, **12** (1992) 685.

[25] C.P. Nicolaides, M.S. Scurrell, *Appl. Catal*., **55** (1989) 259.

[26] H. Knözinger in Handbook of Heterogeneous Catalysis, G. Ertl, H. Knözinger and J. Weitkamp, eds, **Vol. 2**, Wiley-VCH, 1997, Weinheim, 676.

[27] G. Leofanti, G. Tozzola, M. Padovan, G. Petrini, S. Bordiga and A. Zecchina, *Catal. Today*, **34** 1997 307.

[28] J.G. Post and J.H.C. van Hooff, *Zeolites,* **4** (1984) 9.

[29] G.L. Woolery, G.H. Kuehl, H.C. Timken, A.W. Chester and J.C. Vartuli, *Zeolites*, **19** (1997) 288.

[30] S Besselmann, C Freitag, O Hinrichsen and M Muhler, *Phys. Chem. Chem. Phys*., **3** (2001) 4633.

[31] N.W. Hurst, S.J. Gentry, A. Jones and B.D. McNicol, *Catal. Rev.-Sci. Eng*., **24** (1982) 233.

[32] N.A. Seaton, *Chem. Eng. Sci*., **46** (1991) 1895.

[33] M. Thommes, *Zeolites and Ordered Mesoporous Materials by Physical Adsorption*, Quantachrome Instruments, Boynton Beach, FL, USA, p 495-523.

[34] P.E. Hatahway and M.E. Davis, *Catal. Lett*., **5** (1990) 333.

[35] M. Thommes, R. Kohn and M. Froba, *J. Phys. Chem. B,* **104** (2000) 793.

[36] J.C. Groen, L.A.A Peffer and J Pérez-Ramírez, *Microporous and Mesoporous Mater.*, **60** (2003) 1.

[37] S. Brunauer, P.H. Emmett and E. Teller, *Phys. Chem.*, **60** (1938) 309.

[38] S.M. Csicsery, *Catal. Today*, **18** (1970) 30.

[39] S.M. Campbell, D.M. Bibby, J.M. Coddington and R.F. Howes, *J. Catal*., **161** (1996) 350.

[40] X. Cheng, S. Huang, D. Cao and W. Wang, *Fluid Phase Equlibrium*, **260** (2007) 146.

[41] T. Tsai, I. Wang, C. Huang and S. Liu, *Appl. Catal A: General*, **321** (2007) 125.

[42] X. Wang, H. Carabineiro, F. Lemos, M.A.N.D.A Lemos and F. Ramona Riberio, *J. Mol. Catal. A: Chemical*, **216** (2004)131.

[43] Y. Xu and L. Lin, *Appl. Catal.*, **188** (1999) 53.

[45] Y. Shu and M. Ichikawa, *Catal. Today.*, **71** (2001) 55.

[46] Y. Xu, X. Bao and L. Lin, *J. Catal.*, **216** (2003) 386.

[47] M.G. Sanchez, Characterization of Gallium-containing Zeolites for Catalytic Application, PhD Thesis, Eindhoven University of Technology, Netherlands, (2003).

[48] P. Meriaudead and C. Naccache, *Catal. Rev-Sci.Eng.*, **39** (1997) 5.

[49] A. Smieskova, E. Rojasova, P. Hudec and L. Saboet al. *React. Kinet. Catal. Lett*., **82** (2004) 227.

[50] M. Guisnet and N.S. Gnep, *Appl. Catal. A: General*, **146** (1996) 33.

[51] L.H. Nguyen, T.Vazhnova, S.T. Kolaczkowski and D.B. Lukyanov, *Chem. Eng. Sci*., **61** (2006) 5881.

[52] N.S. Gnep, J.Y. Doyement and M.R. Guisnet, *J. Mol. Catal*., **45** (1988) 281.

[53] M.A. Kohler, M.S. Wainwright, D.L. Trimm, and N.W. Cant, *Ind. Eng. Chem. Res.*, **26** (1987) 652.

[54] I. Nakamura and K. Fujimoto, *Catal. Today*, **31** (1996) 335.

[55] J.A. Biscardi and E. Iglesia, *Catal. Today*, **31** (1996) 207.

[56] V.R. Choudhary, S.A.R. Mulla and S. Banerjee, *Microporous and Mesoporous Mater.,* **57** (2003) 317.

[57] T.V. Choudhary, A. Kinage, S. Benerjee and V.R. Choudhary, *Microporous and Mesoporous Mater.*, **83** (2005) 23.

[58] J. Kanai and N. Kawata, *Appl. Catal.,* **55** (1989) 115.

[59] V.R. Choudhary, S.A.R. Mulla and S. Banerjee, *Microporous and Mesoporous Mater*., **57** (2003) 317.

[60] H. Kitagawa, Y. Sendoda and Y.Ono, *J. Catal*., **101** (1986) 12.

[61] R.J. Nash, M.E. Dry and C.T. O'Connor, *Appl Catal A: General*, **134** (1996) 285.

[62] G.L. Price and V. Kanazirev, *J. Mol. Catal*., **66** (1991) 115.

[63] C.R. Bayense and J.H.C. van Hooff, *Appl. Catal. A: General*, **79** (1991) 127.

[64] E.G. Derouane, S.B.A. Hamid, I.I. Ivanova and P.E.H Nielsen, *J. Mol. Catal.,* **86** (1994) 371.

[65] V.R. Choudhary, A.K. Kinage, C. Sivadinarayana, P. Devadas, S.D. Sansare and M. Guisnet, *J. Catal*., **158** (1996) 34.

[66] K. Nishi, S. Komai, K. Inagaki, A. Satsuma and T. Hattoriet, *Appl. Catal. A: General*, **223** (2002) 187.

[67] J. Kanai and N. Kawata *Appl. Catal*. **55** (1989) 115.

[68] J. Scherzer and J.L. Bass*, J. Catal*., **46** (1977) 10.

[69] T. Mole and J.R. Anderson, *Appl. Catal*., **17** (1985) 141.

[70] N. P. Sincadu, PhD Thesis, University of the Witwatersrand, Johannesburg (2003).

[71] J. Heemsoth, E. Tegeler, F. Roessner and A. Hagen, *Microporous and Mesoporous Mater*., **46** (2001) 185.

[72] J. A. Biscardi and E. Iglesia, *Catal. Today*, **31** (1996) 207.

[73] H. Berndt, G.Lietz, B. Lucke and J. Volter, *Appl. Catal. A: General*, **146** (1996) 315.

[74] A. Smieskova, E. Rojasova, P. Hudec and L. Sabo, *Appl. Catal. A: General,* **268** (2004) 235.

[75] E. Rojasova, A. Smeiskova, P. Hudec, Z. Zidek, *React. Kinet. Catal. Lett*., **66** (1999) 91.

[76] L. Wang, L. Tao, M. Xie and G. Xu, *Catal. Lett.,* **21** (1993) 35.

[77] J. Wang, M. Kang, Z. Zhang and A. Wang, *J. Nat. Gas Chem*., **11** (2002) 43.

[78] R. Barthos and F. Solymosi, *J. Catal*., **235** (2005) 60.

[79] A. Szechenyi and F. Solymosi, *Appl. Catal A: General*, **306** (2006) 149.

Chapter 3

Experimental

3.1. REAGENTS

Table 3.1 Reagents that were used in the preparation of catalysts and catalytic reactions are shown below.

Reagent	Supplier
Fumed silica Aerosil 200	Degussa
Aluminium hydroxide	Fluka
Sodium hydroxide	Saarchem
Tetrapropylammonium bromide (TPABr)	Fluka
Silver nitrate	Aldrich
Ammonium heptamolybdate	Saarchem
Gallium nitrate	Aldrich
Zinc Nitrate	Aldrich
n-Hexane	Aldrich

3.2. CATALYST PREPARATION

3.2.1. Preparation of H-ZSM-5 zeolite catalysts

The H-ZSM-5 zeolites were synthesized by a hydrothermal treatment method [1, 2] varying the synthesis temperature between 90 and 150^{o}C so as to obtain samples of different percentage crystallinity. The SiO_2/Al_2O_3 ratio was kept constant at 70. The MFI structure and percentage of the H-ZSM-5 zeolite was confirmed by powder-XRD.

A sodium aluminate solution was prepared by mixing 17.9 g of NaOH with 2.98 g of $Al(OH)_3$ in 75 ml of distilled water. The mixture is then heated and stirred to obtain a clear solution. The template solution was prepared by dissolving 29.7 g of tetrapropylammonium bromide (TPABr) in 75 ml of distilled water. A slurry of fumed silica was prepared by mixing 80.4 g of Aerosil 200 with 650 ml distilled water. And a Kenwood blender was used to stir the mixture until a smooth jellylike form was consistently obtained.

The sodium aluminate and template mixtures were then added to the silica slurry under vigorous stirring and the mixture was transferred to an autoclave equipped with a 1 litre Teflon vessel. The contents were allowed to crystallize at a specific temperature, for 72 hours, under stirring conditions.

After the hydrothermal treatment, the autoclave contents were filtered and washed with deionised water until the filtrate was bromide and hydroxide free. This was detected by using a silver nitrate solution. The resulting product was then dried at 120^{o}C for 16 hours and calcined at 630^{o}C for 3.5 hours to remove the template. The resulting product is Na-ZSM-5.

To obtain the NH_4-ZSM-5 form of the zeolite, the calcined Na form of the zeolite was treated with a 1M NH_4Cl solution at room temperature under stirring conditions for 1 hour. The contents were filtered and washed to remove the chloride ions. The sample was further calcined at 530^{o}C for 3 hours to obtain the acidic form of the zeolite i.e. H-ZSM-5.

3.2.2. Preparation of metal modified H-ZSM-5 zeolite catalysts using the impregnation method

The preparation of Mo/HZSM-5, Ga/H-ZSM-5 and Zn/H-ZSM-5 catalysts involved the impregnation of H-ZSM-5 (SiO_2/Al_2O_3) using the incipient wetness impregnation method with solutions of ammonium heptamolybdate $(NH_4)_6Mo_7O_{24}\cdot H_2O$, gallium nitrate $Ga(NO_3)_3.8H_2O$ and zinc nitrate $Zn(NO_3)_2.6H_2O$ respectively at appropriate concentrations. The samples were then dried overnight at 120^oC and calcined at 500^oC for 6 hours.

3.3. CHARACTERIZATION OF CATALYSTS

The catalysts were characterized by the various techniques presented in the following subsections.

3.3.1. Fourier Transform Infra Red (FT-IR) Spectroscopy

The infrared framework spectra were obtained by using a Brucker Tensor 27 FT-IR spectrometer with maximum resolution of 4 cm^{-1}. The samples were diluted with KCl and pressed into a self supporting disc and then dried at 120^oC for 1 hour. The samples were then analyzed at between 400 and 4000 cm^{-1} at room temperature. The spectral data were collected on the computer equipped with Brucker Opus 4.2 software.

3.3.2. Powder X-Ray Diffraction (XRD)

Powder X-ray diffraction data were collected using a Brucker AXS D8 diffractometer equipped with a primary beam Gobel mirror, a radial Soller slit, a VAntec-1 detector and using Cu-Kα

radiation (40 kV, 40 mA). Data were collected in the 2θ range 5 to 90^{o} in 0.021^{o} steps, using a scan speed resulting in an equivalent counting time of 14.7 s per step.

3.3.3. Ammonia-Temperature Programmed Desorption (TPD)

The NH_3-temperature programmed desorption experiments were performed in a U-shaped quartz tubular reactor charged with 0.2 g sample. The sample was degassed with helium gas flowing at 40 ml/min with temperature increasing to 500^{o}C at a rate of 10^{o}C/min and held at 500^{o}C for 1 hour. It was then allowed to cool down to 100^{o}C under the flow of helium gas. A mixture of ammonia in helium (4%NH_3 balance helium) was passed over the sample for 1 hour at 100^{o}C for the adsorption of ammonia on the surface of the catalyst. Desorption of ammonia was carried out in helium at a flow rate of 40 ml/min while heating the sample from 100 to 700^{o}C at the rate of 10^{o}C/min. The NH_3-TPD profiles were obtained by measuring the amount of ammonia desorbed relative to the temperature, using a thermal conductivity detector.

3.3.4. Hydrogen-Temperature Programmed Reduction (TPR)

Samples of 0.2 g were loaded in a U-shaped quartz tubular reactor and heated under nitrogen gas atmosphere at a rate of 10 °C/min to 500 °C, allowed to settle for 30 minutes, and then cooled to room temperature under nitrogen. When performing the analysis the sample was exposed to a gas mixture of hydrogen and argon (5% H_2 balance argon) at a flow rate of 30 ml/min that was heated to 800 °C at a rate 8 °C/min.

3.3.5. Nitrogen Adsorption (BET) Analysis

BET surface areas were determined using a Micromeritics 3300 series instrument. About 0.2 g of a sample was degassed at 400^{o}C for 4 hours. After the degassing process the samples were then loaded on the analysis station for determination of the isotherms at -195^{o}C.

3.4. CATALYTIC CONVERSION REACTIONS

The conversion of n-hexane as the evaluation reaction was carried out in a fixed bed quartz tubular reactor. A sample of 0.5 g catalyst was loaded to a reactor and pretreated with nitrogen for 1 hour at 500 °C flowing at a rate of 10 ml/min. The purpose of the pretreatment was to remove all the absorbed impurities and the moisture from the catalyst. Finally, the catalyst was exposed to the mixture of pure n-hexane and nitrogen gas at a ratio 1:5, with nitrogen flowing at a rate of 10 ml/min. The products were analyzed using an online HP 5730A Gas Chromatograph equipped with and FID detector and a Supelcoport packed column (6 m x 3 mm) packed column and the results were obtained using Varian 4290 integrator. A typical setup of the reactor system is given in Figure 3.1.

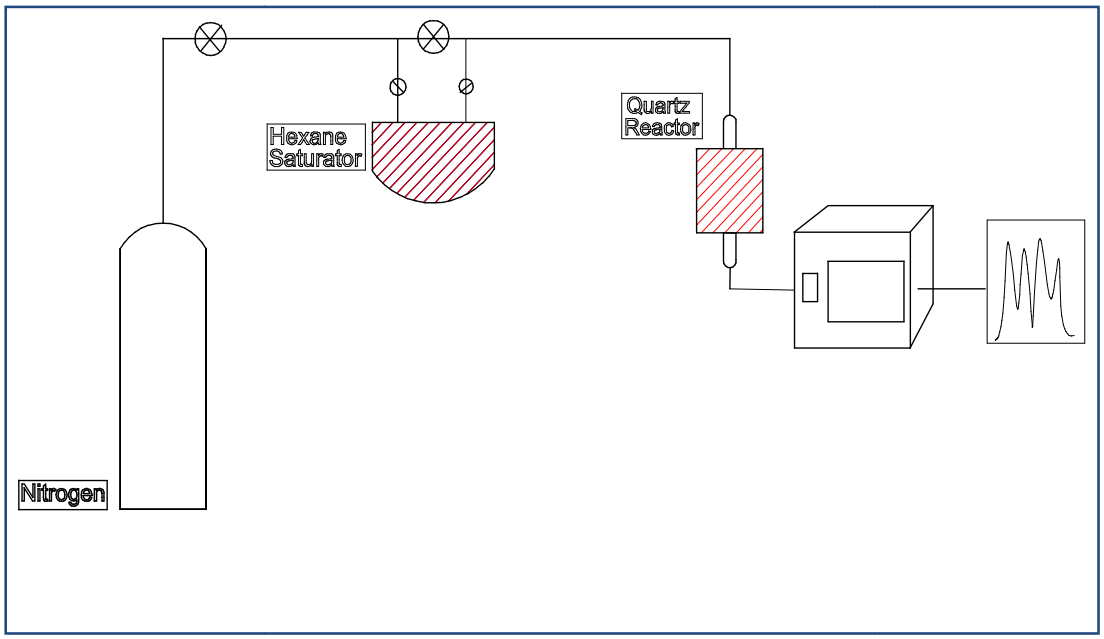

Figure 3.1: The schematic representation of the reactor setup.

The percentage conversion, selectivity and yield of products were calculated using the equations shown below.

$$\%\text{Conversion} = \frac{\%\ \text{Hexane}_{(in)} - \%\ \text{Hexane}_{(out)}}{\%\ \text{Hexane}_{(in)}} \times 100 \qquad 3.1$$

$$\%\ \text{Selectivity} = \frac{\%\ P_i}{\%\ \text{Conversion}} \times 100 \qquad 3.2$$

$$\%\text{Yield} = \frac{\%S_{P_i} \times \%\text{Conversion}}{100} \qquad 3.3$$

3.5. REFERENCE LIST

[1] C. P. Nicolaides, *Appl. Catal. A*, **185** (1999) 211-217.

[2] N.P. Sicandu, PhD Thesis, University of the Witwatersrand, Johannesburg, 2003.

Chapter 4
Results and Discussion

4.1. Introduction

In this chapter we discuss the results on the aromatization of *n*-hexane over H-ZSM-5 zeolite catalysts which were modified by addition of metals i.e. gallium, zinc and molybdenum at different metal loadings. These catalysts were prepared by the incipient wetness impregnation method and calcined at 500^{o}C. The catalysts were further in studied by observing the effect of percentage XRD crystallinity of H-ZSM-5 zeolite samples which were modified by loading 2 wt% of the metal studied on the reaction. The effect of reaction temperature on the aromatization of *n*-hexane between 500 and 600^{o}C was also investigated.

4.2.The Effect of Metal Loading

4.2.1. The Effect of Gallium Loading

The aromatization of *n*-hexane over Ga/H-ZSM-5 (i.e. 66% crystallinity XRD and SiO_2/Al_2O_3 = 70) catalysts prepared by an incipient wetness impregnation method with gallium loadings ranging from 0 to 4 wt% were investigated. The reactions of the aromatization of *n*-hexane were carried out at 500^{o}C and 1 bar pressure. The results of the effect of gallium loading on the surface area and pore volume of H-ZSM-5 samples are shown in the Table 4.1.

Table 4.1: BET surface areas and pore volumes of the calcined Ga/H-ZSM-5 catalysts with different gallium loadings.

Catalysts	BET Surface Area m^2/g	Pore Volume cm^3/g
H-ZSM-5	376	0.28
0.5% Ga/H-ZSM-5	357	0.26
1% Ga/H-ZSM-5	352	0.26
2% Ga/H-ZSM-5	333	0.24
4% Ga/H-ZSM-5	295	0.22

The results show a slight decrease in the surface area and pore volumes of gallium modified H-ZSM-5 catalysts with increase in gallium loading. This pore volume decrease can be attributed to the migration of gallium species into the channels of H-ZSM-5 and leading to the pores being blocked and the decrease in surface areas may be due to the gallium species outside the framework of H-ZSM-5 [1].

The results of the effect of gallium loading on the Lewis and Brønsted acid sites distribution are presented in Figure 4.1 below. It is evident that the addition of gallium in H-ZSM-5 influences the distribution of the acid sites. The TPD profile of H-ZSM-5 has two peaks one at low temperature (LT) 220^{o}C representing the desorption of ammonia from the weak Lewis acid sites and the other at high temperature (HT) 490^{o}C which relates to desorption of ammonia from strong Brønsted acid sites. The intensity of the HT peak decreased with an increase in the gallium loading while the peak at the LT region grew. The band width also widened with increase in gallium loading. It should be noted that at low gallium loading there is no significant change in the temperature of desorption to the LT peak when compared to that at high gallium loading. For the 4%Ga/H-ZSM-5, the intensity of the HT peak decreased and this decrease represents the interaction of the gallium species with the Brønsted acid sites in the channels of H-ZSM-5 decreasing the concentration of Brønsted acid sites.

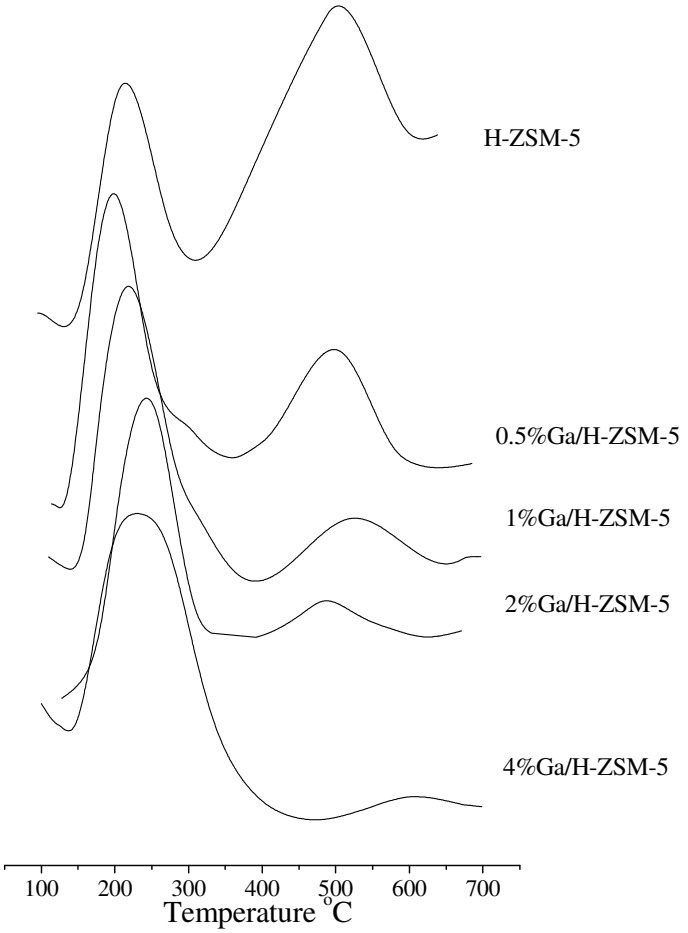

Figure 4.1: NH_3-TPD profiles for Ga/H-ZSM-5 catalysts with different gallium loadings.

The results of the effect of the gallium loading on the catalytic conversion of *n*-hexane studied at a reaction temperature of 500°C are shown in Figure 4.2. The catalytic conversion of *n*-hexane initially increased with the addition of gallium attaining a maximum of 94% conversion at a gallium loading of 0.5 wt%. It then decreased with further increase in the gallium loading. It is worth noting that the conversion of *n*-hexane was within the relative narrow range of 70-94%. The higher activity in *n*-hexane conversion after the addition of gallium can be attributed to the increase in dehydrogenation activity due to the presence of gallium species in the H-ZSM-5 channels [2]. A decrease in conversion observed when the gallium loading was more than 0.5 wt% may attributed to a decrease in the concentration of Brønsted acid sites of the H-ZSM-5 which are occupied by the gallium species in channels of H-ZSM-5 as shown in the ammonia-TPD profiles as shown above in Figure 4.1. The Brønsted acid sites are important for the

facilitation of cracking and cyclization reactions of *n*-hexane and other aromatizable products. And the decrease in the BET surface areas and the pore volumes suggest that high gallium loading resulted in gallium being dispersed on the surface of H-ZSM-5 covering the active sites and blocking the pores of the H-ZSM-5 zeolite. This may also contribute in the decrease in activity for the aromatization of *n*-hexane.

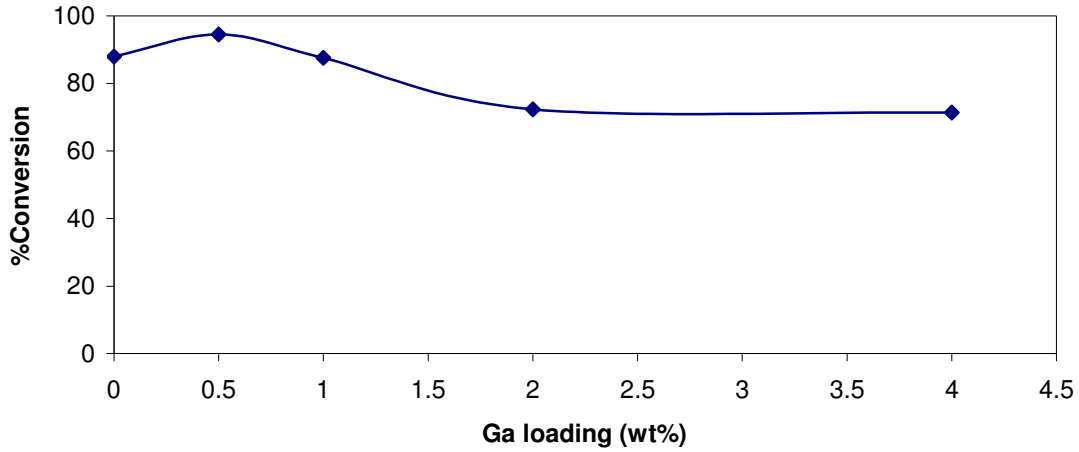

Figure 4.2: The effect of gallium loading on the catalytic conversion of *n*-hexane over Ga/H-ZSM-5 at 500^{o}C taken at time-on-stream of 5 hours.

The stabilities of Ga/H-ZSM-5 catalysts when exposed to *n*-hexane for 12 hours time-on-stream at 500^{o}C are shown in Figure 4.3. The results show that the addition of gallium species has a positive effect on the conversion of *n*-hexane for the catalysts with lower gallium loadings. High conversions raging between 87 and 95% were observed over gallium catalysts with low loadings and this was followed by a subsequent drop to 70% at gallium loadings above 2 wt%. Catalysts with a gallium loading of 1 wt% showed a steady decrease in conversion but later showed a significant decrease after 7 hours on-stream. With further increase in the gallium loading the deactivation of the catalyst became more severe as shown by the rapid decrease in conversion for the catalysts with high gallium loadings. This showed that the catalytic activity of catalysts with low gallium loading is independent of the time. However, as the loading is increased there is some deactivation that is observed for 2 and 4 wt% gallium catalysts. The increased rate of

deactivation of the catalysts can be attributed to deposition of coke on the surface of the H-ZSM-5; at this stage the colour of the catalyst was black. For the catalysts with low gallium loading this was not found to be the case. Lanh et al. [3] reported similar results on catalysts with high loadings of gallium; this was assigned to the increase in amount of non-framework gallium species which are responsible for the strong deactivation by promoting the formation of olefinic compounds which are regarded as coke precursors.

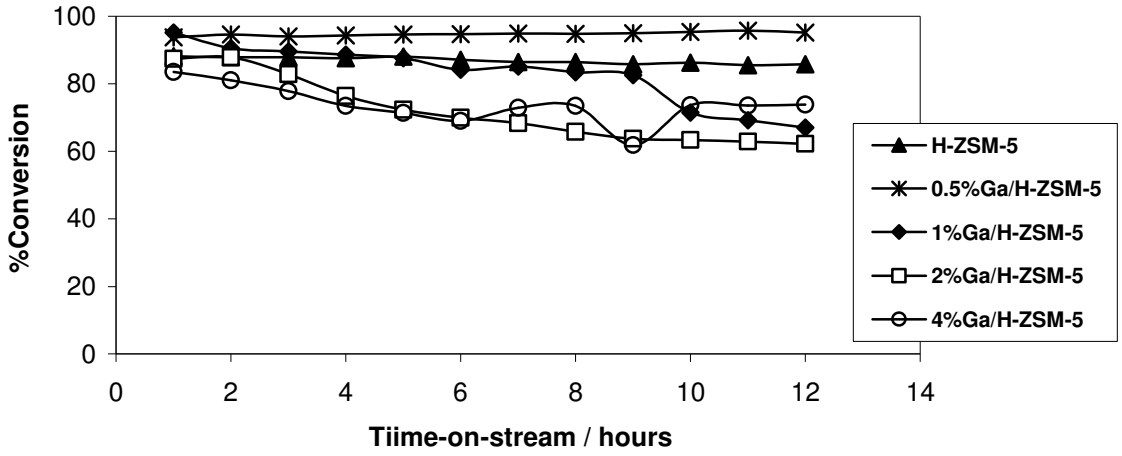

Figure 4.3: The catalytic conversion of *n*-hexane of Ga/H-ZSM-5 with different gallium loading as the function of time-on-stream at 500^{o}C.

The results of the aromatic selectivity of Ga/H-ZSM-5 catalysts with different gallium loadings are presented in Figure 4.4. The aromatic selectivity of gallium loaded H-ZSM-5 catalysts is in the region of 35-42% while the free gallium H-ZSM-5 aromatic selectivity is 25%. Addition of gallium on H-ZSM-5 contributes positively to the enhancement of aromatic selectivity. The formation of aromatic compounds is not dependent on the percentage conversion of *n*-hexane but on the presence gallium species within the channels of H-ZSM-5. An increase in the aromatic selectivity can be attributed to the dehydrogenation activity introduced by the presence of gallium species in the H-ZSM-5 channels [4]. The gallium species in the H-ZSM-5 provide alternative pathways for the formation of aromatic compounds. Hence an increase in the

aromatic selectivity is observed. This can also be observed when looking at the cracking and dehydrogenation activity of the Ga/H-ZSM-5 catalysts, shown in Figure 4.4.

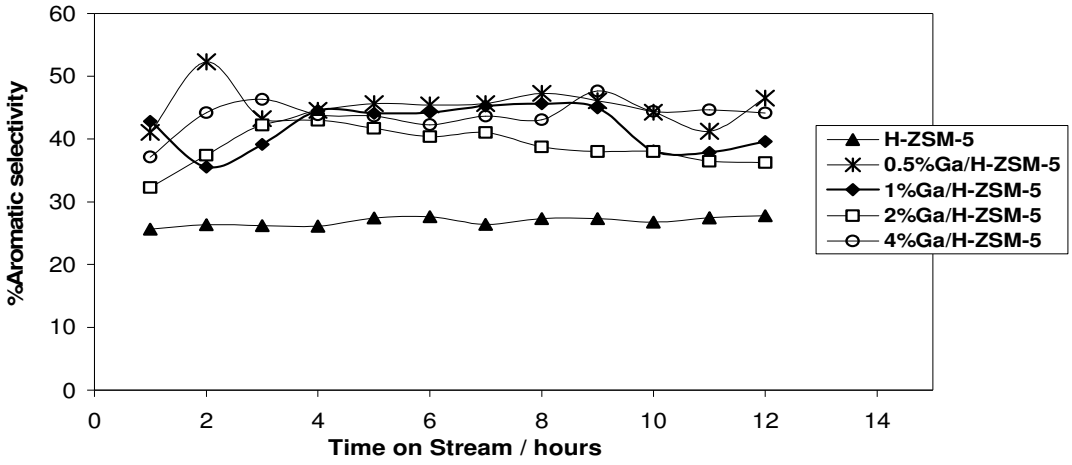

Figure 4.4: The aromatic selectivity of *n*-hexane over Ga/H-ZSM-5 with different loading as a function of time on stream at 500^{o}C.

Figure 4.5 shows the results of the effect of gallium loading on the product distribution of Ga/H-ZSM-5 catalysts with different loadings. The product distribution of aromatic compounds is compared to that of propylene ($C_3^=$) and butenes ($C_{4s}^=$) since the formation of aromatic compounds can be derived from the $C_3^=$ and $C_{4s}^=$ present in the reactor during reaction. From the graph we observe a mirror image behaviour between the plot of aromatic yield and both $C_3^=$ and $C_4^=$ as the gallium loading increased. The aromatic yield increased from 27% to a range of 40 to 50% when 0.5%gallium was loaded on the H-ZSM-5. The yield for $C_3^=$ and $C_{4s}^=$ showed a different trend from the aromatic yield. The percentage yields for $C_3^=$ and $C_{4s}^=$ were 27% and 11% resppectively for the H-ZSM-5 catalyst, but decreased when the H-ZSM-5 zeolite catalyst was impregnated with 0.5%gallium reaching a minimum values of 12% and 4% respectively . However, as the metal loading was increased an increase of $C_3^=$ yield to 15% was observed, while $C_{4s}^=$ showed a slight increase in yield reaching a stabilized state at 1 wt% loading.

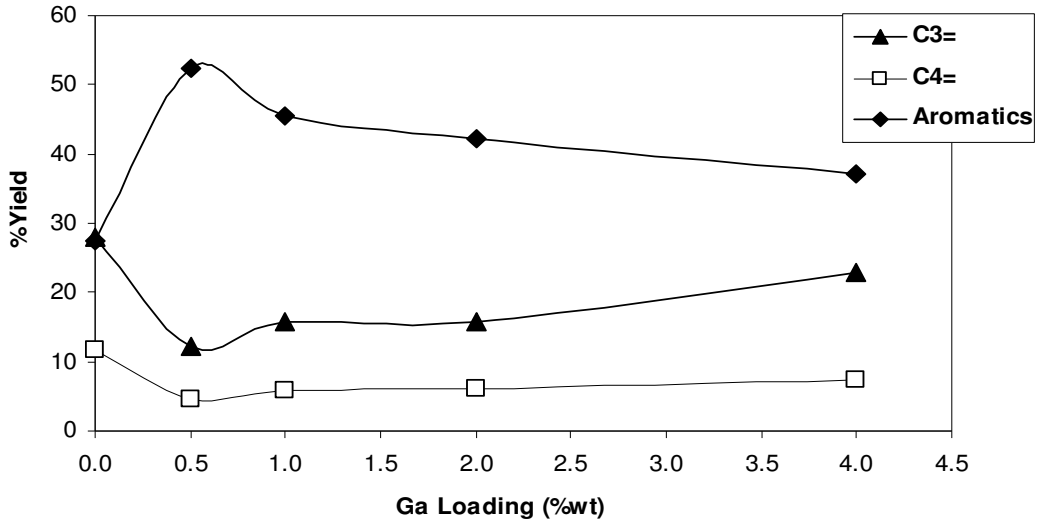

Figure 4.5: The effect of gallium loading on the product distribution taken at iso-conversion at 500^{o}C.

The decrease in $C_3^=$ and $C_{4s}^=$ yields when small amounts of gallium were introduced may be attributed to the decrease of Brønsted acid sites that are occupied by the gallium species. The gallium species inhibit Brønsted acid sites from activating the $C_3^=$ and $C_{4s}^=$ into carbonium form that can be easily converted into some aromatics.

The results of the effect of gallium loading on the aromatic product distribution of Ga/H-ZSM-5 catalysts with different loadings are presented in Figure 4.6.

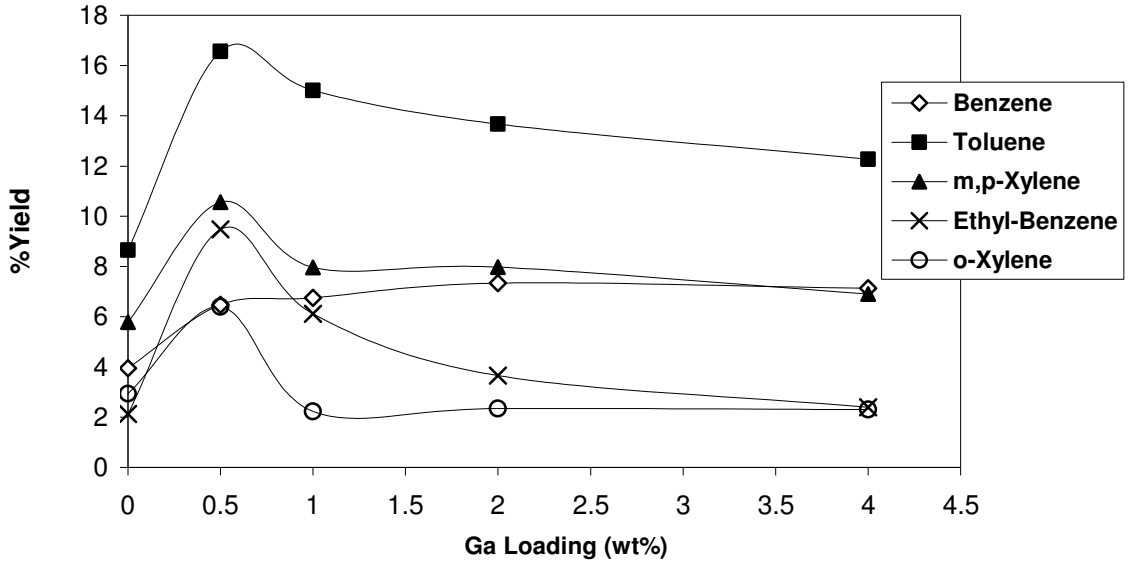

Figure 4.6: The effect of gallium loading on the aromatic product distribution mainly BTX of aromatization of *n*-hexane at 500^{o}C taken at isoconversion of ±85%.

The yield for each aromatic compound reached a maximum value at 0.5 wt% gallium loading with toluene being the dominating product with 17% yield. This high toluene yields are observed for catalysts with 0.5 and 1 wt% gallium loadings and a slight decrease was evident when metal loading was increased. The benzene yield increased with increase in gallium loading and stabalized at 7% yield after 2 wt% loading. For C_8 aromatic products (xylenes and ethylbenzene) an increase in yield was observed when the metal loading was 0.5 wt% and followed by a decrease at 1 wt% loading and stabilized after 2 wt% loaing. Lahn and co-workers [3] observed an increase in benzene and decrease in methylated benzene compounds yields, and they attributed this to the changes in acid sites when metal was loaded on the H-ZSM-5. They reported that the benzene yield depends on the Lewis acid sites while the methylbenzene compounds depend on the Brønsted acid sites. When increasing the metal loading an increase in Lewis acid sites is observed from the NH_3-TPD results. Hence an increase in yield for benzene

was observed for catalyts with high gallium loadings and thus disfavoured the production of methylated benzene compounds.

A summary of results on the aromatization of *n*-hexane over Ga/H-ZSM-5 catalysts of different metal loading is shown Table 4.2.

Table 4.2: The results of the aromatization of *n*-hexane over Ga/H-ZSM-5 catalysts at 500^{o}C taken at isoconversion of about 85%.

Ga Loading (wt%)	0	0.5	1	2	4
%Conversion	85.5	94.6	83.5	82.9	83.6
	Percentage Yields				
Methane	3.2	2.3	3.1	3.0	4.5
Ethylene	4.7	2.7	3.9	3.0	4.4
Ethane	8.4	3.0	4.1	3.4	5.7
Proplyene	26.9	10.3	14.7	15.0	21.0
Propane	5.9	2.6	4.3	4.1	6.5
$C_{4s}^{=}$	10.9	3.8	5.6	5.8	7.2
$C_4^{/}$	2.7	0.9	1.4	1.6	1.6
C_{5s}	3.1	1.0	1.8	1.8	2.1
C_{6s}	0.3	0.0	0.4	0.4	0.2
Benzene	4.6	6.9	8.1	8.9	8.4
Toluene	10.1	17.5	18.0	16.5	14.7
m-p Xylenes	6.8	11.2	9.6	9.6	8.3
o-Xylene	2.5	10.0	7.3	4.4	2.9
Ethyl-Benzene	3.4	6.8	2.7	2.8	2.8
C_{9s}	1.8	14.5	7.6	5.6	0.1
∑Aromatics	27.4	52.3	45.6	42.2	37.1

The aromatization of *n*-hexane over Ga/H-ZSM-5 zeolite catalyst is dependent on the amount of metal loading on the H-ZSM-5 zeolite catalysts. The yield of aromatic products increases with the increase in gallium loading with toluene being the dominant aromatic product. The

selectivity of $C_3^=$ and $C_{4s}^=$ olefins which are the primary products decreased with increasing metal loading. The H-ZSM-5 zeolite catalyst showed 26.9% and 10.9% selectivity to $C_3^=$ and $C_{4s}^=$ selectivity were observed but after addition of 0.5 wt% of gallium there was a noticeable drop of $C_3^=$ and $C_{4s}^=$ yields to 10.3 and 3.8% respectively. However, as the gallium loading was increased to 4 wt% there was an increase in the selectivity of $C_3^=$ and $C_{4s}^=$ olefins. The sum of the aromatic compounds increased sharply to 52% after the addition of gallium and decreased with increase in gallium loadind reaching a minimum of 37% at 4 wt% gallium laoding. A low yield is observed for the C_5 compounds. This can be attributed to the C_5 compounds cracking into smaller compounds. It is evident that the aromatic compounds are not the primary products that are formed from the aromatization of *n*-hexane; they are the result of small compounds undergoing secondary reactions to form the aromatic compounds. The yields for short chain compounds, i.e. C_1, C_{2s}, C_{3s}, C_{4s} and C_{5s} decreased as the gallium was added to the H-ZSM-5. This shows that there is an enahncement on the dehydrogenative activity of gallium modified catalysts as compared to the cracking activity. Similar effects have been reported for the aromatization of propane. The addition of gallium whether prepared by ion-exchange or wet impregnation methods increased the conversion of propane and enhanced the aromatic yield while suppressing the production of small products from cracking [4, 5].

4.2.2. The Effect of Zinc Loading

The influence of zinc on the catalytic activity and selectivity of H-ZSM-5 on the conversion was investigated. This study was conducted over Zn/H-ZSM-5 catalysts with different zinc loadings ranging 0 to 3 wt% loading. These catalysts were prepared by an incipient wetness impregnation method. The reactions of conversion for the *n*-hexane were performed at 500^{o}C.

The results of the effect of zinc loading on the surface area and pore volumes of H-ZSM-5 catalysts are summarized in Table 4.4. The surface area and pore volume of the catalysts decreased with an increase in zinc loading, decreasing from 376 to 327 m^2/g and a decrease in

pore volume from 0.28 to 0.25 cm^3/g also occurred. This small decrease in surface areas and pore volumes may be due to the channel occupation of small contents of zinc species [6].

Table 4.3: BET surface areas and pore volumes of the calcined Zn/HZSM-5 catalysts with different gallium loadings.

Catalysts	BET Surface Area m^2/g	Pore Volume cm^3/g
H-ZSM-5	376	0.28
0.5%Zn/H-ZSM-5	357	0.26
1.5%Zn/H-ZSM-5	349	0.27
3%Zn/H-ZSM-5	327	0.25

The NH_3-TPD results of Zn/H-ZSM-5 zeolite catalysts with different zinc loadings are presented in Figure 4.7. The impregnation of on H-ZSM-5 resulted to a decrease on the HT peak at 490^oC and the intensity and the peak area at 290^oC of the LT peak increased as the zinc loading increased. The temperature of desorption for the LT peak shifted to high temperatures as the zinc loading increased. The increase in the LT peak is due to the formation of Lewis acid sites generated by zinc ions. The addition of zinc led to a third peak appearing at 330^oC that is more visible in the 1.5%Zn/H-ZSM-5 and 3%Zn/H-ZSM-5 profiles. Berndt et al. [7] reported the appearance of the third peak and attributed it to the desorption of NH_3 from new moderate acid sites that are generated as zinc loading is increased. The area and intensity of the HT peak corresponding to the Brønsted acid sites decreased with an increase in zinc loading. This indicates that the concentration of the Brønsted acid sites decreases as the zinc loading is increased.

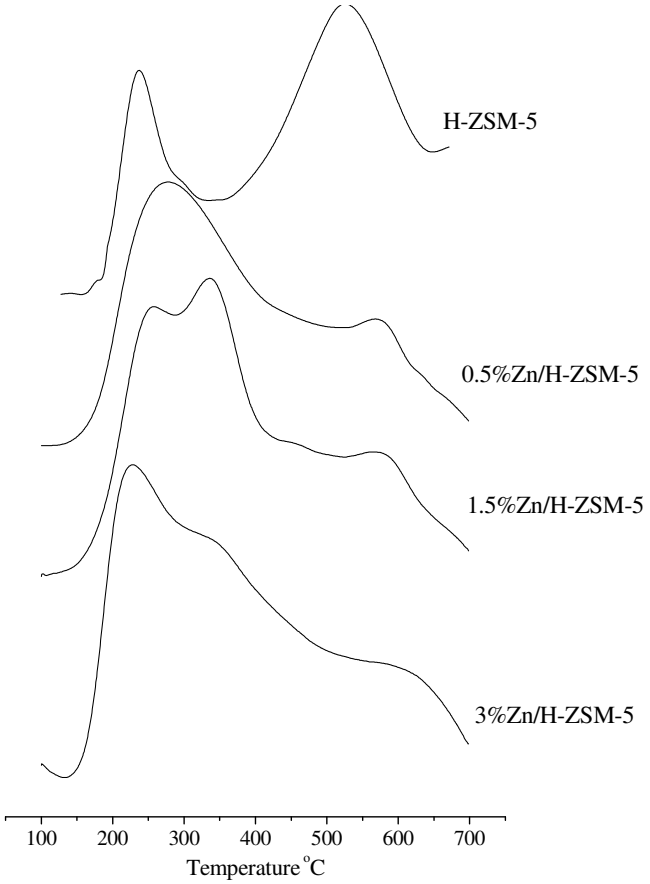

Figure 4.7: NH_3-TPD profiles of Zn/H-ZSM-5 zeolite catalysts with different zinc loadings.

The results on the effect of zinc loading on the catalytic conversion of *n*-hexane over Zn/H-ZSM-5 at time-on-stream of 5 hours are presented in Figure 4.8.

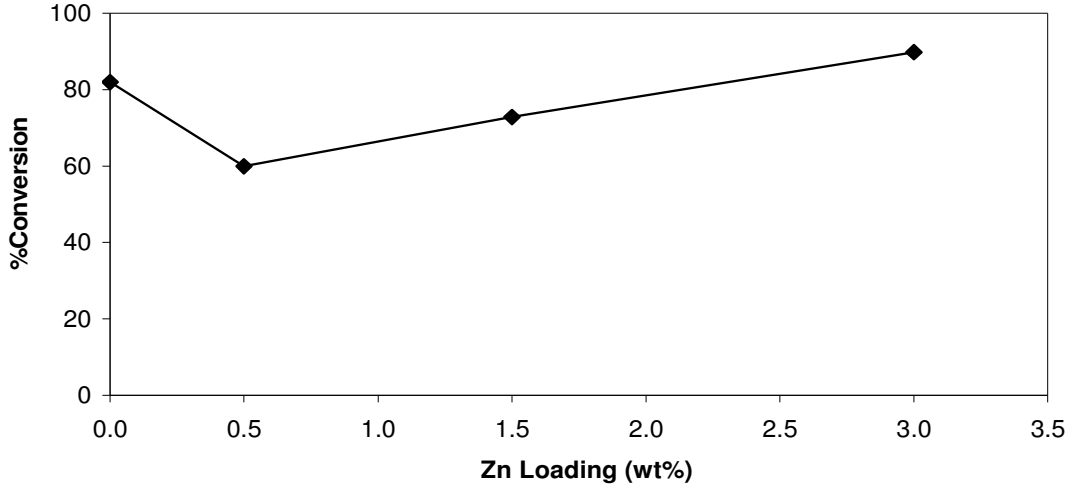

Figure 4.8: The effect of zinc loading on the catalytic conversion of *n*-hexane over Zn/H-ZSM-5 catalysts at 500^{o}C taken at time-on-stream of 5 hours.

The results show that the catalytic conversion of *n*-hexane is dependent on the amount of zinc loaded on the H-ZSM-5 zeolite catalyst. It can be seen that the conversion of *n*-hexane on 0.5%Zn/H-ZSM-5 is low when compared with the zinc free H-ZSM-5 catalyst, but a continuous increase in conversion is observed with increase in zinc loading. The low catalytic conversion of *n*-hexane over 0.5% Zn/H-ZSM-5 catalyst can be attributed to the reduction of the number of Brønsted acid sites by the introduction of Zn species [8]. However an increase in catalytic conversion was observed when zinc loading was increased from 1.5 to 3 wt%. The increase in the activity of Zn/H-ZSM-5 catalysts with zinc loading above 0.5 wt% can be attributed to an increase in the dehydrogenation activity which is associated with Zn species in the H-ZSM-5 zeolite catalysts. It is believed that the introduction of zinc species increases the activity of the catalysts by introducing an alternative pathway to the reaction mechanism since well the catalysts is bifunctional [9]. This is due to the zinc species being able to dehydrogenate *n*-hexane into hexene, which can be further aromatized and fragmented into olefin intermediates

that can undergo secondary intermediate reactions which lead to high aromatic selectivity as shown in Figure 4.10.

The stabilities and aromatic selectivity of Zn/H-ZSM-5 catalysts when exposed to *n*-hexane for a time-on-stream of 12 hours at 500^{o}C are shown in Figure 4.9 and Figure 4.10 respectively. The impregnation of H-ZSM-5 zeolite with zinc species has been shown to have an influence on the catalytic conversion of *n*-hexane and aromatic selectivity. The H-ZSM-5 and Zn/H-ZSM-5 zeolite catalysts with different zinc loadings showed good catalytic stability with time-on-stream, retaining the *n*-hexane conversion. This agrees with the results presented in the gallium catalyst system showing that conversion of *n*-hexane is independent on time-on-stream. Catalysts containing low zinc loadings i.e. below 3 wt% showed low activity towards catalytic conversion *n*-hexane. The zinc-free H-ZSM-5 and 3%Zn/H-ZSM-5 catalysts also showed high *n*-hexane conversion and good catalytic stability with time-on-stream, retaining their conversion of *n*-hexane at 81 and 88% respectively. This high catalytic conversion of the 3%Zn/H-ZSM-5 catalyst can be attributed to the enhancement of the dehydrogenation activity of the zinc species by increase of the zinc loading which is necessary to initiate the reaction of dehydrogenating *n*-hexane to hexene. The aromatic selectivity of the Zn/H-ZSM-5 catalysts showed an increase with metal loading as shown in Figure 4.10. This increase may be attributed to the increase in dehydrogenation activity as the zinc species are introduced. The zinc-free H-ZSM-5 catalyst showed low aromatic selectivity.

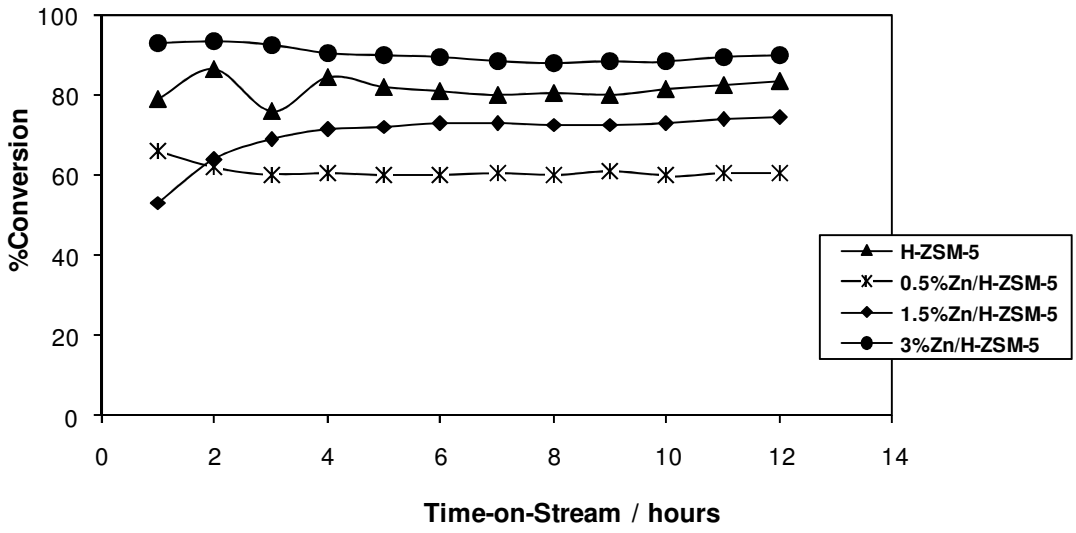

Figure 4.9: The catalytic conversion of *n*-hexane of Zn/H-ZSM-5 with different zinc loadings as the function of time-on-stream at 500°C.

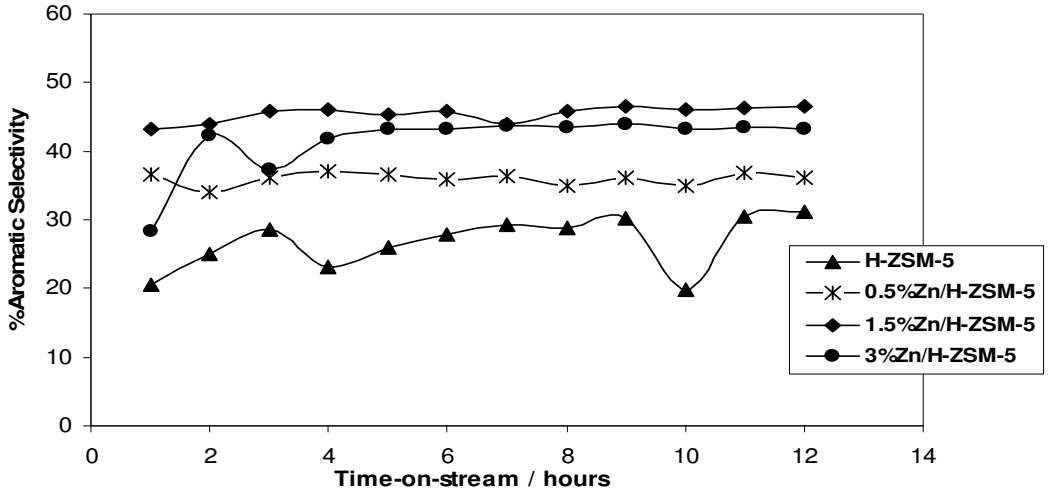

Figure 4.10: The aromatic selectivity of *n*-hexane over Zn/H-ZSM-5 catalysts with different zinc loadings as the function of time on stream at 500°C.

The results on the effect of zinc loading on the product distribution are shown in Figure 4.11.

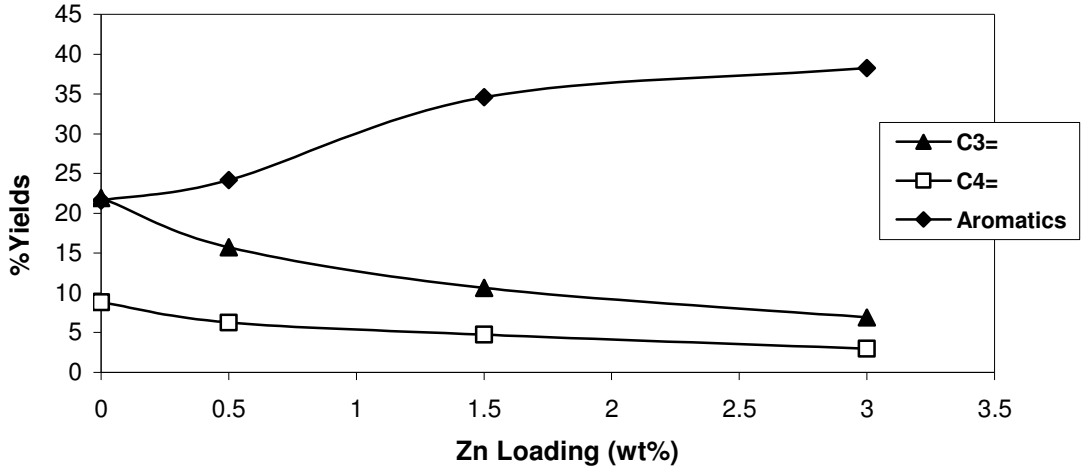

Figure 4.11: The effect of zinc loading on the product distribution taken at iso-conversion at 500^{o}C.

The results show an increase in aromatic yield and a decrease in yield of olefins when the zinc loading was increased. The aromatic yield increased from 22 to 38% with increase in metal loading, however, a different behaviour can be said on the yield of $C_3^=$ and $C_{4s}^=$. The yield of olefins decrease from 22% to yields as low as 10% for the $C_3^=$ and for $C_{4s}^=$ from 10 to 5% yield as the metal loading increased. This results were also reported for the gallium catalyt system. Gnep et al. [10] reported similar results on conversion of propane over Ga/H-ZSM-5 zeolite catalysts. The intoduction of zinc and gallium was associated with an increase in concentration of aromatic compounds. The studies of *n*-hexane[11] and propane[12] cracking showed that the yields of aromatic procducts depend on the concentration of olefins present in the reaction mixture. The zinc species in the bifunctional catalyst facilitates the dehydrogenation of paraffins to olefins and of other intermediates to aromatic compounds and dienes. The dehydrogenation activity is increased as the metal loading increases. The location and nature of zinc species has an important role on the aromatic yield. At a high zinc concentration the performance of Zn/H-ZSM-5 catalysts is diffferent and this is attributed to the different nautre of zinc species that may be present the channels of H-ZSM-5. The distance between the adjacent Al atoms in the zeolite framework affects the position of zinc cations and also detemines if the isolated or oxygen–briged cationic species are also formed in the catalyst. These species are reported to have a

different activity in the aromatiztion of alkanes [13]. So, the increase in the yields of aromatic compounds can be attributed to the increase dehydrogenation activity of the Zn/H-ZSM-5 catalyst systems, as the zinc concentration increases in H-ZSM-5 zeolite catalysts. The decrease in olefin concentration with zinc loading suggests that there was a high concentration of olefins produced in the reaction mixture and that further underwent a secondary reaction and was converted to aromatic compounds.

The product distribution results of Zn/H-ZSM-5 catalysts with different zinc loadings are presented in Figure 4.12.

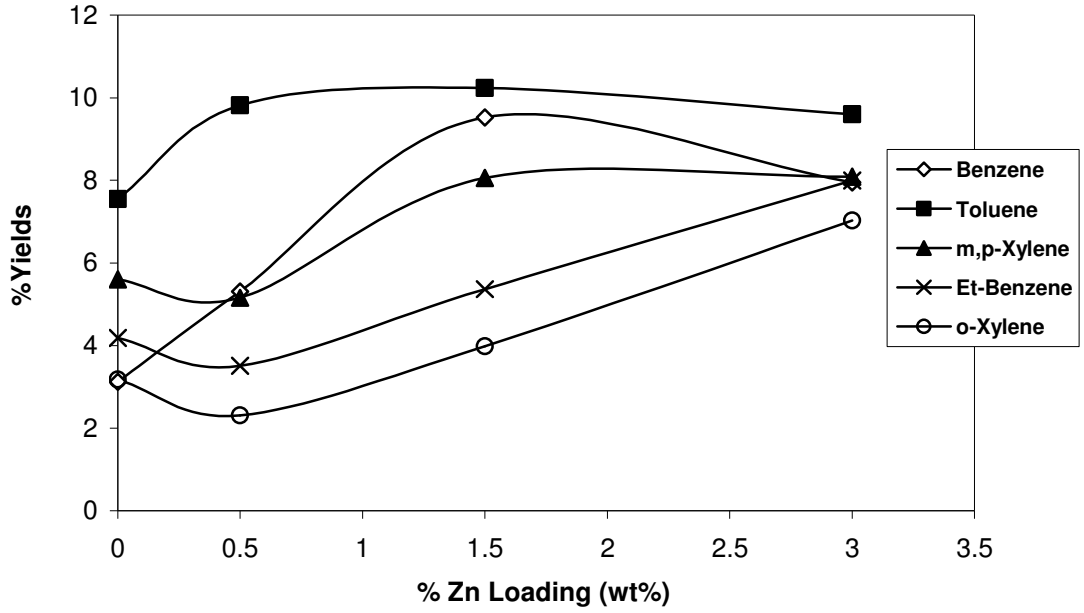

Figure 4.12: The effect of zinc loading on the aromatic product distribution mainly BTX of aromatization of *n*-hexane at 500^{o}C taken at isoconversion.

The addition of zinc to the H-ZSM-5 catalyst influenced the product distribution of the aromatic compounds. An increase in the yield of aromatic products with increase in zinc loading was observed also, the yield C_8 aromatics (xylenes and ethylbenzene) is at a minimum for the catalyst with 0.5 wt% zinc loading. The low yield of benzene over the H-ZSM-5 catalyst can be

attributed to the alkylation of benzene that might be taking place in the zeolite channels that can contribute to the high yield of toluene and low yields of methane [14]. The introduction of zinc species led to an increase in the yield of benzene, reaching an optimum of 9% yield for the catalyst with 1.5 wt% zinc loading. This increase in benzene yield might be due to the zinc species decreasing the Brønsted acid sites which were promoting the alkylation reaction on the zinc free H-ZSM-5 catalyst.

Table 4.4 shows the summarised results of the aromatization of *n*-hexane over Zn/H-ZSM-5 zeolite catalysts.

Table 4.4: The result of of the product distribution of *n*-hexane aromatization over Zn/H-ZSM-5 catalysts at 500^{o}C.

Zn Loading (wt%)	0	0.5	1.5	3
%Conversion	75.9	66.0	74.2	87.9
	Percentage Yields			
Methane	2.3	1.9	2.4	3.8
Ethylene + Ethane	10.3	7.8	8.8	6.3
Propylene	21.9	15.7	10.6	6.9
Propane	5.7	3.5	4.2	2.0
$C_{4s}^{=}$	8.9	6.3	4.8	2.9
$C_{4s}^{/}$	2.0	1.8	1.4	0.9
C_{5s}	2.2	2.0	1.5	0.6
C_{6s}	0.0	0.2	0.1	0.2
Benzene	3.1	5.3	9.5	8.0
Toluene	7.6	9.8	10.2	9.6
m,p-Xylene	5.6	5.2	8.1	8.1
Et-Benzene	2.2	1.6	2.8	5.6
o-Xylene	3.2	2.3	4.0	7.0
$C9_s$	4.6	0	1.4	21.3
∑Aromatics	21.6	24.2	34.6	38.3

The increase in zinc loading resulted in a decrease in the yield of cracked products with increase in the formation of aromatic compounds. The total aromatic yield increased from 21 to 38% with increase in zinc loading. This increase in aromatic loading can be attributed to the dehydrogenation activity that is enhanced when the zinc loading is increased. A simultaneous decrease in the yields of cracked products with increase in zinc loading was observed. An obvious change is on the yield of $C_3^=$ nd $C_{4s}^=$ olefins which decreased with increase in the zinc loading. This can be due to the increase in dehydrogenating activity that surpressed the cracking activity as the zinc loading was increased. But a slight increase in methane yields was observed as the zinc loading increased showing that the alkylation of benzene decreased with increased metal loading. We also observed that the 1.5%Zn/H-ZSM-5 catalyst produced high yields of methane, C_{2s} and propane compared to other catalysts. Also, high yields of benzene that are due to 1.5 wt% are also observed. High yields of methane, C_{2s} and benzene may be attributed to the increase in the alkylation activity of the H-ZSM-5 as the metal loading increased. The increase in metal loading decreased the formation of toluene by inhibiting the alkylation of benzene and low weight alkanes remained unreacted leading to a high concentration of low alkanes.

4.2.3. The Effect of Molybdenum Loading

The aromatization of *n*-hexane was further studied over the molybdenum loaded H-ZSM-5 zeolite catalysts. The Mo/H-ZSM-5 catalysts with loadings between 0 and 10 wt% were prepared an incipient impregnation method and calcined at 500^{o}C. The influence of molybdenum loading was investigated at a reaction temperature set to 500^{o}C.

The results of the effect of molybdenum loading on the BET surface areas and pore volumes of Mo/H-ZSM-5 catalysts with different molybdenum loadings are presented in Table 4.5. The BET surface areas and pore volumes decreased with an increase in the amount of molybdenum loaded in the H-ZSM-5. For the catalysts with 2 to 4 wt% molybdenum loadings a steady decrease in both the BET surface areas and porous volumes was observed, while a more severe decrease was observed for 6 and 10 wt% molybdenum loaded catalysts. The increase in molybdenum up to 10

wt.% loading led to a enormous decrease in surface area and pore volume, in which the surface area decreased by 33% and pore volume by 23%, when compared to the parent H-ZSM-5. Li and Co-workers [15] also reported similar observations and attributed the decrease in BET surface area and pore volume to the molybdenum species being highly dispersed on the zeolite surface and the channels of the zeolite.

TABLE 4.5: The results of the BET surface areas and pore volumes of the calcined Mo/H-ZSM-5 catalysts with different molybdenum loadings.

Catalysts	BET Surface Area (m^2/g)	Pore Volume (cm^3/g)
H-ZSM-5	376	0.28
2%Mo/H-ZSM-5	364	0.27
4%Mo/H-ZSM-5	340	0.25
6%Mo/H-ZSM-5	312	0.23
10%Mo/H-ZSM-5	245	0.20

The XRD patterns and FT-IR spectra of Mo/H-ZSM-5 catalysts with different molybdenum loadings are shown in Figure 4.13 and Figure 4.14 respectively. The powder-XRD profiles show that the structure of H-ZSM-5 was retained as the molybdenum was loaded although there was a slight change in the intensity on the characteristic peaks of H-ZSM-5. At 2 theta values of 12^o and 27^o extra peaks that were visible on the prolife of a sample containing 10 wt% molybdenum loading were noted. These peaks are attributed to the crystallization of molybdenum trioxide on the external surface of H-ZSM-5 [16, 17]. At a loading higher than 6 wt% the presence of molybdenum species on the surface of H-ZSM-5 is detected. This agrees with BET surface area results that the surface areas for samples with high loading decreased due to crystallization of MoO_3 on the external surface of H-ZSM-5. Similar observations were reported by Chen at al. [18] for samples with molybdenum loading exceeding 8 wt%. Comparable conclusions can be drawn from the FT-IR results of Mo/H-ZSM-5 catalysts shown in Figure 4.14. For the catalysts with Mo loading 4 and 6 wt% there is a visible shoulder at 917 cm^{-1}. At 10 wt% loading the peak becomes more visible. This peak is attributed to the Mo-O-Mo vibration of molybdenum oxide. These results correspond with that of the powder-XRD patterns, which indicates that at

Mo loadings of 10 wt%, crystallization of molybdenum trioxide takes place on the surface of H-ZSM-5.

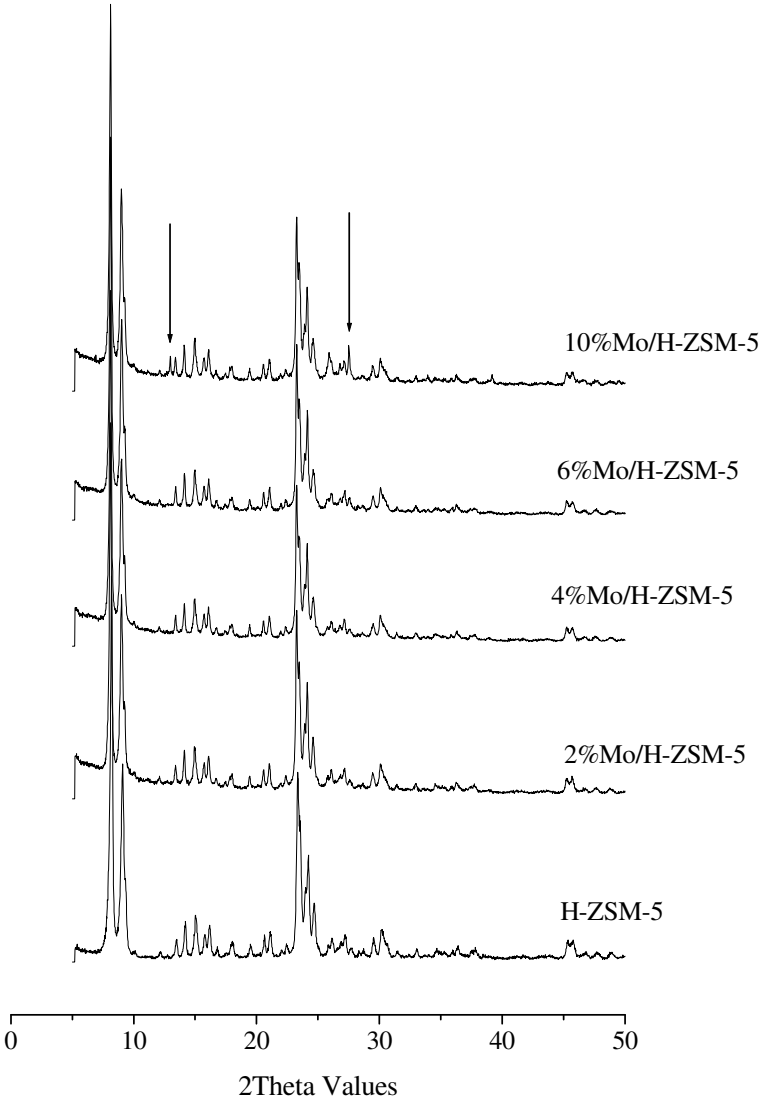

Figure 4.13: XRD Patterns of Mo/H-ZSM-5 with different molybdenum loading.

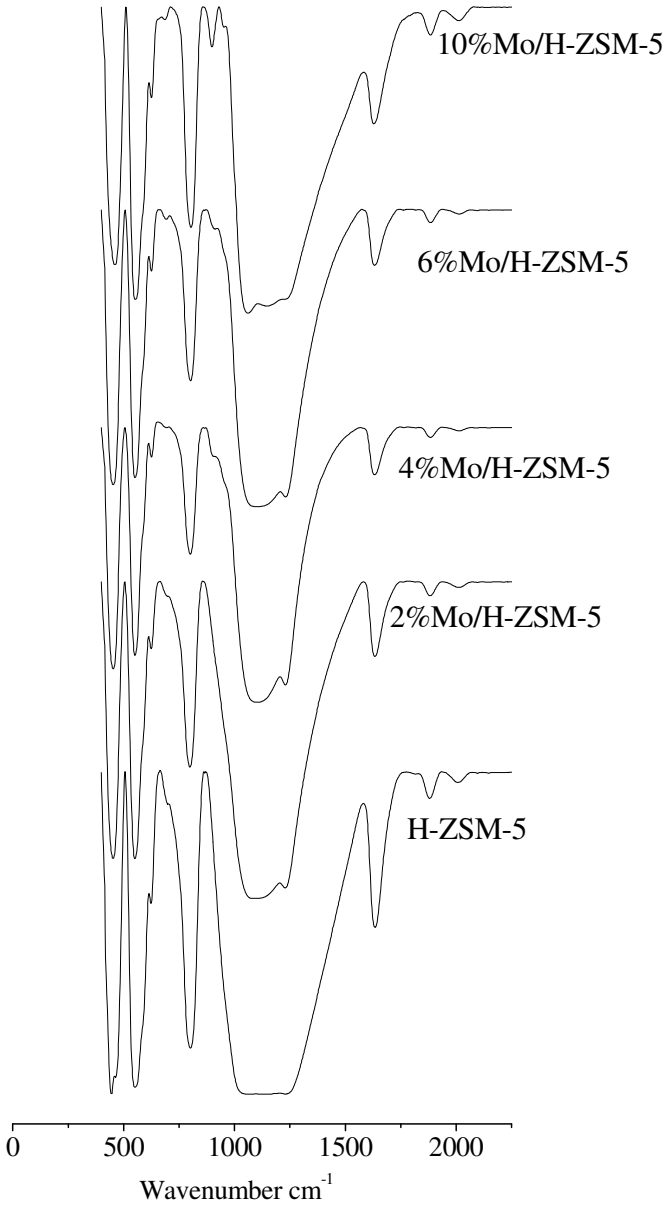

Figure 4.14: FT-IR spectra of Mo/HZSM-5 catalysts with different molybdenum loadings**.**

The catalysts were further characterized using H_2-TPR and the results shown in Figure 4.15 are of the reduction of Mo/HZSM-5 catalysts with different molybdenum loading.

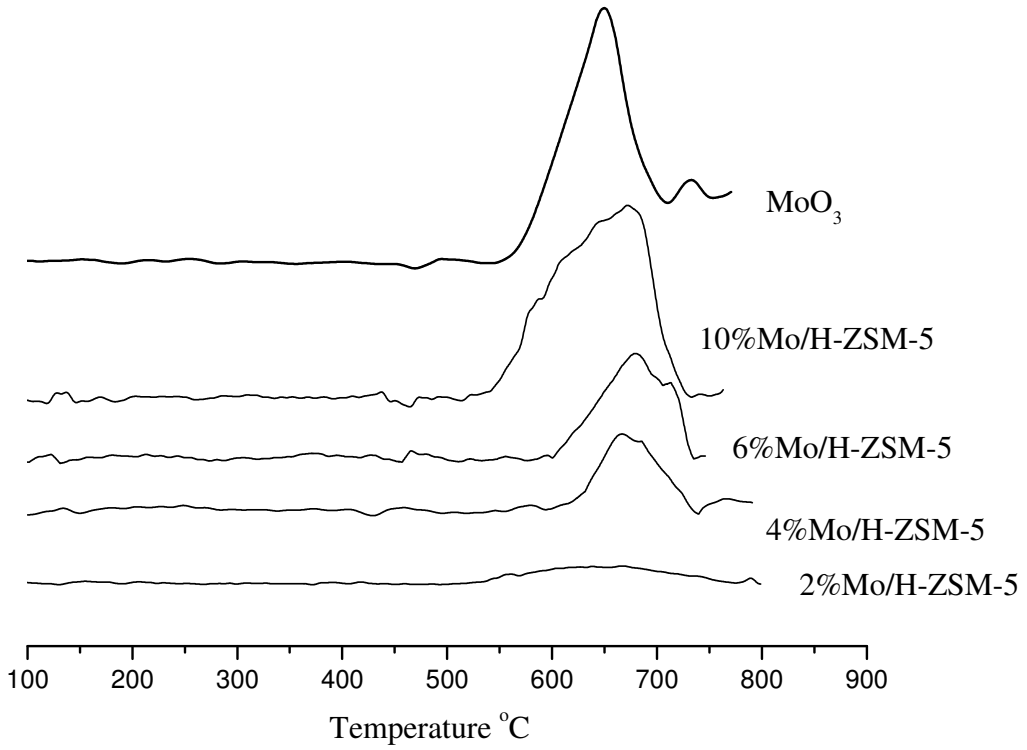

Figure 4.15: H_2-TPR profile of Mo/H-ZSM-5 catalysts with different molybdenum loading.

The profile showing the reduction of molybdenum trioxide has two peaks. The first peak at 647°C represents the reduction of molybdenum from the +3 oxidation state to a +2 oxidation state. The second peak appearing at 730°C represents the reduction of molybdenum species in the +2 oxidation state to a +1 oxidation state. Focusing on the profiles of Mo/H-ZSM-5 catalysts, we observe that the intensity of the reduction peaks, especially at 647°C increased with molybdenum loading. This signifies that the molybdenum species are dispersed on the external surface of the H-ZSM-5 zeolite and exist in a crystallized state for catalysts with loading higher

than 6 wt% [19]. The TPR profiles Mo/H-ZSM-5 catalyst with loading 2 wt% showed that a small amount of hydrogen was taken up at a reduction temperature 627^{o}C. This can be attributed to the reduction of small MoO_3 species in the channels of H-ZSM-5. As the molybdenum loading increased the reduction temperature shifted from 730^{o}C to 647^{o}C and an increase in the hydrogen consumption was also observed. The increase in the intensity of reduction peak when the molybdenum loading was increased may be due to the reduction of the molybdenum trioxide that has crystallized as MoO_3 on the surface of the catalyst as suggested by FT-IR studies.

Figure 4.16 shows the NH_3-TPD profiles Mo/H-ZSM-5 catalytsts with different molybdenum loadings.

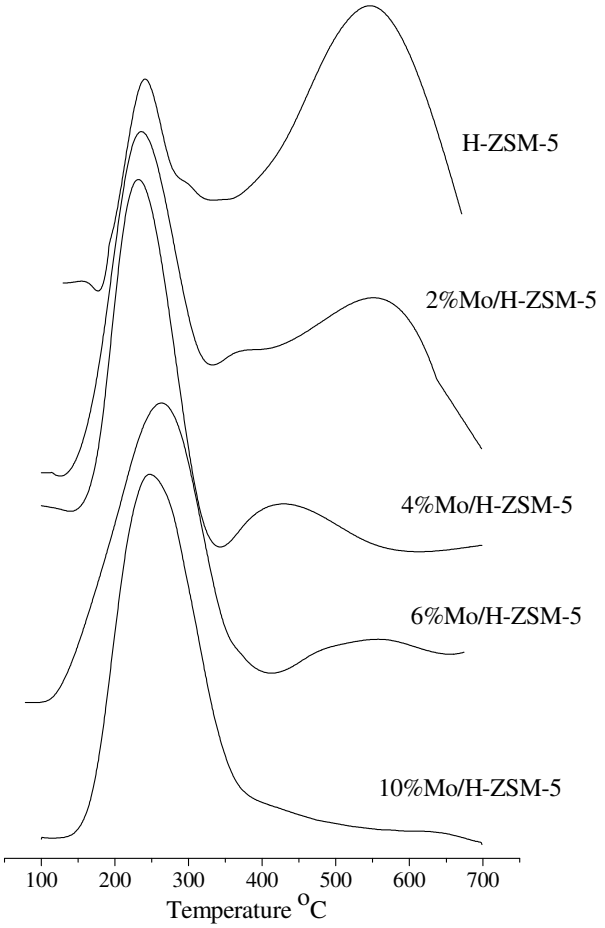

Figure 4.16: NH_3-TPD proile of Mo/H-ZSM-5 ctalysts with different molybdenum loadings.

The addition of molybdenum gave a distinct decrease to the HT peak corresponding to the Bronsted acid site of the H-ZSM-5 while the LT peak area increased with molybdenum loading. At high molybdenum loading the HT peak fades away and this is due the molybdenum trioxide species migration into the channeles of H-ZMS-5. The molybdenum species in the channels interact strongly with the Brønsted acid sites and this interaction result into the Brønsted acid sites being consumed [20]. Hence a decrease in the area and intesinsity of the HT peak is obsersed at higher molybdenum loading. The peak at low temperature increased with increase in loading and the temperature of the desorption shifted to higher temperature.

The catalytic results of the aromatization of *n*-hexane over molybdenum H-ZSM-5 zeolite catalysts are presented below. The effect of molybdenum loading on the catalytic conversion of hexane was studied at reaction temperature of 500^{o}C; the results are shown in Figure 4.17.

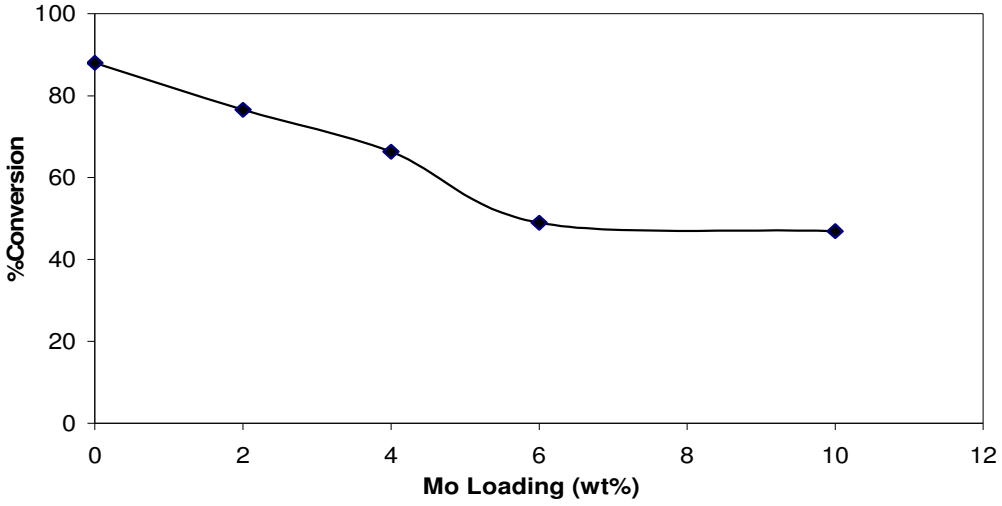

Figure 4.17: The effect of molybdenum loading on the percentage conversion of *n*-hexane taken at time-on-stream of 5 hours.

The *n*-hexane conversion decreased due to the modification of H-ZSM-5 by loading Mo. This decrease may be attributed to a decrease in the surface area, pore volume and concentration of

Brønsted acid sites of the parent H-ZSM-5 due to molybdenum loading. The decrease observed between 2 and 4 wt% was slightly has but between 6 and 10 wt% there was a noticeable decrease in conversion of *n*-hexane.

The results on the catalytic activity as the function of time are shown in Figure 4.18.

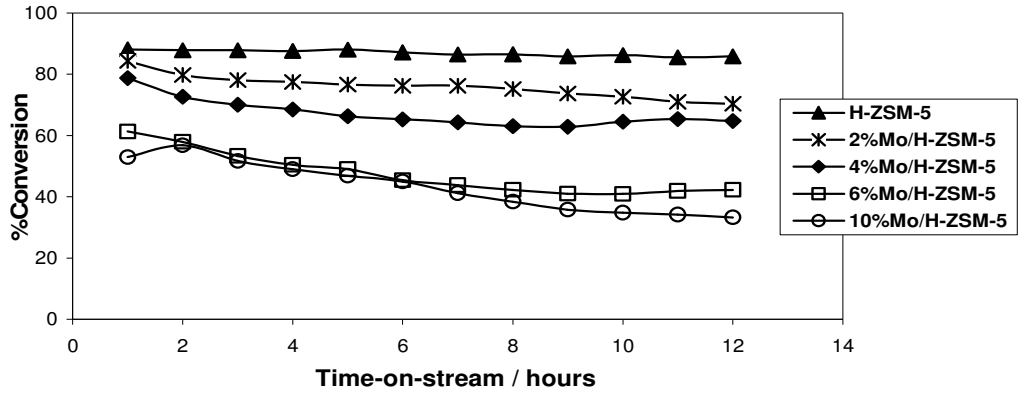

Figure 4.18: The catalytic conversion of *n*-hexane as a function of time-on-stream at 500^{o}C over Mo/H-ZSM-5 catalysts of different molybdenum content.

These results show a decrease in conversion of *n*-hexane with the increase in time-on-stream. This decrease can be attributed to the deactivation of the catalysts associated with the deposition of coke on the active sites of catalysts rendering them inactive. The molybdenum-free H-ZSM-5 catalyst showed stability with respect to time-on-stream with hexane conversion ranging between 89 and 85%. For catalysts with low molybdenum content (2 and 4 wt%) a steady decrease in conversion with time-on-stream was observed. However, catalysts with high molybdenum loading, i.e. 6 and 10 wt% there is an obvious decrease in *n*-hexane conversion from 58 to 34% with time-on-stream. These observations may be attributed to the agglomeration of molybdenum species in the H-ZSM-5 channels. The agglomerated Mo species increased with the increase in

molybdenum loading. This led to the observed crystals of MoO_3 being formed on the H-ZSM-5 channels leading to the blockage of pores.

Results on the aromatic selectivity of the Mo/H-ZSM-5 catalysts with time-on-stream are shown in Figure 4.19.

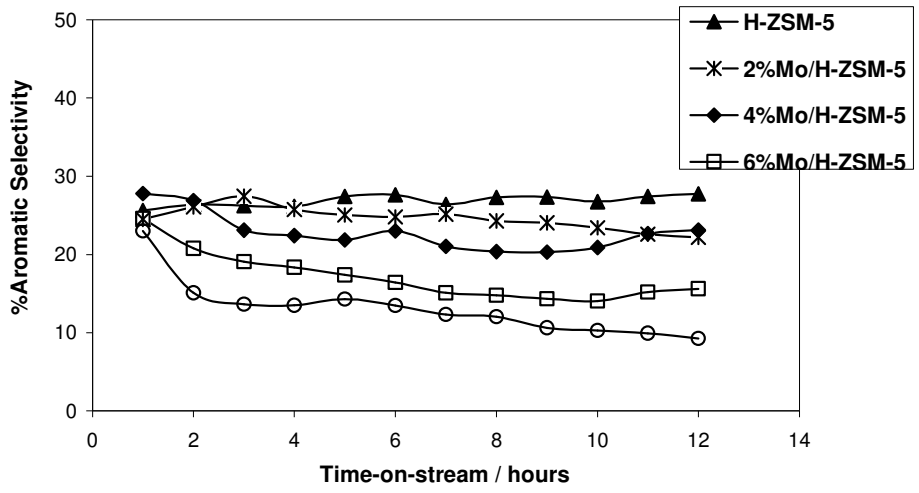

Figure 4.19: The percentage aromatic selectivity as a function of time-on-stream at 500^{o}C over Mo/H-ZSM-5 catalysts with different molybdenum loadings.

A matching trend observed in the catalytic conversion is also observed for the aromatic selectivity with time-on-stream. The selectivity of the catalysts with low molybdenum loading ranged between 21 and 28%, whereas for the 6 and 10 wt% Mo loaded catalysts we observed an obvious decrease in aromatic selectivity from 24 to 9% was observed. Although the catalytic conversion for the H-ZSM-5 molybdenum-free catalyst was higher, the aromatic selectivity was comparable with those of impregnated samples with low molybdenum loading. The aromatic selectivity for H-ZSM-5 was not dependent on the time-on-stream and this is due to the stable activity of the catalyst in (Figure 4.19). However, for samples with molybdenum species we observed a decrease in aromatic selectivity with increase in time-on-stream. This is due to the

decrease in the conversion of *n*-hexane with time. This results show that the aromatic selectivity over molybdenum modified H-ZSM-5 zeolites samples is dependent on the conversion of *n*-hexane.

The product distribution results of Mo/H-ZSM-5 catalysts at different molybdenum loading are presented in Figure 4.20.

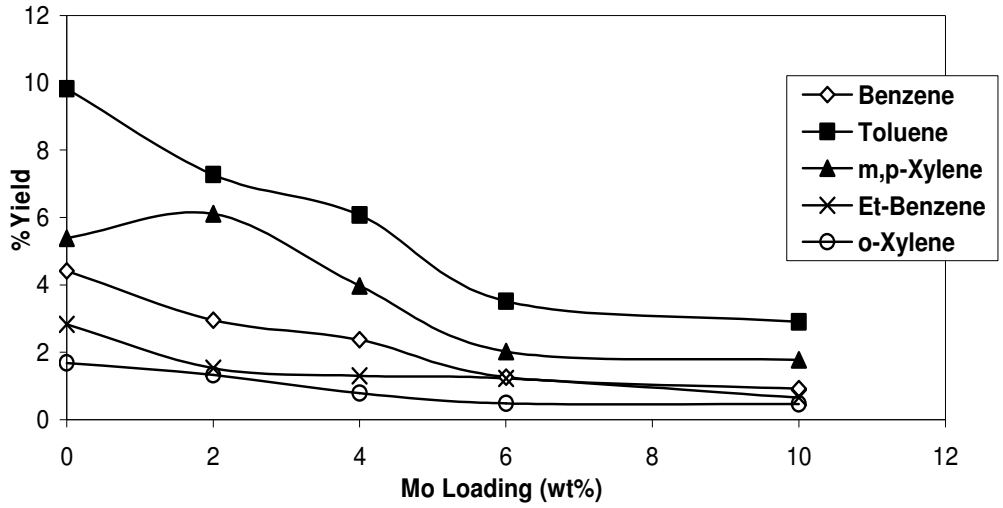

Figure 4.20: The effect of molybdenum loading on the aromatic product distribution mainly BTX of aromatization of *n*-hexane at 500^{o}C taken at time-on-stream of 5 hours.

In these results for the H-ZSM-5 catalyst, which is molybdenum-free possesses high yields for all individual aromatic compounds when compared with other molybdenum loaded H-ZSM-5 zeolite catalysts. Toluene was the dominating product followed by *m,p*-xylene in all the Mo/H-ZSM-5 catalysts. For all aromatic compounds we observed a noticeable decrease in the yield with increase in molybdenum loading from 0 to 6 wt%. However, between 6 and 10 wt% loading a plateau was reached. Equivalent yields that are observed at loadings of 6 and 10 wt% may be due to the similar conversion of *n*-hexane. The trend observed suggests that the loading of molybdenum on H-ZSM-5 catalyst did not favour the formation of aromatic compounds when compared with Ga/H-ZSM-5 and Zn/H-ZSM-5 catalysts.

A summary of results for the aromatization of *n*-hexane over Mo/H-ZSM-5 catalysts of different metal loading is shown Table 4.6.

Table 4.6: The effect of molybdenum loading on product distribution for the aromatization of *n*-hexane at 500^{o}C taken at time-on-stream of 5 hours.

Mo Loading (wt%)	0	2	4	6	10
%Conversion	88.0	76.6	66.3	49.0	46.9
	Percentage Yields				
Methane	3.0	2.3	2.4	2.1	1.6
Ethylene	3.6	5.7	6.9	7.7	7.6
Ethane	9.0	7.9	8.1	9.2	6.4
Propylene	26.5	27.0	27.2	32.44	34.6
Propane	6.1	5.7	4.1	3.4	4.0
$C_{4s}^{=}$	10.5	12.6	12.7	14.7	16.2
$C_{4s}^{/}$	2.5	3.6	4.0	5.2	5.9
C_{5s}	2.9	4.0	4.0	4.5	5.1
C_{6s}	0.3	0.4	1.04	1.4	0.9
Benzene	5.0	3.9	3.6	2.6	1.9
Toluene	11.2	9.5	9.2	7.2	6.2
m,p-Xylene	6.1	7.9	6.0	4.1	3.8
Et-Benzene	3.2	2.0	1.9	2.5	1.4
o-Xylene	1.9	1.7	1.2	1.0	1.0
$C9_s$	2.4	0.9	2.8	1.1	0.6
∑Aromatics	27.4	25.1	21.9	17.4	13.9

The product yield distribution for the aromatization of *n*-hexane over Mo/H-ZSM-5 zeolite catalysts are compared and presented in Table 4.6. The addition of molybdenum to the H-ZSM-5 does not seem to favour the formation of aromatic compounds and the catalytic activity decreased with molybdenum loading. This might be due to the low dehydrogenation activity the molybdenum species leading to the cracking activity dominating over aromatization activity. At a high loading of molybdenum aromatic yields below 20% and the conversion below 50% was observed. This is due to the increase in the molybdenum species that are blocking the active

sites on H-ZSM-5 from interacting with *n*-hexane molecule leading to the low activity and low aromatic yields observed. From the results it was observed that the dominating products are $C_3^=$ and $C_{4s}^=$ olefins, and the yield of these olefins increased with metal loading. High yields of $C_3^=$ and $C_{4s}^=$ olefins can be attributed to the decrease in the dehydrogenation activity of H-ZSM-5 zeolite catalysts as the molybdenum loading increased. High concentrations of molybdenum species hinder these olefins from undergoing the secondary reactions which will convert them to aromatic compounds. Thus low yields of aromatic compounds at high metal loading were observed. Cracking is the main dominating reaction in these molybdenum system catalysts. The yields for lower compounds increased with molybdenum loading. The aromatic activity of the catalyst is suppressed by the addition of molybdenum; this is also shown in the aromatization to cracking i.e. A/C ratio vs. metal loading plot shown in Figure 4.11.

The results on the aromatic:cracking (A/C) ratio of the *n*-hexane for H-ZSM-5 catalysts of different metal loading are presented below in Figure 4.21.

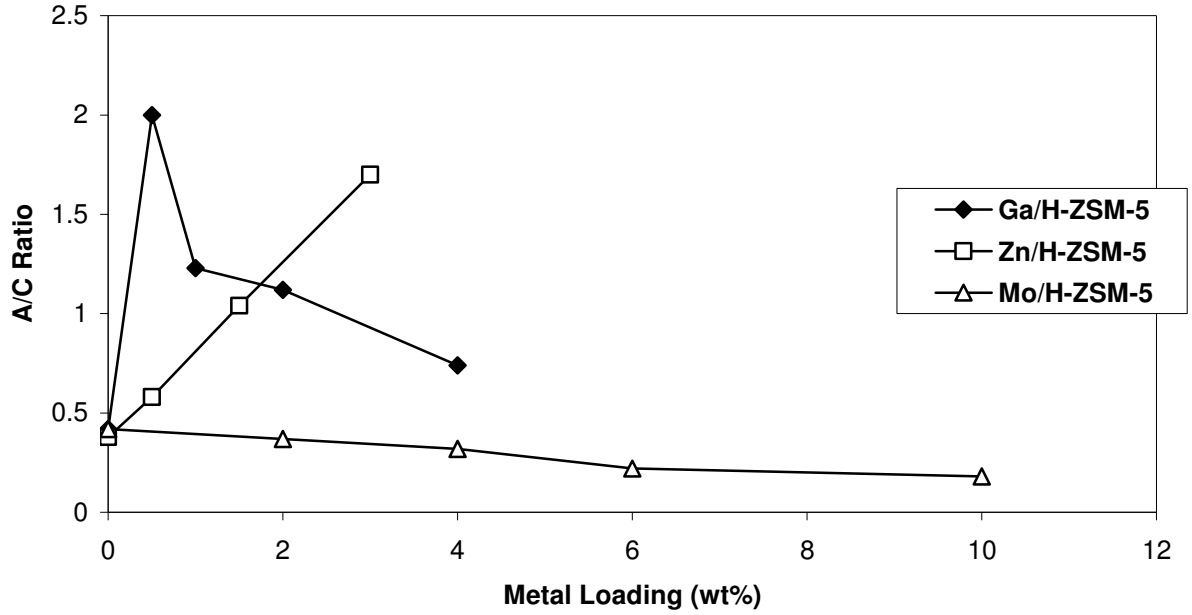

Figure 4.21: The aromatization and cracking activity ratio of *n*-hexane for gallium, zinc and molybdenum catalysts as the fuction of metal loading at 500^{o}C.

The increase in A/C (A = ∑BTX and $\sum C_1$-C_5) ratio can be attributed to the increase in the dehydrogenation activity by introduction of metal species which contribute to the decrease of Brønsted acid sites which are responsible for cracking. Another reason may be due to the formation of a high concentration of olefins in the reaction mixture that further undergo secondary reactions resulting in aromatic compounds being formed. The A/C ratio increased when 0.5 wt% of gallium was introduced to the H-ZSM-5. However, a decrease was also observed when the metal loadings were 1 wt% and higher. The Ga/H-ZSM-5 catalysts with gallium had an A/C ratio higher than the gallium free H-ZSM-5 catalyst due to the presence of gallium species. The incorporation of gallium to the H-ZSM-5 resulted in enhanced dehydrogenation activity and also decreased cracking activity by coating the Brønsted acid sites which are responsible for facilitating the cracking reaction in H-ZSM-5 catalysts. Thus the A/C of Ga/H-ZSM-5 catalysts is higher than of the gallium-free H-ZSM-5 catalysts. An increase in metal loading favoured the formation of aromatic compounds. We observed a linear increase of A/C ratio with zinc loading favouring the formation of aromatic compounds as opposed to cracked products. This is due to the dehydrogenation activity that is possessed by zinc species. The loading of molybdenum led to a decrease in A/C ratio. The decrease in the A/C ratio can be attributed to the decrease in the activity of Mo/H-ZSM-5 catalysts with increased metal loading. This shows that the molybdenum oxide species possess little dehydrogenation activity as opposed to cracking activity. These results may illustrate that the molybdenum species in H-ZSM-5 catalysts possess low dehydrogenation activity compared to gallium and zinc species in the H-ZSM-5 zeolite

4.3. The Effect of Percentage XRD Crystallinity of H-ZSM-5

The effect of H-ZSM-5 percentage XRD crystallinity on the catalytic conversion of n-hexane has been investigated over molybdenum, gallium and zinc modified H-ZSM-5 catalysts at 2 wt% metal loading. Catalysts with %XRD crystallinity ranging from 5 to 86% and with Si/Al ratio = 35 were investigated. The crystallinity of H-ZSM-5 samples is believed to have an influence on the catalytic activity of metal loaded HZSM-5 catalysts. The cracking of n-hexane was

conducted at 500°C with nitrogen flowing at a rate of 10 ml/min through the saturator containing n-hexane.

The results on the influence of %XRD crystallinity on the catalytic conversion of n-hexane over 2wt%Ga/H-ZSM-5, 2wt%Zn/H-ZSM-5 and 2wt%Mo/H-ZSM-5 catalysts with different %XRD crystallinity are presented in Figure 4.22.

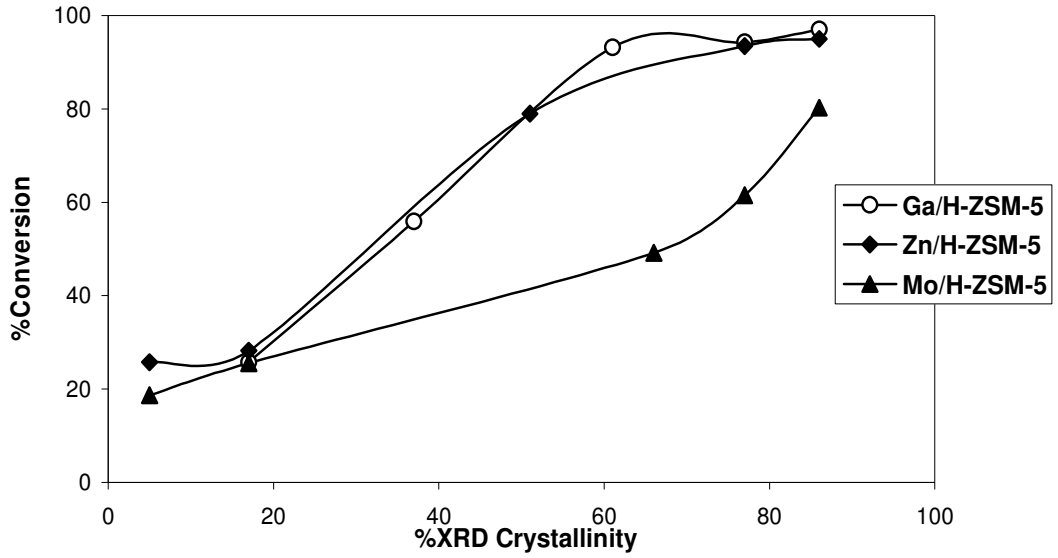

Figure 4.22: The conversion of n-hexane over 2%Ga/H-ZSM-5, 2%Zn/H-ZSM-5 and 2%Mo/H-ZSM-5 catalysts of different %XRD crystallinity at 500°C taken at a time-on-stream of 5 hours.

From the results we observed that the %XRD crystallinity of H-ZSM-5 has an effect on both the catalytic conversion of *n*-hexane and aromatic compound formation. The catalytic conversion of *n*-hexane increased linearly with an increase in %XRD crystallinity of zeolites for the 2%Mo/H-ZSM-5 catalysts. Samples with low %XRD crystallinity (below 30%) showed low catalytic conversion of *n*-hexane. It is expected that samples with low %XRD crystallinity will show low conversions due to the low concentration of acid sites in H-ZSM-5 which are important for the cracking and aromatization of *n*-hexane. For the molybdenum loaded samples with high %XRD crystallinity i.e. 66-86% we observed a slight exponential increase of *n*-hexane conversion from

25 to 80%. For gallium and zinc modified H-ZSM-5 samples, we observed a linear increase in the catalytic conversion of *n*-hexane from 5 to 60% crystallinity and followed by stabilization at high crystallinity attaining conversions above 90%. The %XRD crystallinity of H-ZSM-5 is associated with the acidity of the H-ZSM-5 catalysts. Our results agree with those reported by Makgoba [20]. Makgoba observed an increase in *n*-hexane cracking activity with increase in %XRD crystallinity. This increase in activity with %XRD crystallinity was attributed to the number of Brønsted acid sites present in the H-ZSM-5 zeolite catalyst. The number of Brønsted acid sites increase with an increase in %XRD crystallinity. So, an increase in conversion of *n*-hexane with %XRD crystallinity can be attributed to an increase in the acidity of the H-ZSM-5 zeolite catalysts.

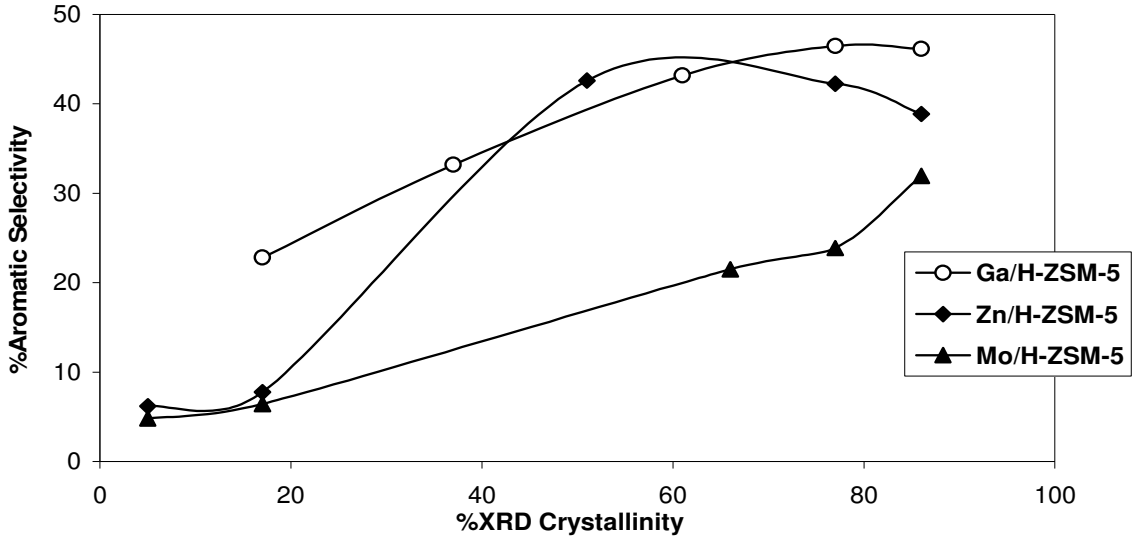

Figure 4.23: The aromatic selectivity of n-hexane over 2%Ga/H-ZSM-5, 2%Zn/H-ZSM-5 and 2%Mo/H-ZSM-5 as the function of percentage XRD crystallinity taken at a time-on-stream of 5 hours at 500^{o}C.

High aromatic selectivity observed in all H-ZSM-5 catalysts of high percentage XRD crystallinity can be attributed to the availability of Brønsted acid sites that are prominent in the samples with high crystallinity as opposed to those with low percentage XRD crystallinity.

Catalysts with %XRD crystallinity above 30% possess good acid site distribution which are able to participate in the cracking of *n*-hexane and are more selective to coke formation on the catalytic surface. High aromatic selectivity and catalytic conversion of n-hexane were observed for Zn/H-ZSM-5 and Ga/H-ZSM-5 samples. This can be attributed to the fact that zinc and gallium possess good dehydrogenation activity. The dehydrogenation activity of gallium and zinc species may be involved in the dehydrogenation of n-hexane to hexene which further undergoes secondary reactions to form aromatic compounds. Thus high conversions of n-hexane and high aromatic selectivity were observed.

The product distribution over 2%Ga/HZSM-5, 2%Zn/H-ZSM-5 and 2%Mo/H-ZSM-5 catalysts of different percentage XRD crystallinity are shown below.

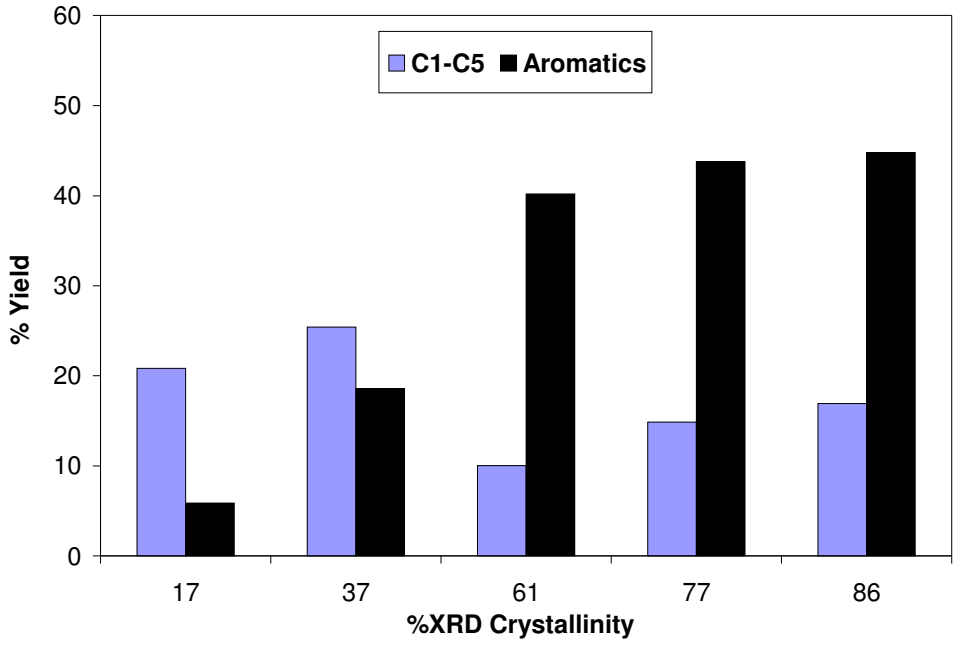

Figure 4.24: The effect of percentage crystallinity on the product distribution of n-hexane over 2%Ga/H-ZSM-5 taken at time-on-stream of 5 hours at 500^{o}C.

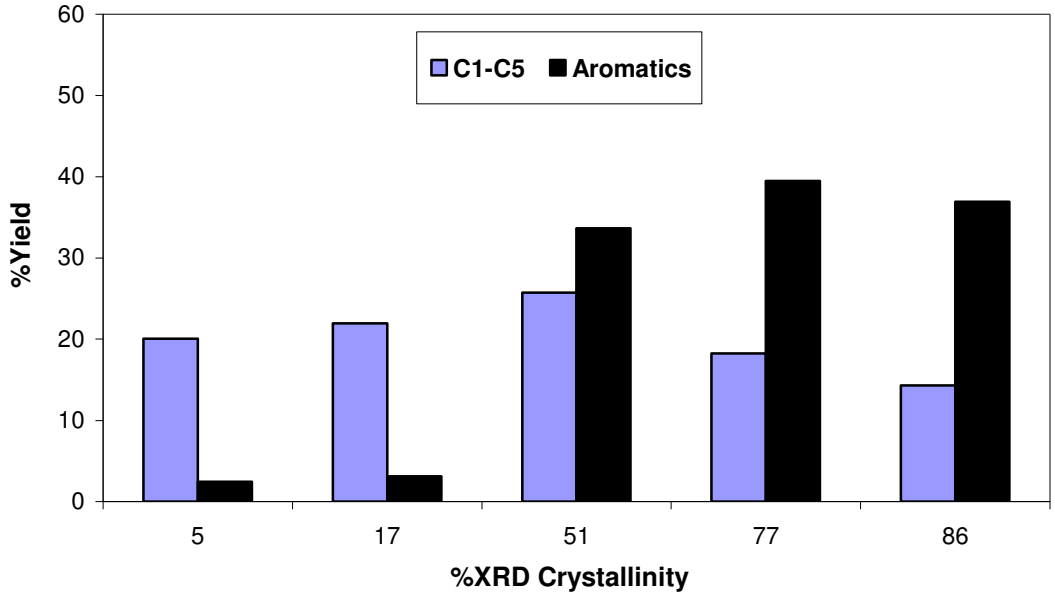

Figure 4.25: The effect of percentage crystallinity on the product distribution of n-hexane over 2%Zn/H-ZSM-5 taken at a time-on-stream of 5 hours at 500^{o}C.

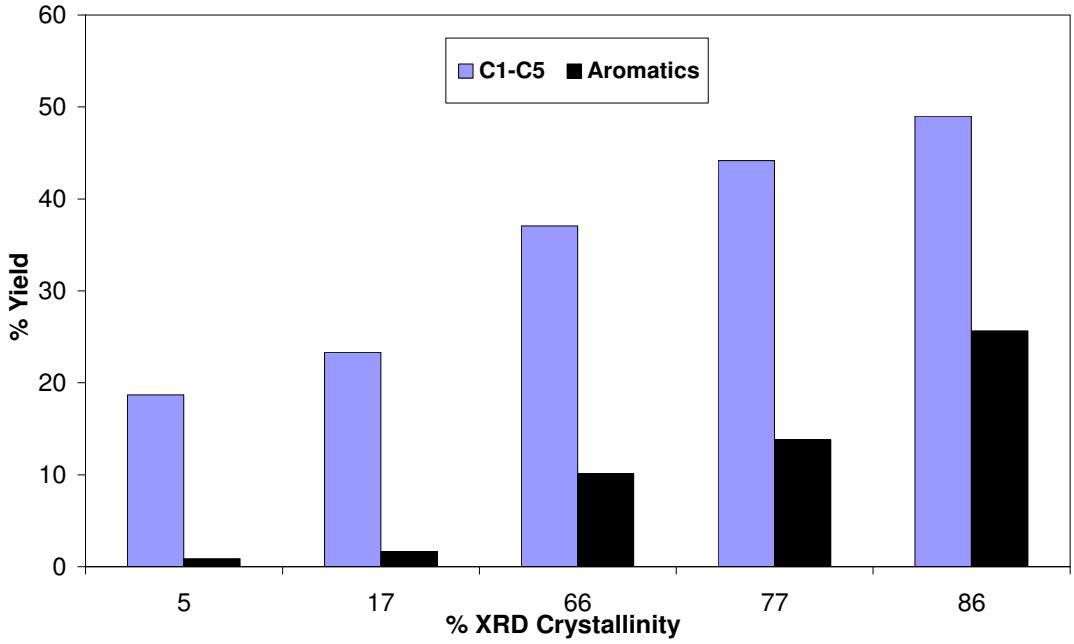

Figure 4.26: The effect of percentage crystallinity on the product distribution of *n*-hexane over 2%Mo/H-ZSM-5 taken at a time-on-stream of 5 hours at 500^{o}C.

From the results presented above we observed that the yields of aromatic compounds show similar trends to those shown for aromatic selectivity (Figure 4.23). This is expected since the percentage yield is a function of both selectivity and conversion. The samples with high %XRD crystallinity show a vast difference between the aromatic yield and cracked product (C_1-C_5) yields. The aromatic yield increased linearly with increase in percentage XRD crystallinity while a decrease in yield of cracked products is simultaneously observed with increase in %XRD crystallinity. These results are only observed for gallium and zinc samples, conversely the molybdenum samples present a different picture. Both the yield of aromatic and cracked products increased linearly with %XRD crystallinity with cracked products being the dominating compounds, reaching values close to 50% yield for highly crystalline samples. The aromatic yield was observed to be below 25%. The aromatic yield at for samples with %XRD crystallinity above 30% was observed to range from 40 to 45% with the 86% XRD sample being the highest for the Ga/H-ZSM-5 catalysts. For the Zn/H-ZSM-5 catalysts we observed a low aromatic yield below 5% for samples with %XRD crystallinity below 30%. However, an increase in the aromatic yields was observed reaching an optimum yield of 39% at 77% XRD crystallinity followed by a slight decrease at 86% XRD crystallinity. These results imply that at low percentage crystallinity there are more olefins produced in the reaction mixture which are not converted into the desired aromatic compounds, leading to the low aromatic yields. This can be attributed to the low catalytic activity which is due to the low number of Brønsted acid sites present in the catalyst. The increase in the aromatic yield and decrease in cracked products with an increase in %XRD crystallinity can be attributed to the high concentration of olefins that are produced in the reaction mixture which further undergo secondary reactions and are converted into aromatic compounds via oligomerization, cyclization then dehydrogenation reactions.

The results of the BTX product distribution analysis for *n*-hexane reaction over Ga/H-SM-5, Zn/H-ZSM-5 and Mo/H-ZSM-5 zeolite catalysts (2 wt% metal loaded at 500^{o}C) for H-ZSM-5 samples with high percentage XRD crystallinity ranging from 51-86% are presented in Table 4.7. The results show that that aromatic product distribution is affected by the choice of the metal loaded on the H-ZSM-5 for the aromatization of n-hexane. The yields of the individual aromatic compounds increase with %XRD crystallinity for Ga/H-ZSM-5 samples. The

percentage yield of toluene increased with the %XRD crystallinity from 10% reaching 15% yield at 86% XRD crystallinity while the benzene increased and reached an optimum yield of 9.8% at 77% XRD crystallinity. This decrease in benzene yield can be attributed to the alkylation that might be taking place between the C_2 compounds and benzene on the Brønsted acid sites which are prominent in samples with high %XRD crystallinity. The alkylation of benzene might contribute to the increase in yields of toluene and ethylbenzene. But a different behaviour was observed for the *m,p*-xylenes yields which decreased for 8.5 to 5.4% with increase in %XRD crystallinity.

Table 4.7: The effect of %XRD crystallinity on the aromatic product distribution comparing H-ZSM-5 samples with high %XRD crystallinity.

			Percentage Yields				
Metal	%XRD	%Conversion	Benzene	Toluene	Et-Benzene	*o*-Xylene	*m,p*-Xylene
Ga	61	93.2	8.2	10.0	7.6	5.9	8.5
	77	94.2	9.9	13.3	6.2	6.6	7.7
	86	97.0	8.2	15.5	9.0	6.7	5.4
Zn	51	79.0	9.5	13.3	6.6	3.3	0.9
	77	93.5	11.1	12.1	7.5	5.7	6.1
	86	95.0	11.7	9.8	5.5	3.8	3.0
Mo	66	49.2	1.5	4.1	2.5	1.2	1.0
	77	61.5	1.9	5.7	3.8	1.3	1.1
	86	80.3	5.3	10.6	6.0	2.0	1.7

A different aromatic product distribution from Ga/H-ZSM-5 samples was observed for Zn/H-ZSM-5. The dominance of toluene over other aromatic products decreased with increase in the %XRD crystallinity while the yield of benzene increased to 10%. Also observed drop in the yield of ethylbenzene, *m,p*-xylene, and o-xylene reaching low values of 5.5, 3.0 and 3.8% respectively at 86% XRD crystallinity was noted. This drop can be attributed to the crystalline material being formed on the mouths of the pore of H-ZSM-5 by crystallization during the

synthesis of H-ZSM-5. This crystalline material blocks the methyl and ethlybenzene compounds from diffusing through the channels of H-ZSM-5 [21]. Another reason may be that the dealkylation occurred from methylbenzene compounds, increasing the yield of benzene from the zinc species. For Mo/H-ZSM-5 catalysts there is an exponential increase in the yield of individual aromatic compounds, with toluene being the dominate product and *m,p*-xylene having the lowest yields. However, these aromatic yields are low when compared with the cracked products as shown in Figure 4.26.

4.4. The Effect of Reaction Temperature

The influence of temperature on the conversion of n-hexane was studied on the 2%Mo/H-ZSM-5, 2%Ga/H-ZSM-5 and 2%Zn/H-ZSM-5 catalysts that were prepared by incipient wetness impregnation method and calcined at 500^{o}C. The catalysts were pretreated at the reaction temperature of the study with nitrogen flowing at 10 ml/min for 1 hour. The n-hexane aromatization reactions were studied at temperatures between 500 and 600^{o}C.

Table 4.8 presents the results of the effect of temperature on the aromatization of *n*-hexane taken after 1, 5 and 10 hours of time-on-stream. The results shown suggest that conversion of *n*-hexane is dependent on the reaction temperature. For the time-on-stream of 1 and 5 hours the conversion of *n*-hexane increased with reaction temperature. However, for longer times on stream a decrease in the conversion of *n*-hexane with increase in reaction temperature was observed. Even though a decrease in conversion is observed with increase in temperature there is a different behaviour for the reactions performed at 550^{o}C. The catalysts at this reaction temperature appear to be showing good activity and are stable with time-on-stream for gallium catalysts. The conversion of *n*-hexane was shown to be within the range of 99 and 96% for gallium catalyst with aromatic selectivity above 50%. As the reaction temperature was increased to 600^{o}C a decrease in aromatic selectivity 43 to 27% was noted with time-on-stream.

Table 4.8: The effect of temperature on the conversion of *n*-hexane and aromatic selectivity of Ga/H-ZSM-5, Zn/H-ZSM-5 and Mo/H-ZSM-5 catalysts containing 2 wt% metal loading taken at 1, 5 and 10 hours time-on-stream.

	Temperature	%Conversion			%Aromatic Selectivity		
Metal	^{o}C	1 hour	5 hour	10 hour	1	5	10
Ga	500	87.4	70.0	62.2	32.2	41.7	36.2
	550	99.8	99.4	97.1	54.5	50.8	49.4
	600	98.7	81.3	59.1	43.2	39.6	27.5
Zn	500	82.6	88.3	88.5	23.6	29.7	35.5
	550	99.1	90.4	74.9	56.9	34.8	18.7
	600	99.9	79.9	53.9	46.5	24.1	7.0
Mo	500	61.2	49.2	41.1	25.2	20.6	19.9
	550	67.1	68.1	59.5	28.7	34.9	30.0
	600	73.0	63.3	47.7	34.8	33.6	27.2

For zinc catalysts the conversion of *n*-hexane increased with reaction temperature for the first hour on stream reaching a maximum of 100% at 600^{o}C followed by a rapid decrease as the time increased at 550 and 600^{o}C. This decrease is due to the volatility of zinc; zinc tends to escape the reactor system at high reaction temperatures due to its low melting and boiling points [22]. This also led to a decrease in the aromatic selectivity from 56 to 18% for the reactions performed at 550^{o}C and at 600^{o}C. A decrease from 46 to 7% was also observed due to the decrease in the dehydrogenation activity as the zinc concentration decreased. The conversion of *n*-hexane was 61 and 73% for the first hour on stream over molybdenum catalysts with an increase in aromatic selectivity from 25 to 35% with increase in temperature. As the time-on-stream increased there was a decrease in the conversion of *n*-hexane at the three reaction temperatures. However, this decrease in conversion is more severe at 600^{o}C, where the conversion decreased from 73 to almost 48%. This decrease in conversion serves to show that deactivation of catalysts that can be attributed to the formation of coke on the surface of the catalysts. This coke formed on the surface of the catalyst acts as a poison on the active sites of zeolite [23]. Hence, we observed a decrease in the conversion of *n*-hexane. A decrease in aromatic selectivity with time on stream

at 500 and 600°C was observed but at a reaction temperature 550°C a stable in aromatic selectivity was maintained. The decrease in the aromatic selectivity can be attributed to the decrease in conversion of *n*-hexane since selectivity is a function of conversion and other factor that may be contributing is the change in the geometry of the zeolite pores due to coke deposition. This alteration may hinder the diffusion of aromatic compounds through the pores and channels of the zeolite structure and some molecules will then be trapped within the microstructure of zeolite. These aromatic compounds will further convert to polyaromatic compounds which contribute in the formation of coke with time [24].

The results on the effect of temperature on the product distribution of *n*-hexane over 2%Ga/H-ZSM-5 catalysts at different temperatures are shown in Figure 4.27.

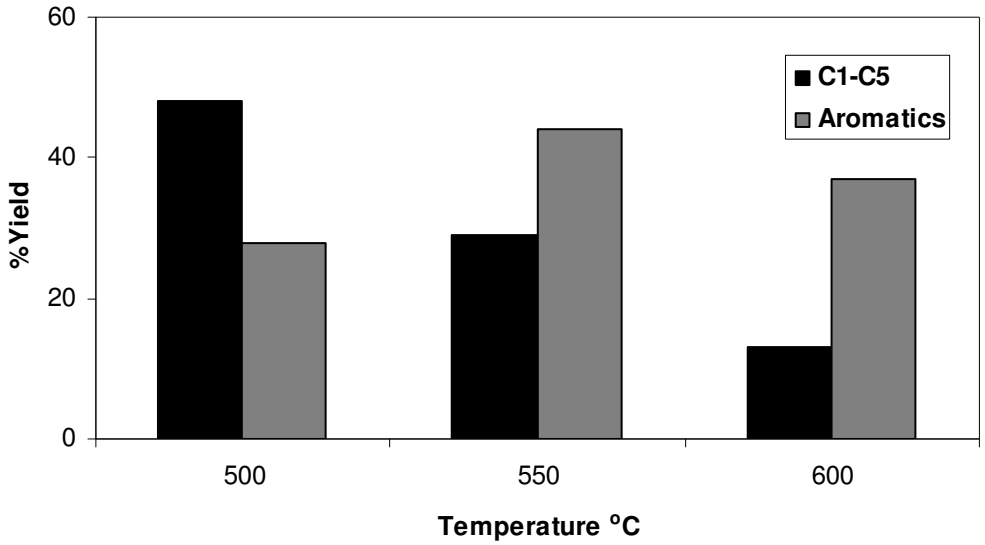

Figure 4.27: The effect of temperature on the product distribution of *n*-hexane over 2%Ga/H-ZSM-5 catalysts at isoconversion of 90%.

The aromatic yield mainly made of BTX products appears to show a dependency on the reaction temperature. In the results shown in Figure 4.27, the aromatic yield increased with temperature reaching an optimum of 44% at 550°C followed by a decrease to 37% at 600°C. It was noted

previously that the %yield of aromatic products depended on the concentration of olefins present in the reaction mixture. So, high yields of aromatic compounds at 550°C can be attributed to high concentration of olefins that are converted into the aromatic compounds, to give a decrease in the yield of the cracked products. The decrease in the yield of the cracked products can be attributed to the secondary reactions that are converting the $C_3^=$ and $C_4^=$ olefins in the reaction mixture. These olefins are converted into aromatic compounds. The decrease in the aromatic yield at 600°C can be ascribed to deactivation of the catalyst.

The effect of temperature on the product distribution of *n*-hexane over 2%Zn/H-ZSM-5 catalysts at different temperatures are shown in below in Figure 4.28

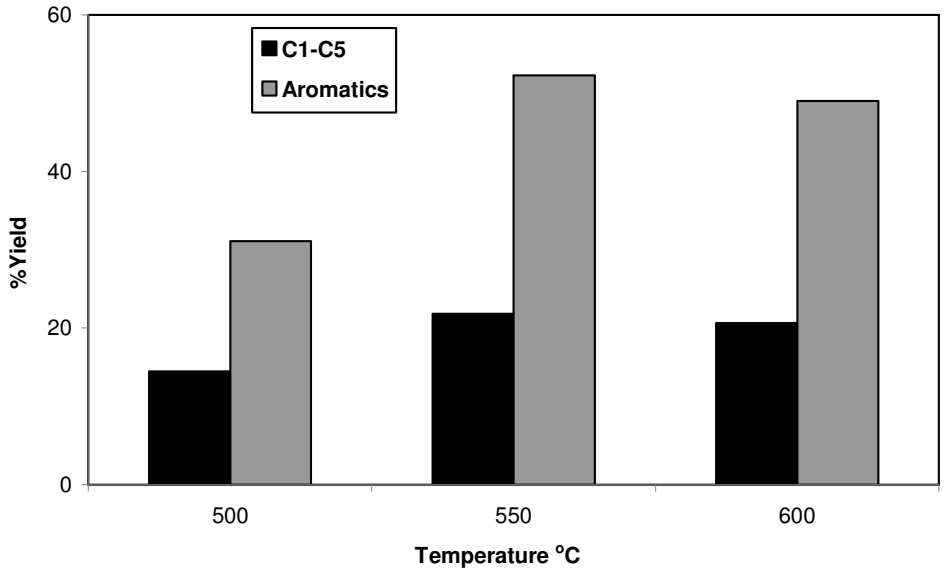

Figure 4.28: The effect of temperature on the product distribution of n-hexane over 2%Zn/H-ZSM-5 catalyst at isoconversion of 92%.

From the results presented above it is evident that the increase in reaction temperature favoured the formation of aromatic compounds. As the reaction temperature was increased from 500 to 600°C, an increase in aromatic yield from 31 to 50% was noted with an optimum at 550°C. There is a decrease in the yield of the cracked products when comparing the reactions performed

at 500 and 550°C. This is due to the formation of aromatic compounds from olefinic cracked compounds as highlighted in the gallium system above. This also shows that the increase in reaction temperature enhanced the dehydrogenation activity of the catalyst over the cracking activity.

The results of effect of reaction temperature on the cracked and aromatic products over 2%Mo/H-ZSM-5 zeolite catalysts at different temperatures are presented in Figure 4.29

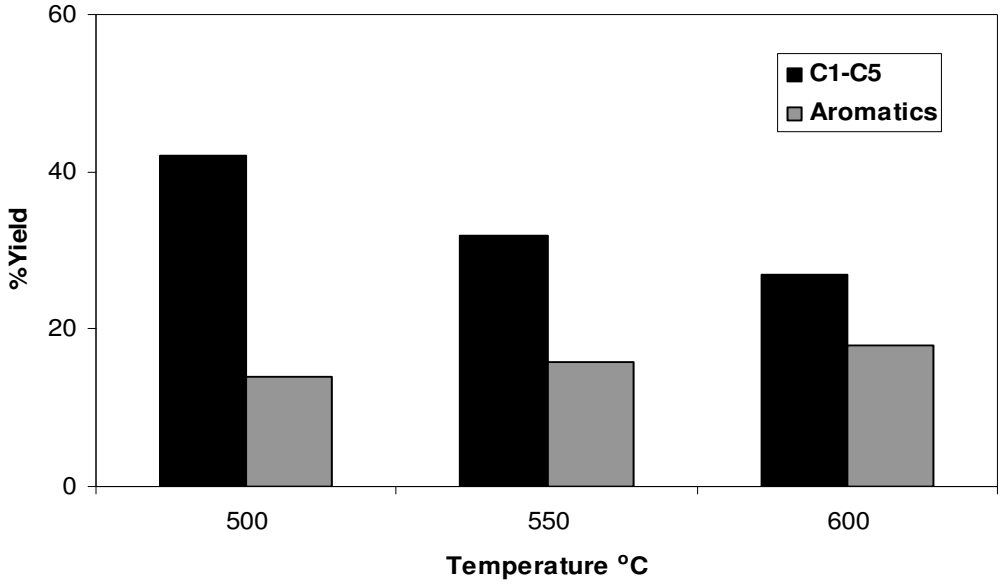

Figure 4.29: The effect of temperature on the product distribution of n-hexane over 2%Mo/H-ZSM-5 catalyst at 60% isoconversion.

The results presented above show that the yield of cracked products decreased from 42 to 27% as the reaction temperature increased while the yield of the aromatic compound did not change much (15 to 18%). The decrease in cracking activity without the increase in the aromatic compounds formation may be due to coke formation on the surface of the catalyst which inhibits reaction of the catalyst active sites with the reactants.

Table 4.9: The effect of reaction temperature on the aromatic product distribution mainly BTX of aromatization of *n*-hexane over Ga/H-ZSM-5, Zn/H-ZSM-5 and Mo/H-ZSM-5 zeolite catalysts. taken at reaction temperatures between 500 and 600 ^{o}C.

			%Yields				
Metal	%XRD	%Conversion	Benzene	Toluene	Et-Benzene	*o*-Xylene	*m,p*-Xylene
Ga	500	87.4	6.6	11.3	2.0	2.5	5.9
	550	96.4	18.3	14.4	2.7	1.8	6.0
	600	90.4	16.4	12.0	1.7	1.5	5.3
Zn	500	88.3	6.9	7.7	7.1	3.5	5.8
	550	92.2	12.0	10.1	4.9	2.8	4.8
	600	92.8	13.7	8.4	4.6	2.3	1.9
Mo	500	61.2	2.0	5.7	1.6	1.4	4.7
	550	58.0	6.8	6.2	0.9	0.6	2.9
	600	58.4	7.9	6.1	0.9	0.9	2.9

The results in Table 4.9 show that the aromatic product distribution is affected by the reaction temperature. The major effect is noticeable for benzene and toluene. At a reaction temperature of 500^{o}C toluene was the dominant product and as the reaction temperature was increased the percentage yield for benzene increased reaching maximum values of 18 and 12% for the gallium and zinc catalyst respectively at 550^{o}C. This increase in the yield of benzene was compensated for by the decrease in the yield of the C_8 aromatic compounds (ethylbenzene and xylenes) as the temperature increased. An increase in reaction temperature inhibited the alkylation reactions and favoured the dealkylation of methylated and ethylated benzene compounds. Hence a decrease in the C_8 aromatic compounds is observed with increase in reaction temperature. The low yields of *o*-xylene relative to *m,p*-xylenes is due to the shape selective character of zeolites. The *p*-xylene contributes in increasing the yields of *m,p*-xylenes hence the *m,p*-xylenes appeared to be favoured over o-xylene [25]. The distribution of the C_8 aromatic compounds seems to show a consistency with temperature. The increase in benzene yield and the slight decrease in toluene yield can be attributed to the demethylation that might be taking place from toluene and C_8 aromatics. This would contribute to the formation of benzene and small traces of methane. The

molybdenum catalyst demonstrated a similar effect to that shown for gallium and zinc catalysts but the yields of for each aromatic compound were below 9%. This may be attributed to low aromatic selectivity that is show by the molybdenum loaded H-ZSM-5 zeolite catalyst. The yield of benzene increased from 2 to 8% while toluene remained constant with increase in reaction temperature. In the case of C_8 aromatics a decrease in the yield was observed from 500 to 550^oC and remained constant at 600^oC. The *m,p*-xylenes were also dominant in the C_8 aromatics composition.

4.5. Brief Comparison Study

A comparison study was done on the H-ZSM-5 and on the metal modified H-ZSM-5 catalysts. The metal modified catalysts were loaded with 2 wt% loading of gallium, zinc and molybdenum prepared by the incipient impregnation method. The catalysts were calcined at 500^oC for 6 hours and the aromatization of *n*-hexane was then performed at 500^oC with nitrogen flowing at 10 ml/min.

The results of the conversion of *n*-hexane over H-ZSM-5 and metal modified zeolite catalysts are presented in Figure 4.30. The conversion of *n*-hexane the over metal free H-ZSM-5 catalyst was around 85% with time-on-stream. The introduction of metal species in the H-ZSM-5 resulted in a decrease in the conversion of *n*-hexane and the activity decreased with an increase in time-on-stream. This decrease in the activity may be due to the decrease in the number of active sites of H-ZSM-5 as the metal species are introduced into H-ZSM-5. The molybdenum catalyst seemed to be more stable than the gallium and zinc catalysts. The conversion of *n*-hexane over Mo/H-ZSM-5 catalyst was ca. 70% and that of Ga/HZSM-5 and Zn/H-ZSM-5 were ca. 60% but with the Ga/H-ZSM-5 suffering a more rapid decrease with time-on-stream than molybdenum and zinc catalyst.

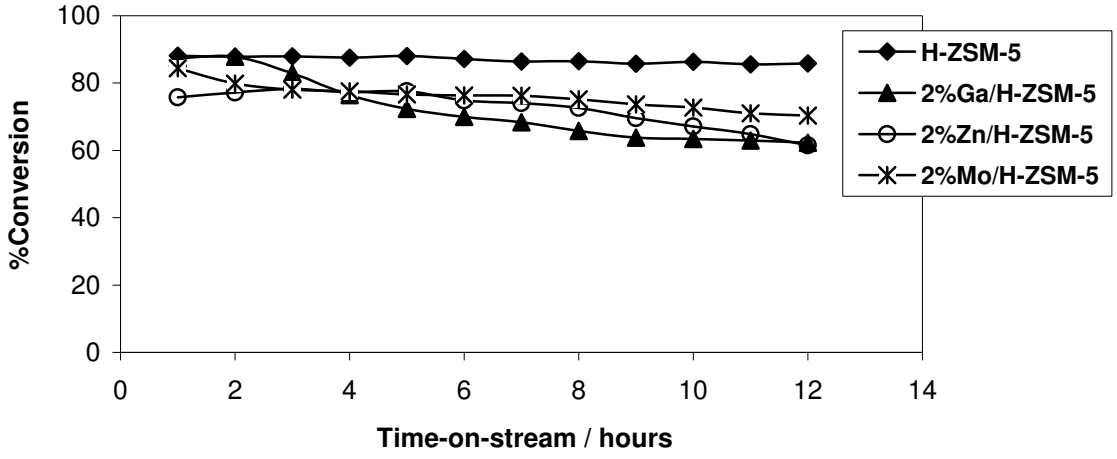

Figure 4.30: The catalytic conversion of *n*-hexane over metal promoted H-ZSM-5 catalysts of 2wt% loading as the function of time-on-stream at 500^{o}C.

The results of the aromatic selectivity of H-ZSM-5 and metal modified H-ZSM-5 zeolite catalysts are presented below.

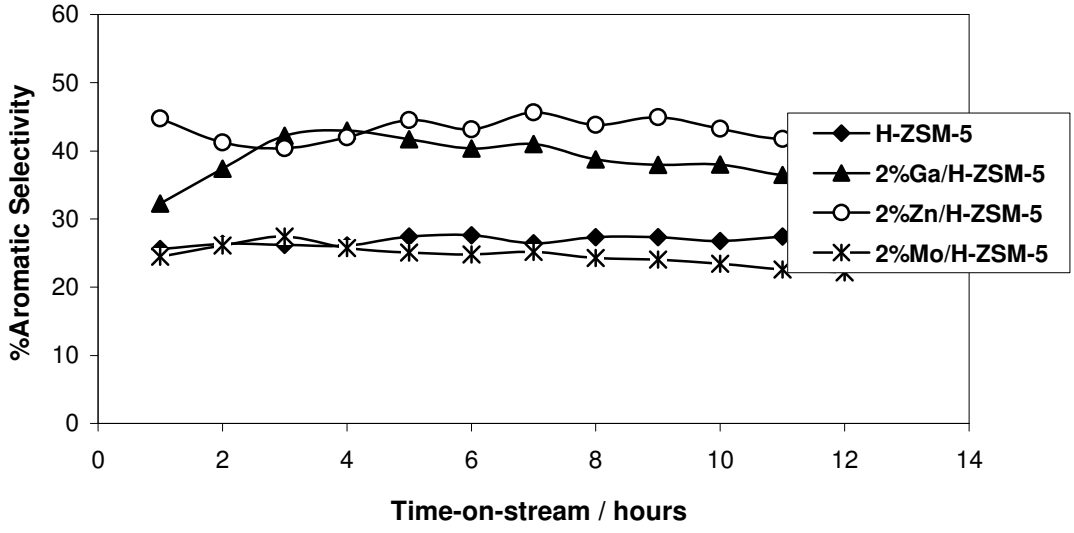

Figure 4.31: The percentage aromatic selectivity as a function of time-on-stream over metal promoted H-ZSM-5 catalysts.

The aromatic selectivity showed a different trend from that of conversion. Catalysts with low conversions exhibited good aromatic selectivities. The aromatic selectivity of gallium and zinc catalysts was around 38 and 41% respectively. And those for metal free H-ZSM-5 and molybdenum loaded were below 30%. The high aromatic selectivity from gallium and zinc loaded H-ZSM-5 zeolite catalysts is due to the dehydrogenation activity that is possessed by the two metals. Low aromatic selectivity of H-ZSM-5 and Mo/H-ZSM-5 may be due to the cracking activity that might be dominating in these catalysts.

The comparison results of cracking activity and aromatic compound formation of H-ZSM-5, Mo/H-ZSM-5, Ga/H-ZSM-5 and Zn/H-ZSM-5 are shown in the Figure 4.32.

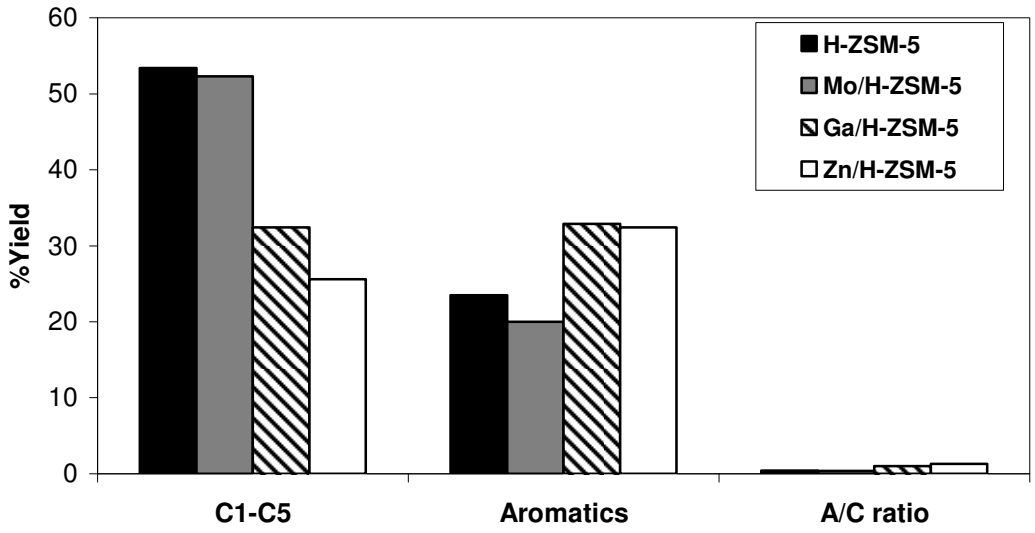

Figure 4.32: The cracking and aromatic activity of the metal modified H-ZSM-5 zeolite catalysts.

From the comparison results of the cracking activity and aromatic compound formation, it is shown that the addition of gallium and zinc to the H-ZSM-5 catalyst increased the formation of aromatic products while the production of cracked products decreased. This is due to the dehydrogenation activity of these metals which is effective in the conversion of small cracked

products especially $C_3^=$ and $C_{4s}^=$ olefins that are mostly converted into aromatic compounds by secondary reactions. The introduction of molybdenum on the H-ZSM-5 gave a material that did not show any activity in transforming the cracked products into aromatics. The yields of the main C_3 and C_4 compounds were almost similar to those produced by the metal-free H-ZSM-5 zeolite catalysts. This might be due to the absence of the dehydrogenation activity; in this catalyst the cracking activity is dominant. The A/C ratio of gallium and zinc was high compared with that of molybdenum.

Table 4.10: The product distribution of the aromatic compounds of *n*-hexane over metal modified H-ZSM-5 zeolite catalysts taken at isoconversion of ±77%.

Catalysts	H-ZSM-5	Ga/H-ZSM-5	Zn/H-ZSM-5	Mo/H-ZSM-5
%Conversion	85.3	76.4	77.3	77.5
	Percentage Yield			
Methane	2.3	2.1	2.4	1.8
Ethylene	4.0	4.3	0.93	3.9
Ethane	6.3	2.6	3.8	6.5
Propylene	21.9	12.1	9.8	20.5
Propane	5.7	3.5	1.9	4.3
$C_{4s}^=$	8.9	5.0	4.3	9.5
$C_{4s}^/$	2.0	1.6	1.4	2.7
C_{5s}	2.4	1.3	1.1	3.0
C_{6s}	0.3	0.4	1.04	1.4
Benzene	4.0	6.4	10.2	3.0
Toluene	8.7	12.1	10.0	7.2
m,p-Xylene	5.8	8.9	7.9	4.1
Et-Benzene	2.1	3.3	2.3	2.5
o-Xylene	2.9	2.1	2.1	1.0
$C9_s$	1.5	3.9	9.7	1.0
∑Aromatics	23.5	32.9	32.4	19.9

The results show that the addition of a metal has an influence on the aromatization of *n*-hexane over H-ZSM-5 zeolite catalysts. The product distribution is affected and depends on the properties of the metal that is added in H-ZSM-5. The obvious characteristic yields that differ

depending on the metal used can be noted. These are the high yields of olefins and aromatics obtained over gallium and zinc catalysts when compared with those found over H-ZSM-5 and molybdenum catalysts. The aromatic yield over H-ZSM-5 is about 24% and the Mo/H-ZSM-5 yielded 20% of aromatic compounds. This shows that the addition of molybdenum did not have a major effect on the product distribution when compared with that of the H-ZSM-5 catalyst. The yields of the major olefins i.e. propylene and the butenes, remained constant after the addition of molybdenum species. Addition of gallium and zinc enhanced the yield of aromatic compounds. The increase in the aromatic yield is accompanied by the decrease in the yields of $C_3^=$ and $C_{4s}^=$ olefins. This is attributed to the dehydrogenation activity that is possessed by gallium and zinc that provided an alternative reaction pathway for the reactant. The cracking of n-hexane is compromised by the presence of gallium and zinc species. This is evident by looking at the yield of C_5 which is around 1% for gallium and zinc catalysts and for H-ZSM-5 and molybdenum catalysts is found to be 2.4 and 3% respectively.

4.6 REFERENCE LIST

[1] J. Kanai and N. Kanata*, Appl. Catal*., **55** (1989) 115.

[2] V.R Choudhary, K. Mantri, C. Sivadinarayana, *Microporous and Mesoporous Mater.,* **37** (2000) 1.

[3] H.D. Lanh, V.A. Tuan, H. Kosslick, B. Parlitz, R. Fricke, J. Völter, *Appl Catal. A: General*, **103** 1993 205.

[4] G.J Buckel and G.J Hutchings, *J. Catal*., **151** (1995) 33.

[5] V. Kanazirev,G. L. Price, and K. M. Dooleyb, *J. Chem. Soc., Chem. Commun.*, (1990) 721.

[6] N. Viswanadham, A.R. Pradhan, N.Ray, S.C.Vishnoi, U. Shanker, T.S.R. Prasada Rao, *Appl. Catal. A: General*, **137** (1996) 225.

[7] H. Berndt, G.Lietz, B. Lucke and J. Volter, *Appl. Catal. A: General*, **146** (1996) 315.

[8] E. Rojasova, A. Smeiskova, P. Hudec, Z. Zidek, *React. Kinet. Catal. Lett*., **66** (1999) 91.

[9] J. Kanai and N. Kawata, *J. Catal*., **114** (1988) 284.

[10] N.S. Gnep, J.Y. Doyement and M.R. Guisnet, *J. Mol. Catal*., **45** (1988) 281.

[11] D.B. Lukyanov, V.I. Shtral, S. N. Khadzhiev, *J. Catal*., **146** (1994) 87.

[12] D.B. Lukyanov, N.S Gnep and M.R. Guisnet, *Ind. Eng. Chem Res.*, **34** (1995) 516.

[13] A. Smieskova, E. Rojasova, P. Hudec and L. Sabo, *Appl. Catal. A: General,* **268** (2004) 235.

[14] C. Bigey and B.L. Su, *J. Mol. Catal. A: Chem*., **209** (2004) 179.

[15] B. Li, S. Li, N. Li, H. Chen, W. Zhang, X. Bao and B. Li, *Microporous and Mesoporous Mater*., **88** (2006) 244.

[16] J. Wang, M. Kang, Z. Zhang and X. Wang, *J. Nat. Gas Chem.*, **11** (2000) 43.

[17] L.Y. Chen, L.W. Lin, Z.S. Xu, X.S. Li and T. Zhang, *J. Catal.*, **157** 1(995) 190.

[18] H. Lui and Y. Xu, *Chin. J. Catal*., **27** (2006) 319.

[19] D. Ma, W. Zhang, Y. Shu, X. Liu, Y. Xu and X. Bao, *Catal. Lett*., **66** (2000) 155.

[20] N.P. Makgoba, MSc. Thesis, University of the Witwatersrand, 2002.

[21] C.P. Nicolaides, N.P. Sincadu and M.S. Scurrell, *Catal. Today*, **71** (2002) 429.

[22] T. Yu and J.H. Qian, *Petroleum Science and Technology*, **24** (2006) 1001.

[23] N. Mori, S. Nishiyama, S. Tsuruya* and M. Masai, *Appl. Catal.,* **14** (1991) 37.

[24] C. Li and P.C Stair, *Catal. Today*, **33** (1997) 353.

[25] T.V Choudhary, A.K Kinage, S Banerjee and V.R Choudhary, *Microporous and Mesoporous Mater*., **70**, (2004) 37.

Chapter 5

Conclusions

- The study of the effect of metal loading on the aromatization of *n*-hexane was undertaken with three metals; gallium, zinc and molybdenum. The addition of gallium showed good activity and stability for the aromatization of *n*-hexane. Higher conversions within the 70-90% band were obtained for catalysts with low gallium loadings while aromatic selectivity increased from below 25% to above 40% after the addition of gallium.

- Similar results were obtained after addition of zinc. Zinc addition gave catalysts that showed good catalytic activity and the catalytic activity was dependent on the amount of zinc loaded on the H-ZSM-5 catalysts. Conversions higher than 80% were obtained over H-ZSM-5 containing 3 wt% zinc loading and the aromatic yield increased with increase in zinc loading reaching 38% yields. The aromatic product distribution results showed that at high zinc loading the Zn/H-ZSM-5 is more selective to the formation of benzene rather than toluene which is more dominant in the aromatization of *n*-hexane.

- The addition of molybdenum had a negative effect on the aromatization of n-hexane. Conversion of n-hexane decreased with molybdenum loadings, reaching values below 50% with catalysts containing 6 and 10 wt% molybdenum. The catalysts showed less stability, with rapid deactivation with time-on-stream. The aromatic selectivity was low for the molybdenum modified catalysts when compared with the molybdenum free H-ZSM-5 catalyst.

- The high aromatization activity that is associated with both gallium and zinc metal is due to the dehydrogenation activity that is possessed by the metals. Impregnation of H-ZSM-5 with gallium and zinc provides an alternative pathway reaction for the aromatization of *n*-hexane which gives a high conversion and a high concentration to aromatic compounds. On the other hand addition of molybdenum to H-ZSM-5 gave different results. When the aromaticity and cracking activity of the three metals were compared, it was observed that the aromatic products obtained from Ga/H-ZSM-5 and Zn/H-ZSM-5 dominated over the cracking activity. This showed that the dehydrogenation activity contributes for the aromatization and hence these catalysts are more selective to the formation of aromatics. Molybdenum-containing catalysts were more selective for cracking reactions.

- The effect of the percentage XRD crystallinity of H-ZSM-5 samples which were modified by a loading of 2 wt% of metal on the aromatization of *n*-hexane revealed interesting trends. The conversion of *n*-hexane increased with increase in percentage crystallinity. Samples with %XRD crystallinity below 30% were less active and less selective to the formation of aromatic compounds irrespective of the metal loaded on H-ZSM-5. The aromatization of *n*-hexane over H-ZSM-5 samples with higher %XRD crystallinity resulted in an increase in conversion. The conversions between 80 and 90% were obtained for Zn/H-ZSM-5 and Ga/H-ZSM-5 catalysts. The aromatic yield was within the 40 to 50% band for both catalysts. The conversion of *n*-hexane over Mo/H-ZSM-5 reached 80% for the 86%XRD sample but exhibited a low aromatic yield when compared with the yield of cracked products. The aromatization reaction is not entirely dependent on the %XRD crystallinity of H-ZSM-5 but the metal species loaded are considered to balance cracking and dehydrogenation activity.

- The aromatization of *n*-hexane was further investigated by varying the reaction temperature from 500 to 600^{o}C. At 550^{o}C catalysts showed good activity giving 99% conversions with aromatic selectivity being 57% for the first hour on-stream. The

gallium catalyst showed good stability as the time-on-stream increased. Deactivation was observed on the zinc system as time-on-stream increased and this can be due to the zinc species volatilizing from the catalyst bed due to their volatility of zinc. This deactivation led to a decrease in the aromatic selectivity from 57%, which reached to 18% after 10 hours on-stream.